

トランスポーター科学に基づくホウ素中性子 捕捉療法 BNCT 用新規増感化合物開発

平成26年度～平成28年度
私立大学戦略的研究基盤形成支援事業
研究 成 果 報 告 書

平成29年5月

学校法人名 獨協学園

大 学 名 獨協医科大学

研究組織名 大学院医学研究科

研究代表者 加藤 広行

(獨協医科大学医学部教授)

は し が き

獨協医科大学大学院医学研究科は基礎医学、臨床医学、社会医学の各分野から構成され、それぞれの領域から様々な研究が行われており、それに加え、最近では研究科内の共同研究が進んできている。本プロジェクトの基盤となった細胞膜の物質輸送を担うタンパク質であるトランスポーターの研究は、当初本プロジェクトの研究代表者を務めた薬理学講座主任教授の安西尚彦が、前任地の杏林大学にて約10年に渡り研究を継続してきたものであり、平成23年後に安西が杏林大学から獨協医科大学に異動後、基礎医学では生化学講座と病理学講座、臨床医学では第一外科、呼吸器外科、泌尿器科、産婦人科とそれぞれ個別に学内の共同研究として進めていたものでもある。

本プロジェクトは安西を中心としたそれまでの個別の共同研究というベースのある「トランスポーター研究」を特色とし、基礎から臨床に渡る双方向性の学内外多講座融合研究の活性化を担うものとして企画された。具体的には、主に細胞の生存のために欠くことのできない必須アミノ酸を運ぶL型中性アミノ酸トランスポーターLAT (L-type neutral amino acid transporter)に着目し、同分子を現在国家プロジェクトの一つとして進められている院内設置型小型加速器を用いたホウ素中性子捕捉療法 BNCT (Boron Neutron Capture Therapy) の抗腫瘍効果発現に必須のホウ素化合物をトランスポーターの視点から検討を加えることで、より有効な新規化合物を同定することを目標とした。本プロジェクトの推進のため学内の基礎医学および臨床医学の複数の講座が参画し、さらに院内設置型小型加速器が設置される国立がん研究センター中央病院放射線治療部を初めとして、同センター研究所、ジェイファーマ株式会社、米国 Colorado 大学などの参画を促し国外にまで及ぶ共同研究体制を構築して腫瘍型トランスポーター指向性新規ホウ素化合物の同定を目指す研究を実施した。本プロジェクトは近年の治療法の進歩で多くのがんが治るようになったと言われる中で、未だ治療法の無い難治性がんも存在し、それらに向けた新たながん治療法開発に道を開くための基となる機序の解明に大きく貢献した。

冒頭に、多くの研究者の方々のご協力に深い感謝を表したい。

研 究 組 織

研究代表者：加藤 広行 (獨協医科大学医学部・教授)

研究プロジェクトに参加する主な研究者：

杉本 博之 (獨協医科大学医学部・教授)
林 啓太郎 (獨協医科大学医学部・准教授)
中里 宜正 (獨協医科大学医学部・准教授)
Jutabha P (獨協医科大学医学部・助教)
川又 均 (獨協医科大学医学部・教授)
金 彪 (獨協医科大学医学部・教授)
窪田 敬一 (獨協医科大学医学部・教授)
千田 雅之 (獨協医科大学医学部・教授)
川又 均 (獨協医科大学医学部・教授)
金 彪 (獨協医科大学医学部・教授)
窪田 敬一 (獨協医科大学医学部・教授)
千田 雅之 (獨協医科大学医学部・教授)
石井 芳樹 (獨協医科大学医学部・教授)
深澤 一雄 (獨協医科大学医学部・教授)
釜井 隆男 (獨協医科大学医学部・教授)
植木 敬介 (獨協医科大学医学部・教授)
平林 秀樹 (獨協医科大学医学部・教授)
村上 昌雄 (獨協医科大学附属病院・教授)
坂本 攝 (獨協医科大学附属病院・教授)
越川 千秋 (獨協医科大学附属病院・薬剤部長)

主な共同研究機関等：

安西 尚彦 (千葉大学大学院医学研究院・教授
／獨協医科大学医学部・特任教授)
伊丹 純 (国立がん研究センター中央病院・科長)
上園 保仁 (国立がん研究センター研究所・分野長)
遠藤 仁 (ジェイファーマ株式会社・代表取締役)
Michel F. Wempe (米国 University of Colorado・准教授)

ポスドク研究員 (PD)：

Hasaya Dokduang (獨協医科大学大学院医学研究科・平成 26・27 年度)
森田 亜洲華 (獨協医科大学大学院医学研究科・平成 28 年度)
野原 正勝 (獨協医科大学大学院医学研究科・平成 28 年度)

研 究 経 費

平成 2 6 年度	63,873	千円
平成 2 7 年度	28,122	千円
<u>平成 2 8 年度</u>	<u>32,205</u>	<u>千円</u>
合 計	124,200	千円

研究プロジェクトの目的・意義・及び計画の概要

ホウ素中性子捕捉療法 BNCT (Boron Neutron Capture Therapy,) とは、原子炉などからの中性子とガン組織に取り込まれた中性子との反応断面積が大きい元素 (ホウ素) との核反応によって発生する粒子放射線によって、選択的にがん細胞を殺すという原理に基づく放射線療法である。中性子発生には、これまでは原子炉を必要としたため、BNCT の利用は限定的であったが、最近原子炉に代る病院設置型小型加速器が開発され、都市型病院にも設置可能となり、平成 27 年度より共同研究先である国立がん研究センターで BNCT の施行が可能となった。BNCT による治療は、1. 正常細胞を巻き込むことなくがん細胞を超選択的に死滅させることができる、2. 一度で十分な治療を行うことができるため長期入院が不要、3. 原発性はもちろん、現在の治療方法では治療が困難な、再発・転移・末期がんにも有効、4. 放射線治療後、陽子線治療後、重粒子線治療後の再発がんにも治療可能、など今までの治療方法とは異なる利点を持つ。この BNCT の抗腫瘍効果に大きな影響を与えるのががん細胞に入って中性子の受け手となるホウ素を如何にがん細胞に蓄積させるかである。これまで第一世代のホウ素化合物としてホウ素化フェニルアラニン BPA (p-boronophenylalanine) が使用されているが、BPA に替わる有効な化合物は未だ生み出されておらず、その開発が期待されている。

がん細胞は、正常細胞に比較し亢進した増殖能を持つが、それを支えるのは、生命活動に必要なエネルギー源および細胞を構成するタンパク質の原料である糖やアミノ酸といった栄養素の細胞外からの取込みである。糖やアミノ酸などの栄養素は、「トランスポーター」と呼ばれる特殊な膜タンパク質を介して細胞内に取込まれる。糖と異なりアミノ酸には多様なトランスポーターが存在し、正常細胞とがん細胞でアミノ酸取込みに関与するタンパク質 (アミノ酸トランスポーター) は量的だけでなく質的にも異なることを報告している。本プロジェクト開始時、本学医学部薬理学講座の主任教授として在籍していた安西尚彦が研究対象とする L 型アミノ酸トランスポーター LAT1 は必須アミノ酸取込みを担い、多くのがんで発現が亢進するが正常組織には殆ど発現しない。先の BPA も LAT1 によって輸送されると当時推定されていて、LAT1 を高発現するがん細胞にのみ取込まれるため、BNCT に有効であると考えられる。

そこで腫瘍型アミノ酸トランスポーター研究を行う本学がその特色を生かし、トランスポーター科学の視点から新規化合物合成と LAT 発現細胞を用いたスクリーニングにより高いがん集積性を示す新たなホウ素化合物を同定することで、BNCT という極めて有効な医用原子力技術の推進を通じて、難治性がん治療成績改善に貢献するだけでなく、我が国の目指す医療イノベーションに寄与することが意義として挙げられる。

予定された計画の概要は以下の通りである。平成 26 年度：各臓器由来がんにおける L 型アミノ酸トランスポーター LAT1 発現を、がん患者組織検体を対象にした抗 LAT1 抗体を用いた免疫染色、特異的オリゴを用いた定量 PCR の点から、さらにはがん由来培養細胞を対象に質量分析計による低分子物質解析および RI トレーサー測定によりアミノ酸輸送特性の点から詳細な検討を加える。並行して BPA 構造を基にした化合物設計を行う。平成 27 年度：LAT1 安定発現細胞を用いた候補化合物のスクリーニングを行う。選別された少数の候補化合物に対しその蛍光標識体合成を行い、がん動物モデルへの投与によりがん細胞への集積性と体内動態の解析を蛍光を指標に評価する。平成 28 年度：集積性の確認された化合物をがん動物モデルに投与して中性子照射を行い、*in vivo* での腫瘍細胞における *in vitro* での影響を検討する。さらに蓄積の認められた正常組織の培養細胞にて細胞毒性効果を検討する。

この中で、平成 27 年度までに、腫瘍型トランスポーター LAT1 選択的な阻害を示す化合物のホウ素化を実施したところ、LAT1 特異的な阻害を示さないという状況が出現した。そこでその解決策として、平成 28 年度には当初の予定の代わりに以下の検討を行った：1、化合物の異なる部位にホウ素化を行うことでの LAT1 特異的阻害効果が回復するか、2、化合物を溶解する溶媒の違いが LAT1 特異的阻害効果に影響するか。検討は現在も進行中である。

研 究 組 織

本研究プロジェクトを代表する研究代表者は、獨協医科大学医学部第一外科学主任教授の加藤広行（申請時は薬理学講座主任教授の安西尚彦、現千葉大学）であり、当大学院医学研究科の基礎から臨床にわたる重要なトランスレーショナル研究の一つとして本プロジェクトを位置付けた。その観点から代表者は本プロジェクトを全てにわたり、研究の進展についての統括を行った。

本研究プロジェクトは、当初研究代表者を務めた当時本学薬理学講座主任教授であった安西らが行っている、国内外で評価の高い「トランスポーター」研究の成果を展開する形で行われた。そのため、本学薬理学講座が基礎研究の主体となり、合計3名のポスドク研究員（PD）を雇用し、生化学講座（タンパク質解析）と病理学講座（組織切片作成）との連携をとりながら体内各臓器由来のヒトがん培養細胞株におけるアミノ酸輸送の多角的解析を行う（基礎系研究者5名）ことと並行して、消化器、呼吸器、腎泌尿器、婦人科などの各臨床科からのがん患者の臨床検体の解析を行った（基礎系研究者17名）。

研究チーム間の連携は実際の研究室内にて個別の共同研究として組まれた他、それを全体としてまとめる体制は、薬理学講座において開催された毎週月曜日の朝9時からの定例セミナーにおいて保障された。また、基礎臨床連携に関しては、3月、7月、12月の年3回打合せを定期的に行い開催した他、薬理学（前代表者所属）、第一外科（現代表者所属）、呼吸器外科、泌尿器科のコアとなる教室間では特に、1月、4月、7月、10月の年4回の打合せを行い、進捗状況を確認した。本プロジェクトの遂行には膨大な費用が必要であるため、各研究室に対する大学からの講座研究費も一部導入され、研究の支援・実施体制が確立された。

他の共同研究機関として 新規ホウ素化合物群の設計・合成に関する共同研究をジェイファーマ株式会社とその連携先である米国Colorado大学と行った他、院内設置型小型加速器の設置される国立がん研究センター中央病院・研究所とは、*in vivo* 薬効および毒性評価の共同研究体制をとるなど、外部施設も参画する学際的共同研究開発体制を構築した。

研 究 施 設 ・ 設 備 等

本プロジェクトを実施する研究施設としては、獨協医科大学医学部基礎医学棟（7,652 m²、5名）および臨床医学棟（21,154 m²、12名）、実験動物センター（1,916 m²、5名）に所属する各研究室・実験室が用いられた。参画した計22名の研究者は全てフルタイムで連日上記施設を利用した。主な研究装置・設備としては、主たるものとして以下のものが用いられた。

（研究装置）

共焦点レーザー顕微鏡 LSM780	20 時間／週
イメージング質量顕微鏡 iMScope	6 時間／週
質量分析装置 QTRAP 5500	12 時間／週
質量分析装置 TRIPLE TOF6600	9 時間／週

（研究設備）

in vivo イメージング装置 Clairvivo Opt plus	1 時間／週
-------------------------------------	--------

研究成果の概要

本研究プロジェクトとしての計画は次の2点に要約できる。

①腫瘍指向性蓄積を示す新規ホウ素化合物同定

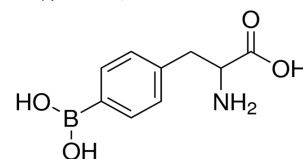
②各種がん細胞における治療標的としての腫瘍特異的L型アミノ酸トランスポーターの検証

そこで研究成果の概要をこれら2点に分けて記載する。

①腫瘍指向性蓄積を示す新規ホウ素化合物同定

本プロジェクトの当初の研究代表者である薬理学講座の安西らは、これまでに必須アミノ酸の細胞内取り込みに注目し、杏林大学の遠藤 仁氏（現ジェイファーマ株式会社）、金井好克氏（現大阪大学教授）らが世界に先駆けて同定した L 型中性アミノ酸トランスポーターLAT（L-type neutral amino acid transporter）が、ホウ素中性子捕捉療法 BNCT（Boron Neutron Capture Therapy）の抗腫瘍効果発現に現在利用されているホウ素化フェニルアラニン BPA（boronophenylalanine）を輸送する可能性を着想した。

Chemical structure of BPA



(a) LAT ファミリーによる BPA 輸送の可能性の検討

これまでに LAT ファミリーには4つのアイソフォーム（LAT1, LAT2, LAT3, LAT4）があることが知られている。さらに BPA はラセミ体（光学異性体である L 体と D 体との等量混合物）であることが知られており、光学異性体であることがトランスポーター活性に影響する可能性を検討するため、LAT1 から LAT4 までに対する BPA のラセミ体、L 体、D 体の作用を検討した。必須のホウ素化合物をトランスポーターの視点から検討を加えることで、より有効な新規化合物を同定することを目標とした。

図1に示すように LAT1 および LAT2 は BPA のラセミ体によりともに濃度依存性に阻害されたが、LAT1 に対する阻害の方が親和性が高かった。LAT3 と LAT4 に対する作用は見出されなかった。また光学異性体ごとの検討では L-BPA による LAT1 阻害が強力で (>LAT2) あったが、D-BPA は LAT2 を阻害しない LAT1 選択性であることが明らかになり、化合物のキラリティの考慮の有効性を見出した（論文投稿中）。

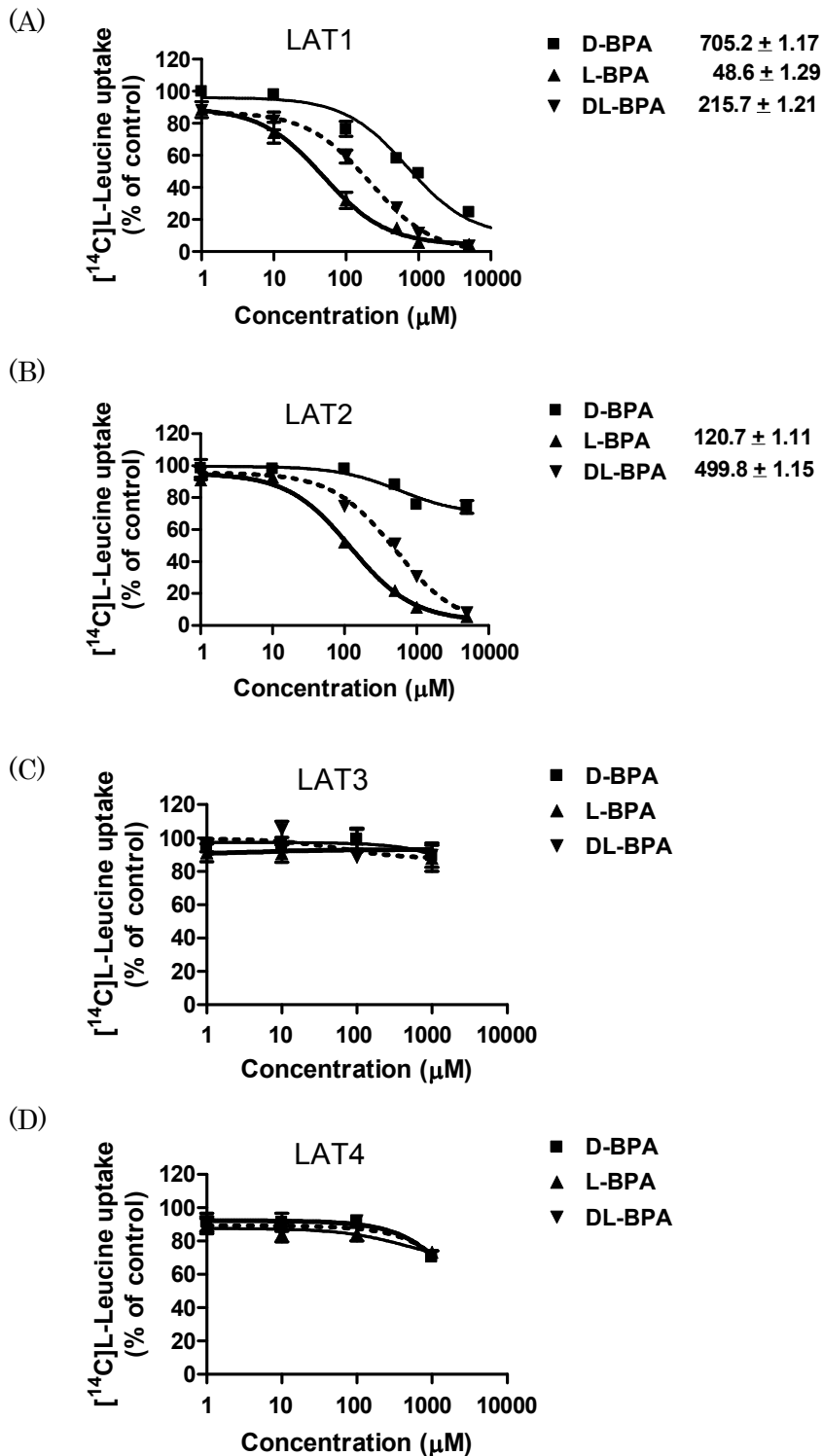


図1. L型アミノ酸トランスポーターに対するBPAの抑制効果

(b) LATを介して細胞内に蓄積する新規ホウ素化合物創製

安西らは既に腫瘍型のL型アミノ酸トランスポーターLAT1と正常型のL型アミノ酸トランスポーターLAT2の安定発現細胞を樹立し、その中性

アミノ酸ロイシン輸送に対する阻害効果のプロファイルから LAT1 特異的阻害薬の基幹構造情報を取得し、現在臨床試験が行われている化合物 JPH203 創製の基礎とした経験を持つ (*Morimoto, Anzai et al. J Pharmacol Sci* 108(4):505-16, 2008)。そこで本プロジェクトでは BNCT 治療に必要な増感薬の開発を目指し、LAT を介して細胞内に蓄積する新規ホウ素化合物の基幹構造の取得を試みた。

細胞内への化合物の蓄積を検討するために、以前に樹立した LAT1 および LAT2 安定発現細胞に加え、もう一つの輸送実験系であるアフリカツメガエル卵母細胞系を導入し、トランスポーターの交換輸送特性により細胞内からのロイシンの流出が化合物の蓄積の指標となることに着目して、実験を行った。

ジェイファーマ株式会社を通じて海外の共同研究先である米国 Colorado 大学に化合物合成を依頼し、まずは trial としてホウ素化されていない状態のアミノ酸類似構造を持つ 13 種類の化合物 (set 1) を得た。

初めに LAT1 および LAT2 安定発現細胞を用いた阻害実験を行った。

Inhibition test on S2-stably expressed LAT1 (S2-LAT1)
or LAT2 (S2-LAT2)

Compound	Molecular Weight	IC50 (μM)	
		S2-LAT1	S2-LAT2
S1	469.01	33.14	>100
S2	183.18	11.83	29.81
S3	199.18	18.65	49.44
S4	183.18	14.73	46.27
S5	215.63	16.17	38.11
S6	338.98	45.2	>100
S7	307.09	9.97	23.29
S8	216.66	17.11	48.27
S9	183.18	13.58	33.79
S10	244.09	11.04	30.36
S11	195.22	14.85	50.13
S12	179.22	26.6	>>>100
S13	291.09	14.54	32.07

上記の表に示すように、程度の差はあれ多くの set 1 化合物が LAT1 選択性を示した。そこで続いてアフリカツメガエル卵母細胞発現系を用いたロイシン排出実験を行った (図 2)。

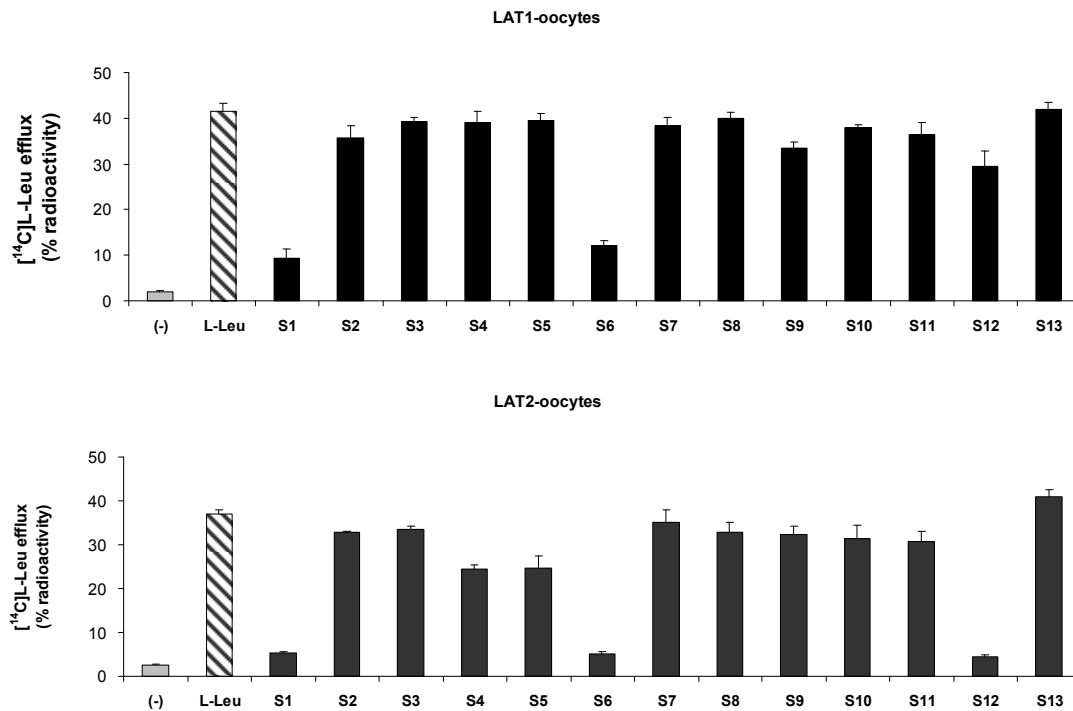


図 2. Set 1 化合物に対する LAT1 および LAT2 を介したロイシン排出

この中で、S1, S6, S12 が LAT2 に比し、LAT1 においてロイシン排出の増加 (すなわち化合物の細胞内蓄積) を認めた。そこでこれらの 3 化合物について濃度依存性変化を確認した (図 3)。その結果 S12 が LAT1>LAT2 の顕著な変化を示したので、これを最初の基幹構造とした。

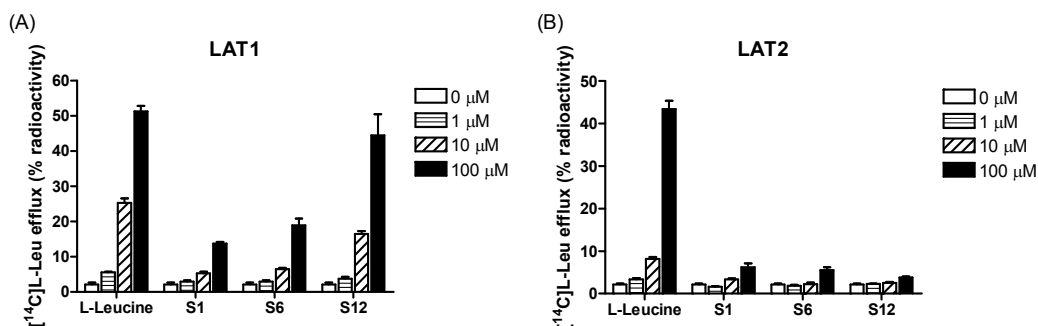


図 3. Set 1 化合物 S1, S6, S12 の濃度依存性変化

S12 の構造を元に 8 化合物 (set 2) を合成し, LAT1 および LAT2 への阻害効果 (図 4) と LAT1 および LAT2 を介するロイシン排出 (蓄積効果) (図 5) の解析を行った。

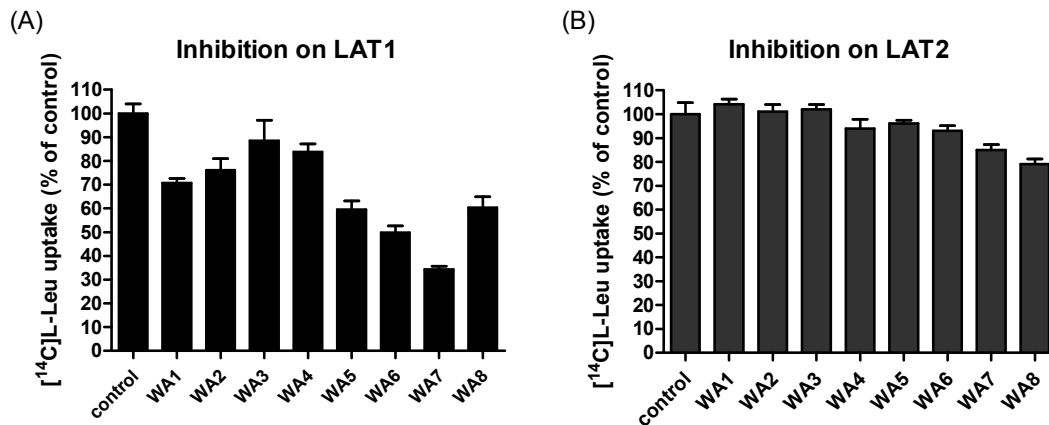


図 4. Set 2 化合物に対する LAT1 および LAT2 の輸送阻害

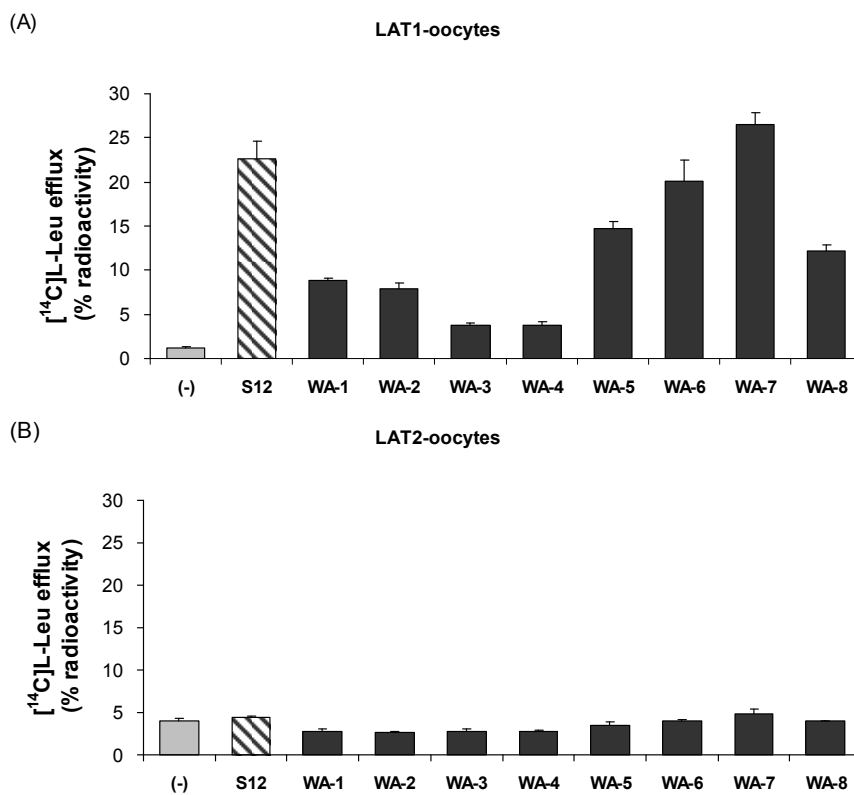


図 5. Set 2 化合物に対する LAT1 および LAT2 を介したロイシン排出

Set 2 化合物の中では WA-7 において顕著な LAT1 選択的阻害効果とロイシン排出を認め、これを第二の基幹構造とした。そこで S12 と WA-7 を基幹構造としてホウ素を導入した 10 化合物 (set 3) の合成を行い、LAT1 および LAT2 への阻害効果 (図 6) の解析を行った。

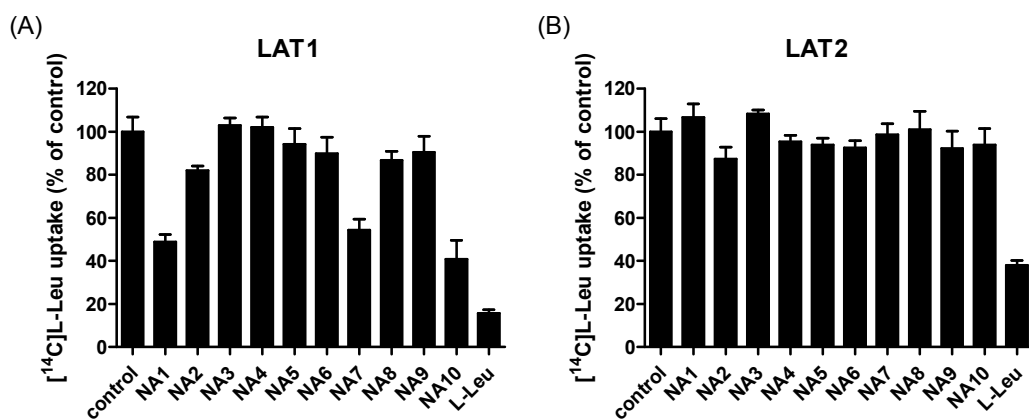
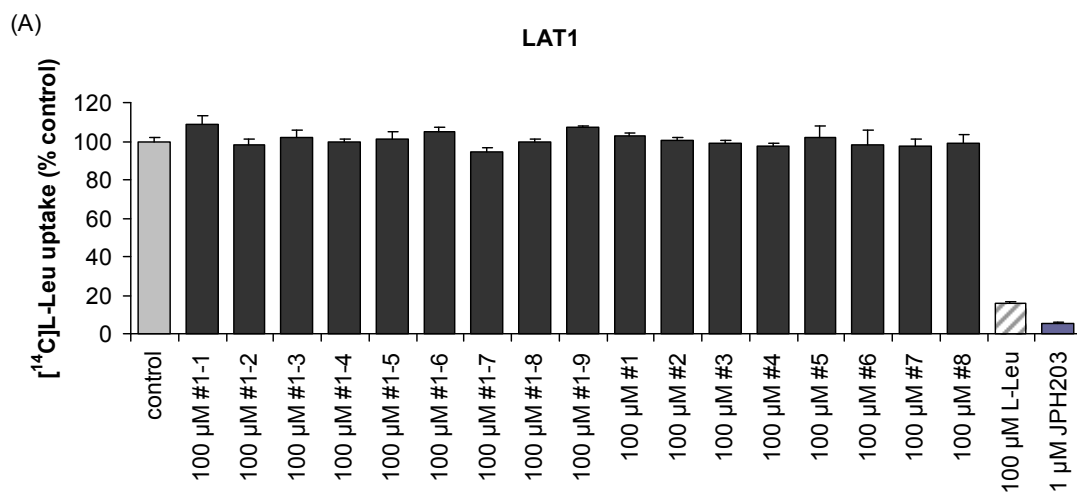


図 6. Set 3 化合物に対する LAT1 および LAT2 の輸送阻害

この中では NA1, NA7, NA10 が LAT1>LAT2 のプロファイルを示したが、これらは上述の S12 と WA-7 を超える阻害効果を示さなかった。すなわち、化合物へのホウ素原子の導入がかえって LAT1 による認識の親和性が低下したことを意味する。理由としてはホウ素導入が化合物の物性を変化させた可能性、さらには化合物を溶かしている溶媒の影響などが考えられたため、その可能性をにらみつつ、化合物の合成を 3 度行い (set 4, 5, and 6)、LAT1 および LAT2 への阻害効果 (図 7、8) の解析を行った。



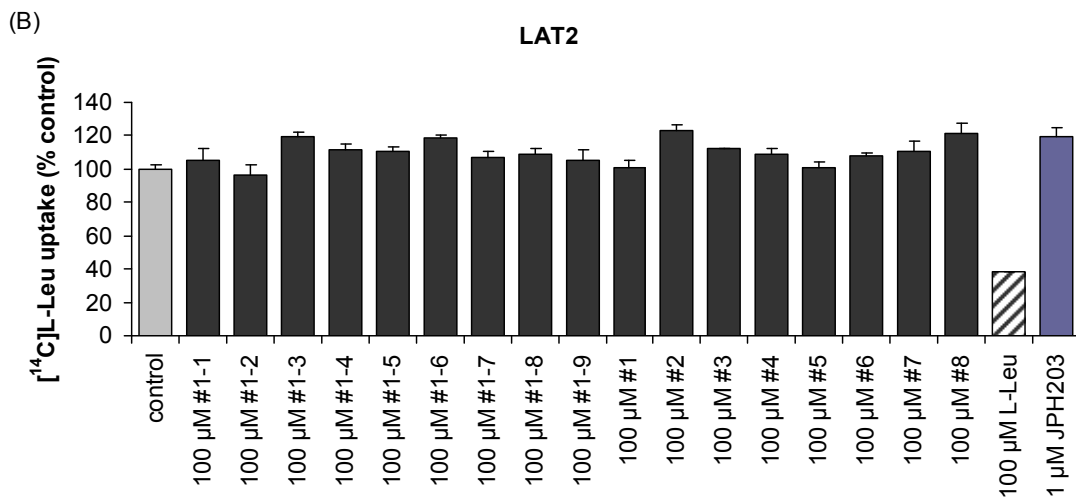


図 7. Set 4 & 5 化合物に対する LAT1 および LAT2 の輸送阻害

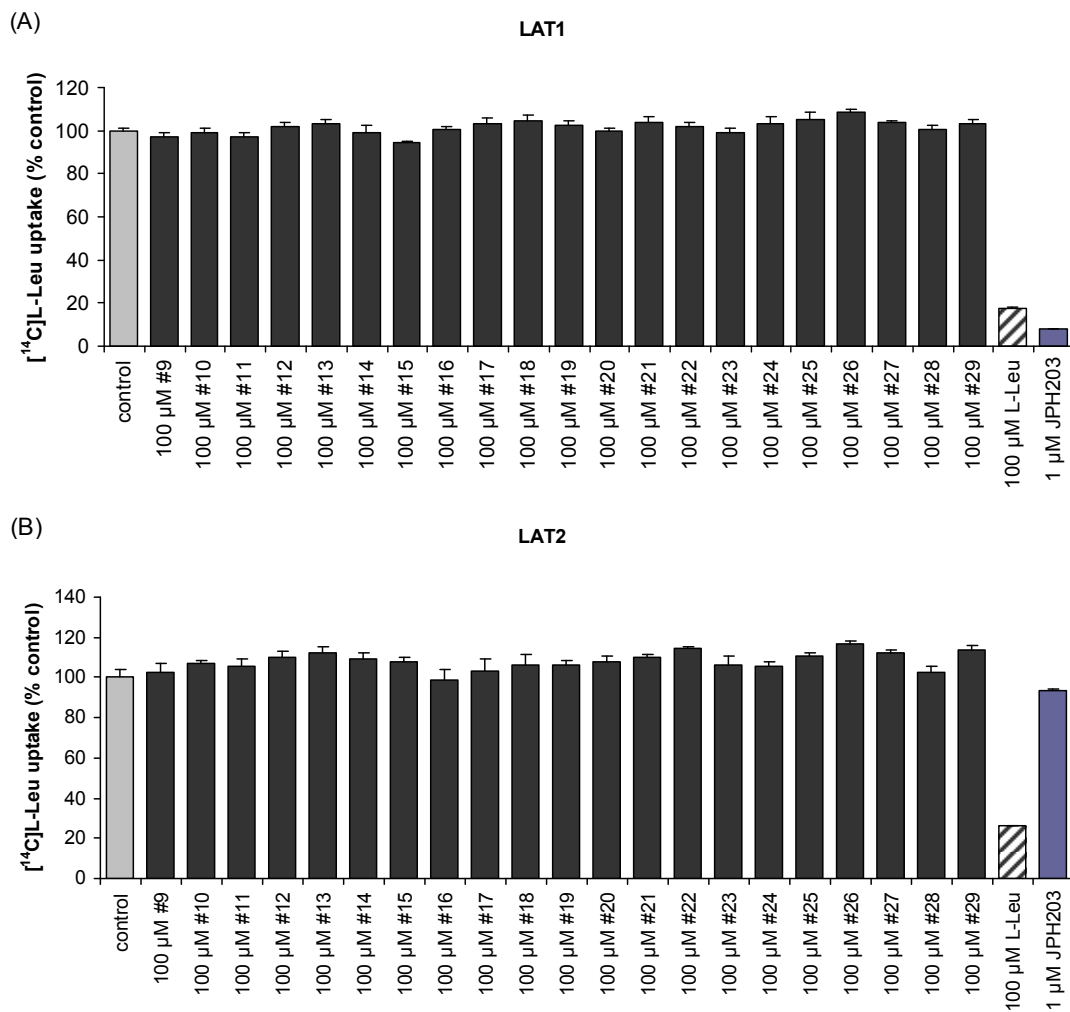


図 8. Set 4 & 5 化合物に対する LAT1 および LAT2 の輸送阻害

図7、8に示すように set 4, 5, 6 の計38化合物に関してその効果を検討したが、これらの中にはLAT1 特異的な阻害を示す化合物を見出すことはできなかった。

<優れた成果が上がった点>

今回検討した69化合物の中で、S12 と WA-7 という LAT1 選択性の高い細胞内蓄積性を示す化合物の構造情報を得られた。これは本プロジェクトの目的を超え、他の標識体、特に新しいがん診断のための PET プローブ創製や、 α 線照射性の細胞内治療薬作成の際に利用が可能となるこれまで世界中でも未だ報告のなされていない貴重な情報であると言える。

<課題となった点>

図6で示したように、ホウ素化されていない段階では高い細胞蓄積性、高いLAT1 特異的阻害効果を示す化合物 (S12 と WA-7) が、ホウ素化によりその有用性を失うことを初めて確認した。科学的には意義のあるものではあるが、本プロジェクトの達成という意味ではそれが障害となり、3年間での新規ホウ素化合物同定という点では達成に至らなかった。

<自己評価の実施結果と対応状況>

年3回(3月、7月、12月)定期的に開催した基礎臨床連携打合せ会の3月の会合(2016年、2017年)、および本プロジェクトのコアとなる教室(薬理学、第一外科、呼吸器外科、泌尿器科)で年4回(1月、4月、7月、10月)定期的に開催したコア打合せ会の1月の会合(2016年、2017年)で、各教室単位での研究の進捗状況の調査を行うとともに、論文公表数、学会発表数、研究費使用状況などの点から評価を行い、貢献度の低い教室への研究費の再配分を行うことで対応した。

<外部(第三者)評価の実施結果と対応状況> 実施せず。

<研究期間終了後の展望>

LATファミリーによるBPA輸送とLATを介して細胞内に蓄積する新規ホウ素化合物創製の両課題は引き続き継続して実施する。ホウ素化によりその有用性を失うという障害に対し、平成28年度から始めた取り組み

である2点：1、化合物の異なる部位にホウ素化を行うことでの LAT1 特異的阻害効果が回復するか、2、化合物を溶解する溶媒の違いが LAT1 特異的阻害効果に影響するかは、本研究の成功の鍵であるため、精力的に検討を行う。

＜研究成果の副次的効果＞

特になし。

②各種がん細胞における治療標的としての腫瘍特異的L型アミノ酸トランスポーターの検証

本研究プロジェクトは、当初の研究代表者である当時本学薬理学講座主任教授の安西らの研究グループがこれまで行ってきた、がん細胞特異的に発現するアミノ酸トランスポーターLAT1が、多くのがんで高発現を示し、その盛んな増殖能を支えているという戦略に基づき、本検討を行った。

呼吸器外科と薬理学の共同研究をベースにして、林らは世界で初めてヒト胸腺癌検体におけるL型中性アミノ酸トランスポーターLAT1の高発現を見出すとともに、Ty82ヒト胸腺癌由来細胞において代表的な中性アミノ酸であるロイシンの腫瘍細胞への高い取り込みと、LAT1選択的阻害薬JPH203の細胞増殖抑制効果を初めて明らかにし、これまでその治療法の確定していなかった胸腺癌でのLAT1の貢献を示唆するとともに、治療標的としての重要性を明らかにした（雑誌論文36）。

また以前からの薬理学の共同研究先であるタイ国 Khon Kaen 大学で樹立されたヒト胆管癌由来培養細胞を用いた *in vitro* および *in vivo* の検討を行ったところ、文部科学省国費外国人留学生として薬理学に在籍した Yothaisong らはヒト胆管癌検体におけるL型中性アミノ酸トランスポーターLAT1の高発現を見出すとともに、ヒト胆管癌由来細胞 KKU-055, KKU-213 および MMNK1 を用いた解析により、ロイシンの腫瘍細胞への高い取り込みと、LAT1 選択的阻害薬 JPH203 の *in vitro* および *in vivo* での細胞増殖抑制効果を初めて明らかにし、これまでその治療法の確定していなかった胆管癌でのLAT1の貢献を示唆するとともに、治療標的としての重要性を明らかにした（雑誌論文11, 39）。

婦人科と薬理学の共同研究をベースにして、森田らはヒト卵巣癌由来細胞 JAR および JEG3 においてL型中性アミノ酸トランスポーターLAT1

の高発現を見出すとともに、ロイシンの腫瘍細胞への高い取り込みと、LAT1 選択的阻害薬 JPH203 による抑制効果を初めて明らかにし、ヒト卵巣癌での LAT1 の貢献を示唆するとともに、治療標的としての重要性を明らかにした（論文投稿準備中）。

<優れた成果が上がった点>

世界に先駆けてこれまで治療法の無いヒト胸腺癌と治療抵抗性の悪性腫瘍であるヒト胆管癌における L 型中性アミノ酸トランスポーターLAT1 の重要性を明らかに出来た。この成果は評価の高い国際科学雑誌に公表することが出来た。これらの成果は本プロジェクトが開発を目指すホウ素化合物を用いた BNCT 治療の科学的根拠を与えることに貢献した。

<課題となった点>

特になし。

<自己評価の実施結果と対応状況>

年 3 回（3 月、7 月、12 月）定期的で開催した基礎臨床連携打合せ会の 3 月の会合（2016 年、2017 年）、および本プロジェクトのコアとなる教室（薬理学、第一外科、呼吸器外科、泌尿器科）で年 4 回（1 月、4 月、7 月、10 月）定期的で開催したコア打合せ会の 1 月の会合（2016 年、2017 年）で、各教室単位での研究の進捗状況の調査を行うとともに、論文公表数、学会発表数、研究費使用状況などの点から評価を行い、貢献度の低い教室への研究費の再配分を行うことで対応した。

<外部（第三者）評価の実施結果と対応状況>

実施せず。

<研究期間終了後の展望>

本プロジェクト期間中に成果の得られたヒト胸腺癌、胆管癌、卵巣癌に関しては、今後現行の BNCT 増感剤である BPA の腫瘍細胞への蓄積を引き続き解析するとともに現在進行中の新規ホウ素化合物の合成がなされた際には、BPA 同様に解析を進めていく。

また期間中には検討に至らなかったヒト食道癌、胃癌、大腸癌、腎癌、膀胱癌、等についても継続して解析を進めて行く。

<研究成果の副次的効果>
特になし。

研究発表の状況

<雑誌論文>

1. Kojima S, Tohei A, Kojima K, Anzai N. Evidence for tachykinin NK3 receptors-triggered peptide YY release from isolated guinea-pig distal colon. *Eur J Pharmacol.* 740:121-6, 2014.
2. Hayashi K, Anzai N. Role of LAT1 in the promotion of amino acid incorporation in activated T cells. *Crit Rev Immunol.* 34(6):467-79, 2014.
3. Satomura H, Sasaki K, Nakajima M, Yamaguchi S, Onodera S, Otsuka K, Takahashi M, Muroi H, Shida Y, Ogata H, Okamoto K, Kato H. Can expression of CXCL12 and CXCR4 be used to predict survival of gastric cancer patients? *Anticancer Res.* 34(8):4051-7, 2014.
4. Sohda M, Miyazaki T, Honjyo H, Hara K, Ozawa D, Suzuki S, Tanaka N, Sano A, Sakai M, Yokobori T, Nakajima M, Fukuchi M, Kato H, Higuchi T, Tsushima Y, Kuwano H. L-[3-¹⁸F]- α -methyltyrosine uptake by lymph node metastasis is a predictor of complete response to CRT in esophageal cancer. *Anticancer Res.* 34(12):7473-7, 2014.
5. Kojima S, Tohei A, Ikeda M, Anzai N. An Endogenous Tachykinergic NK2/NK3 Receptor Cascade System Controlling the Release of Serotonin from Colonic Mucosa. *Curr Neuropharmacol.* 13(6):830-5, 2015.
6. Lee EY, Kaneko S, Jutabha P, Zhang X, Seino S, Jomori T, Anzai N, Miki T. Distinct action of the α -glucosidase inhibitor miglitol on SGLT3, enteroendocrine cells, and GLP1 secretion. *J Endocrinol.* 224(3):205-14, 2015.
7. Ouchi M, Oba K, Saigusa T, Watanabe K, Ohara M, Matsumura N, Suzuki T, Anzai N, Tsuruoka S, Yasutake M. Association between pulse wave

velocity and a marker of renal tubular damage (N-acetyl- β -D-glucosaminidase) in patients without diabetes. *J Clin Hypertens (Greenwich)*. 17(4):290-7, 2015.

8. Takayanagi K, Shimizu T, Tayama Y, Ikari A, Anzai N, Iwashita T, Asakura J, Hayashi K, Mitarai T, Hasegawa H. Downregulation of transient receptor potential M6 channels as a cause of hypermagnesiuric hypomagnesemia in obese type 2 diabetic rats. *Am J Physiol Renal Physiol*. 308(12):F1386-97, 2015.

9. Bulacio RP, Anzai N, Ouchi M, Torres AM. Organic Anion Transporter 5 (Oat5) Urinary Excretion Is a Specific Biomarker of Kidney Injury: Evaluation of Urinary Excretion of Exosomal Oat5 after N-Acetylcysteine Prevention of Cisplatin Induced Nephrotoxicity. *Chem Res Toxicol*. 28(8):1595-602, 2015.

10. Jaiyen C, Jutabha P, Anzai N, Lungkaphin A, Soodvilai S, Srimaroeng C. Interaction of green tea catechins with renal organic cation transporter 2. *Xenobiotica*. 46:641-650, 2015.

*11. Yothaisong S, Namwat N, Yongvanit P, Khuntikeo N, Puapairoj A, Jutabha P, Anzai N, Tassaneeyakul W, Tangsucharit P, Loilome W. Increase in L-type amino acid transporter 1 expression during cholangiocarcinogenesis caused by liver fluke infection and its prognostic significance. *Parasitol Int*. pii: S1383-5769(15)00195-6, 2015.

12. Muroi H, Nakajima M, Satomura H, Takahashi M, Domeki Y, Murakami M, Nakamura T, Takada A, Kato H. Effectiveness of proton beam therapy on liver metastases of esophageal cancer: report of a case. *Int Surg*. 100(1):180-4, 2015.

13. Muroi H, Nakajima M, Satomura H, Takahashi M, Yamaguchi S, Sasaki K, Yokobori T, Miyazaki T, Kuwano H, Kato H. Low PHLDA3 expression

in oesophageal squamous cell carcinomas is associated with poor prognosis. *Anticancer Res.* 2015 Feb;35(2):949-54.

14. Miyazaki T, Sohda M, Tanaka N, Suzuki S, Ieta K, Sakai M, Sano A, Yokobori T, Inose T, Nakajima M, Fukuchi M, Ojima H, Kato H, Kuwano H. Phase I/II study of docetaxel, cisplatin, and 5-fluorouracil combination chemoradiotherapy in patients with advanced esophageal cancer. *Cancer Chemother Pharmacol.* 2015 Mar;75(3):449-55.

15. Toyoda S, Inami S, Masawa T, Shibasaki I, Yamada Y, Fukuda H, Kubo T, Nakajima M, Kato H, Inoue T. Hypopharyngeal perforation caused by intraoperative transesophageal echocardiography. *J Med Ultrason* (2001). 42(2):247-50, 2015.

16. Sasaki K, Miyachi K, Yoda N, Onodera S, Satomura H, Otsuka K, Nakajima M, Yamaguchi S, Sunagawa M, Kato H. Long-term comparison of boomerang-shaped jejunal interposition and Billroth-I reconstruction after distal gastrectomy. *World J Surg.* 39(5):1127-33, 2015.

17. Okamoto K, Tani Y, Yamaguchi T, Ogino K, Tsuchioka T, Nakajima M, Yamaguchi S, Sasaki K, Kato H, Ohya T. Asymptomatic Mesenchymal Hamartoma of the Chest Wall in Child With Fluorodeoxyglucose Uptake on PET/CT-Report of a Case. *Int Surg.* 100(5):915-9, 2015.

18. Satomura H, Nakajima M, Sasaki K, Yamaguchi S, Domeki Y, Takahashi M, Muroi H, Kubo T, Kikuchi M, Otomo H, Ihara K, Kato H. Phase I Dose-Escalation Study of Docetaxel, Cisplatin, and 5-Fluorouracil Combination Chemotherapy in Patients With Advanced Esophageal Carcinoma. *Int Surg.* 100(6):1153-8, 2015.

19. Nakajima M, Kato H, Sakai M, Sano A, Miyazaki T, Sohda M, Inose T, Tanaka N, Suzuki S, Masuda N, Fukuchi M, Kuwano H. Planned Esophagectomy after Neoadjuvant Hyperthermo-Chemoradiotherapy

using Weekly Low-Dose Docetaxel and Hyperthermia for Advanced Esophageal Carcinomas. *Hepatogastroenterology*. 62(140):887–91, 2015.

20. Miyazaki T, Ojima H, Fukuchi M, Sakai M, Sohda M, Tanaka N, Suzuki S, Ieta K, Saito K, Sano A, Yokobori T, Inose T, Nakajima M, Kato H, Kuwano H. Phase II Study of Docetaxel, Nedaplatin, and 5-Fluorouracil Combined Chemotherapy for Advanced Esophageal Cancer. *Ann Surg Oncol*. 22(11):3653–8, 2015.

21. Miyazaki T, Honjyo H, Sohda M, Sakai M, Hara K, Tanaka N, Yokobori T, Nakajima M, Kato H, Kuwano H. Successful Tumor Navigation Technique During Intrathoracoscopic Esophagectomy: Laparoscopic Ultrasonography Using Endoscopically Placed Marking Clips. *J Am Coll Surg*. 2015 Dec;221(6):e125–8.

22. Ljubojević M, Breljak D, Herak-Kramberger CM, Anzai N, Sabolić I. Expression of basolateral organic anion and cation transporters in experimental cadmium nephrotoxicity in rat kidney. *Arch Toxicol*. 90(3):525–41, 2016.

23. Mishima M, Hamada T, Maharani N, Ikeda N, Onohara T, Notsu T, Ninomiya H, Miyazaki S, Mizuta E, Sugihara S, Kato M, Ogino K, Kuwabara M, Hirota Y, Yoshida A, Otani N, Anzai N, Hisatome I. Effects of Uric Acid on the NO Production of HUVECs and its Restoration by Urate Lowering Agents. *Drug Res (Stuttg)*. 66(5):270–4, 2016.

24. Hayashi K, Ouchi M, Endou H, Anzai N. HOXB9 acts as a negative regulator of activated human T cells in response to amino acid deficiency. *Immunol Cell Biol*. 94(6):612–7, 2016.

25. Breljak D, Ljubojević M, Hagos Y, Micek V, Balen Eror D, Vrhovac Madunić I, Brzica H, Karaica D, Radović N, Kraus O, Anzai N, Koepsell H, Burckhardt G, Burckhardt BC, Sabolić I. Distribution of organic

anion transporters NaDC3 and OAT1-3 along the human nephron. *Am J Physiol Renal Physiol.* 311(1):F227-38, 2016.

26. Sakoh T, Nakayama M, Tsuchihashi T, Yoshitomi R, Tanaka S, Katafuchi E, Fukui A, Shikuwa Y, Anzai N, Kitazono T, Tsuruya K. Associations of fibroblast growth factor 23 with urate metabolism in patients with chronic kidney disease. *Metabolism.* 65(10):1498-507, 2016.

27. Kokura K, Kuromi Y, Endo T, Anzai N, Kazuki Y, Oshimura M, Ohbayashi T. A kidney injury molecule-1 (Kim-1) gene reporter in a mouse artificial chromosome: the responsiveness to cisplatin toxicity in immortalized mouse kidney S3 cells. *J Gene Med.* 18(10):273-281, 2016.

28. Hayashi K, Jutabha P, Maeda S, Supak Y, Ouchi M, Endou H, Fujita T, Chida M, Anzai N. LAT1 acts as a crucial transporter of amino acids in human thymic carcinoma cells. *J Pharmacol Sci.* 132(3):201-204, 2016.

29. Tsuchiya G, Hori T, Onizawa N, Otani N, Tanaka-Nakadate S, Iseki T, Ouchi M, Hayashi K, Jutabha P, Oba T, Fukuda H, Anzai N. Molecular mechanism of the urate-lowering effects of calcium channel blockers. *Dokkyo J Med Sci* 43(1): 23-29, 2016

30. Hanada K, Nakata T, Ouchi M, Ohtsubo M, Isono M, Morita A, Okamoto K, Otani N, Kobayashi Y, Anzai N. Identification of carnitine transporter CT1 binding protein Lin-7 in nervous system. *Dokkyo J Med Sci* 43(1): 31-38, 2016

31. Tani Y, Nakajima M, Kikuchi M, Ihara K, Muroi H, Takahashi M, Domeki Y, Okamoto K, Yamaguchi S, Sasaki K, Tsuchioka T, Sakamoto S, Kato H. ¹⁸F-Fluorodeoxyglucose Positron Emission Tomography for Evaluating the Response to Neoadjuvant Chemotherapy in Advanced

Esophageal Cancer. *Anticancer Res.* 36(1):367-73, 2016.

32. Ihara K, Yamaguchi S, Ueno N, Tani Y, Shida Y, Ogata H, Domeki Y, Okamoto K, Nakajima M, Sasaki K, Tsuchioka T, Mitomi H, Kato H. Expression of DNA double-strand break repair proteins predicts the response and prognosis of colorectal cancer patients undergoing oxaliplatin-based chemotherapy. *Oncol Rep.* 35(3):1349-55, 2016.

33. Kikuchi M, Nakajima M, Muroi H, Takahashi M, Itoh J, Yamaguchi S, Sasaki K, Kato H. Significance of Expression of Complement C4d in Esophageal Squamous Cell Carcinoma. *Anticancer Res.* 36(9):4553-7, 2016.

34. Nakajima M, Takahashi M, Domeki Y, Satomura H, Muroi H, Kikuchi M, Ogata H, Yamaguchi S, Sasaki K, Sakai M, Sohda M, Miyazaki T, Kuwano H, Kato H. Effective Mediastinal Lymphadenectomy for Esophageal Cancer Using Slender Tracheal Forceps in Prone Position Thoracoscopic Esophagectomy. *In Vivo.* 30(6):893-898, 2016.

35. Miyazaki T, Sakai M, Sohda M, Tanaka N, Yokobori T, Motegi Y, Nakajima M, Fukuchi M, Kato H, Kuwano H. Prognostic Significance of Inflammatory and Nutritional Parameters in Patients with Esophageal Cancer. *Anticancer Res.* 36(12):6557-6562, 2016.

*36. Hayashi K, Anzai N. Novel therapeutic approaches targeting L-type amino acid transporters for cancer treatment. *World J Gastrointest Oncol.* 9(1):21-29, 2017.

37. Furihata T, Morio H, Zhu M, Suzuki Y, Ide H, Tsubota A, Fu Z, Anzai N, Chiba K. Human organic anion transporter 2 is an entecavir, but not tenofovir, transporter. *Drug Metab Pharmacokinet.* 32(1):116-119, 2017.

38. Shimizu Y, Satou M, Hayashi K, Nakamura Y, Fujimaki M, Horibata

Y, Ando H, Watanabe T, Shiobara T, Chibana K, Takemasa A, Sugimoto H, Anzai N, Ishii Y. Matrix-assisted laser desorption/ionization imaging mass spectrometry reveals changes of phospholipid distribution in induced pluripotent stem cell colony differentiation. *Anal Bioanal Chem.* 409(4):1007–1016, 2017.

*39. Yothaisong S, Dokduang H, Anzai N, Hayashi K, Namwat N, Yongvanit P, Sangkhamanon S, Jutabha P, Endou H, Loilome W. Inhibition of l-type amino acid transporter 1 activity as a new therapeutic target for cholangiocarcinoma treatment. *Tumour Biol.* 39(3):1010428317694545, 2017.

40. Otani N, Ouchi M, Hayashi K, Jutabha P, Anzai N. Roles of organic anion transporters (OATs) in renal proximal tubules and their localization. *Anat Sci Int.* 92(2):200–206, 2017.

41. Kiuchi K, Morita A, Ouchi M, Otani N, Jutabha P, Nohara M, Fukasawa I, Fujita T, Anzai N. Characterization of urate transport system in JAR and JEG-3 cells, human trophoblast-derived cell lines. *Dokkyo J Med Sci* 44(1): 31–38, 2017

42. 大内基司, 大谷直由, 安西尚彦. 【遺伝性腎疾患】 尿酸代謝異常. *日本腎臓学会誌* 57(4): 766–773, 2015.

43. 鬼澤信之, 安西尚彦. さまざまな病態における栄養のポイント 高尿酸血症・痛風治療 栄養療法と薬物療法. *Medicina* 51(13): 2320–2323, 2014.

44. 大谷直由, 大内基司, 安西尚彦. 高血圧と高尿酸血症. *循環器内科* 76(4): 403–409, 2014.

45. 堀 貴行, 安西尚彦. 尿酸トランスポーターの役割を教えてください. *尿酸と血糖* 1(2): 88–89, 2015.

46. 安西尚彦, 大内基司. 腎尿細管トランスポーター 尿酸およびグルコース再吸収 revisit. 腎と透析 79(1): 141-145, 2015.
47. 大内基司, 児嶋修一, 安西尚彦. 摘出モルモット大腸標本からのタキキニンNK3受容体作動性peptide YY放出. 消化と吸収 37(3): 231-233, 2015.
48. 安西尚彦, 岡本和久, 花田健治, 阿部篤朗, 大谷直由, 大内基司. ビタミン・バイオフィクタートランスポーター研究の最前線 プロスタグランジンと有機アニオンのトランスポーター. ビタミン 89(9): 441-445, 2015.
49. 安西尚彦, 大内基司. SGLT2 阻害薬を使用すると血清尿酸値が低下するのはなぜですか?. 尿酸と血糖 1(3): 150-151, 2015.
50. 岡本和久, 大内基司, 森田亜州華, 花田健治, 阿部篤朗, 大谷直由, 林啓太郎, Jutabha Promsuk, 安西尚彦. ヒト腎臓尿酸トランスポーター URAT1 と水溶性ヨード系造影剤 iodipamide の相互作用. Dokkyo J Med Sci. 43(1): 73-78, 2016.
51. 安西尚彦, 大内基司, 森田亜州華. 尿酸トランスポーターと糖代謝. 尿酸と血糖 2(1): 6-9, 2016.
52. 大野雄太, 大塚裕介, 野原正勝, 安西尚彦. Hartnup 病. 腎臓内科・泌尿器科 4(5): 459-464, 2016
53. 安西尚彦, 大塚裕介, 大野雄太, 野原正勝. 尿酸関連トランスポーターとその異常. 内分泌・糖尿病・代謝内科 43(1): 8-12, 2016.
54. 大塚裕介, 森田亜州華, 安西尚彦. 代謝 Hartnup 病. 小児科診療 79(Suppl.): 274, 2016.
55. 安西尚彦, 若新英史. GLUT9 その電位差駆動性尿酸輸送特性 (URATv1) とグルコースとの関連性. 尿酸と血糖 3(1): 15-17, 2017.

56. 大内基司, 大谷直由, Jutabha Promsuk, 安西尚彦. リン酸・有機酸トランスポーターNPT 群の概要と尿酸輸送メカニズム. 尿酸と血糖 3(1):27-30, 2017

<図書>

1. 大内基司, 大谷直由, 安西尚彦. 内分泌 基礎分野での進歩 腎尿細管尿酸輸送の分子機序. Annual Review 糖尿病・代謝・内分泌 2015, 160-164, 2015.
2. 安西尚彦, 大谷直由, 降幡知巳. プリン・尿酸代謝の基礎 尿酸排泄機構. 日本臨床 74(Suppl. 9) 高尿酸血症・低尿酸血症, 51-55, 2016.
3. 安西尚彦, 大内基司, 森田亜州華. SGLT2 阻害薬による尿酸排泄機序. 日本臨床 74(Suppl. 9) 高尿酸血症・低尿酸血症, 431-434, 2016.

<学会発表>

1. 林啓太郎, Jutabha Promsuk, 遠藤 仁, 安西尚彦. 中性アミノ酸トランスポーターLAT1 阻害薬の胸腺がんに対する増殖抑制効果. 第 73 回日本癌学会総会 2014. 09
2. 土屋 豪, 鬼澤信之, 堀 貴行, Promsuk Jutabha, 大谷直由, 長谷川元, 福田宏嗣, 安西尚彦. Ca 拮抗薬による尿酸降下作用の解析. 第 37 回日本高血圧学会総会 2014. 10
3. 大内基司, 児嶋修一, 安西尚彦. 摘出モルモット大腸標本からのタキキニン NK3 受容体作動性 peptide YY 放出. 日本消化吸収学会総会 2014. 10
4. 安西尚彦, 大内基司, 大谷直由, Promsuk Jutabha. 尿酸トランスポーター研究 最近の展開. 第 48 回日本痛風・核酸代謝学会総会 2015. 02
5. 土屋 豪, 堀 貴行, 鬼澤信之, 大谷直由, 大内基司, Promsuk Jutabha, 福田宏嗣, 安西尚彦. カルシウム拮抗薬による尿酸降下作用

の解析. 第 48 回日本痛風・核酸代謝学会総会 2015.02

6. 鬼澤信之, 井関 賛, 大谷直由, 大内基司, 長谷川元, 安西尚彦. zotepine、chlorprothixene による尿酸降下作用の解析. 第 48 回日本痛風・核酸代謝学会総会 2015.02

7. 大谷直由, 大内基司, 相馬良一, 井上晃男, 安西尚彦. ヒト臍帯静脈内皮細胞を用いた低酸素血管内皮障害に対する尿酸の影響. 第 48 回日本痛風・核酸代謝学会総会 2015.02

8. 佐藤元康, 沢登祥史, 安西尚彦, 杉本博之. 分子イメージングをもちいた新規消化管ペプチドの探索. 第 回獨協医学会 2015.07

9. 井関 賛, 鬼澤信之, 中舘佐和子, 林啓太郎, 安西尚彦, 堀 貴行. Zotepine 及び Chlorprothixene が持ちうる血中尿酸濃度低下作用及びその機作に関する考察. D 第 回獨協医学会 2015.07

10. 鬼澤信之, 大谷直由, 大内基司, 長谷川元, 安西尚彦. Na⁺依存性モノカルボン酸トランスポーターSMCT2 の結合タンパク質の解明. 第 38 回日本高血圧学会総会 2015.10

11. Jutabha Promsuk, 大谷直由, 大内基司, 井上晃男, 安西尚彦. Functional Analysis of Monocarboxylate Transporter 9(MCT9) as a Urate Transporter. 第 38 回日本高血圧学会総会 2015.10

12. Naohiko Anzai. 「Renal tubular urate transporters as targets for new drug development」(シンポジウム) The 13th Asia Pacific Federation of Pharmacologists Meeting (APFP) 2016/2/1~3 バンコク (タイ)

13. 堀 貴行, 大谷直由, 大野雄太, 大内基司, 福田宏嗣, 安西尚彦. 「腎尿酸排泄低下型動物モデルの創製とカルシウム拮抗薬の尿酸効果作用の検討」第 89 回日本薬理学会年会 2016/3/9~11 パシフィコ横浜 (横浜市)

14. Promsuk Jutabha、林啓太朗、安西尚彦. 「ヒト膵臓癌由来細胞における Na^+ 非依存性中性アミノ酸トランスポーターによる boronophenylalanine 取込み」第 89 回日本薬理学会年会 2016/3/9~11 パシフィコ横浜 (横浜市)
15. 林啓太朗、Promsuk Jutabha、遠藤 仁、安西尚彦. 「アミノ酸トランスポーターLAT1 阻害薬による破骨細胞分化の抑制」第 89 回日本薬理学会年会 2016/3/9~11 パシフィコ横浜 (横浜市)
16. 大谷直由、堀 貴行、大野雄太、大内基司、安西尚彦. 「新規高尿酸血症動物とカルシウム拮抗薬の尿酸低下作用の分子機序の解明」第 93 回日本生理学大会 2016/3/22~24 札幌コンベンションセンター (札幌市)
17. Jutabha Promsuk、大谷直由、大内基司、井上晃男、安西尚彦. 「モノカルボン酸トランスポーター9は腎臓の新規尿酸トランスポーターである」第 93 回日本生理学大会 2016/3/22~24 札幌コンベンションセンター (札幌市)
18. 安西尚彦 「マウスモノカルボン酸トランスポーター9 (mMct9) は尿酸トランスポーターである」第 89 回日本内分泌学会学術総会 2016/4/21~23 国立京都国際会館 (京都市)
19. 森田亜州華、野原正勝、林啓太朗、安西尚彦. 「ホウ素中性子捕捉療法 BNCT 増感物質 boronophenylalanine (BPA) の L 型アミノ酸トランスポーターによる輸送特性」第 20 回がん分子標的治療学会学術集会 2016/5/30~6/1 別府国際コンベンションセンター (別府市)
20. 大塚裕介、大野雄太、森田亜州華、大谷直由、Jutabha Promsuk、大内基司、鶴岡秀一、安西尚彦 「アンセリンによる尿酸降下作用の分子機序解明」第 59 回日本腎臓学会学術総会 2016/6/17~19 パシフィコ横浜 (横浜市)
21. 大野雄太、堀 貴行、大塚裕介、大谷直由、大内基司、伊藤善規、

安西尚彦. 「腎尿酸排泄低下型の創製と Ca 拮抗薬およびロサルタンにより尿酸降下作用の検討」第 134 回日本薬理学会関東部会 2016/7/9 国際医療福祉大学 (栃木県大田原市)

22. 安西尚彦 「腎臓尿酸トランスポーターと高尿酸血症」(特別講演) 東京理科大学 薬理学特別セミナー 2016/8/5 東京理科大学野田キャンパス (千葉県野田市)

23. 安西尚彦 「腎臓の薬物輸送の分子機序 revisit」第 38 回日本小児体液研究会 2016/8/27 大村進・美恵子 聖路加臨床学術センター

24. Naoyuki Otani, Motoshi Ouchi, Promsuk Jutabha, Naohiko Anzai. "monocarboxylate transporter 9 is a novel urate transporter in kidney" APCN/ANZSN2016 (15th Asian Pacific Congress of Nephrology & 52th Australian and New Zealand Society of Nephrology ASM) 2016/9/17~21 Perth Convention and Exhibition Centre

25. 安西尚彦 「突発性腎性低尿酸血症と腎尿細管トランスポーター」(講演) 2016 年度稀少疾患研究会 2016/9/3 立命館大学びわこ・くさつキャンパス (草津市)

26. 安西尚彦 「尿酸トランスポーターと高尿酸血症」(講演) 河田町循環器セミナー 2016/9/26 東京女子医科大学 (東京都)

27. 安西尚彦、大内基司、大谷直由、JUTABHA Promsuk 「ヒトの血清尿酸値制御の分子機序」(教育講演) 第 39 回日本高血圧学会総会 2016/9/30~10/2 仙台国際センター

28. 大谷直由、堀 貴行、森田亜州華、野原正勝、大野雄太、大塚裕介、Promsuk Jutabha、大内基司、福田宏嗣、安西尚彦 「新規尿酸排泄低下型高尿酸血症モデルマウスの創製とカルシウム拮抗薬とアンジオテンシン II 受容体拮抗薬による尿酸効果作用の検討」第 39 回日本高血圧学会総会 2016/9/30~10/2 仙台国際センター

29. 若新英史、安西尚彦、Jeffery Kopp 「変異型 APOL1 は細胞内炎症性シグナリングを促進しポドサイト障害を増悪させる」 第9回トランスポーター研究会九州部会 2016/10/1~2 宮崎市民プラザ (宮崎市)
30. 安西尚彦、大内基司 「腎尿細管尿酸輸送と糖輸送のクロストーク」 (教育講演) 第46回日本腎臓学会東部学術大会 2016/10/7~8 京王プラザホテル (東京都)
31. 森尾花恵、降幡知巳、朱 美艶、鯉渕明良、井出秀行、澁谷実香、上市敦子、千葉 寛、安西尚彦、秋田英万 「In vitro 肝臓モデル構築を目指した新規ヒト不死化肝類洞内皮細胞の樹立およびその特性解明」 日本薬物動態学会第31回年会 2016/10/13~15 キッセイ文化ホール、松本総合体育館 (松本市)
32. 安西尚彦. 「腎尿細管トランスポーター分子標的創薬」 (講演) 第38回日本薬学会九州支部コロキウム 2016/11/12 熊本大学薬学部 (熊本市)
33. 安西尚彦. 「腎尿細管トランスポーターと抗糖尿病薬作用」 (特別講演) 第10回氷川フォーラム 2016/11/26 大宮ソニックシティ (大宮市)
34. 若新英史、安西尚彦、Jeffery Kopp 「変異型 APOL1 は細胞内炎症性シグナリングを促進し、ポドサイト障害を増悪させる」 2016年度生理研研究会 「上皮膜輸送調節蛋白の異常と病態生理学の融合」 2016/11/24~25 自然科学研究機構 生理学研究所 (岡崎市)
35. Naohiko Anzai 「Uricosuric agents and renal tubular urate transporters」 (シンポジウム) 第6回日中薬理学・臨床薬理学ジョイントミーティング 第37回日本臨床薬理学会学術総会 2016/12/1~3 米子コンベンションセンター、米子市文化ホール (米子市)



Contents lists available at ScienceDirect

Parasitology International

journal homepage: www.elsevier.com/locate/parint

Increase in L-type amino acid transporter 1 expression during cholangiocarcinogenesis caused by liver fluke infection and its prognostic significance

Supak Yothaisong^{a,f,g}, Nisana Namwat^{a,f,g}, Puangrat Yongvanit^{a,f,g}, Narong Khuntikeo^{b,f,g}, Anucha Puapairoj^{c,f}, Promsuk Jutabha^d, Naohiko Anzai^d, Wichitra Tassaneeyakul^e, Panot Tangsucharit^e, Watcharin Loilome^{a,f,g,*}

^a Department of Biochemistry, Faculty of Medicine, Khon Kaen University, Khon Kaen 40002, Thailand

^b Department of Surgery, Faculty of Medicine, Khon Kaen University, Khon Kaen 40002, Thailand

^c Department of Pathology, Faculty of Medicine, Khon Kaen University, Khon Kaen 40002, Thailand

^d Department of Pharmacology and Toxicology, Dokkyo Medical University School of Medicine, Tochigi 321-0293, Japan

^e Department of Pharmacology, Faculty of Medicine, Khon Kaen University, Khon Kaen 40002, Thailand

^f Liver Fluke and Cholangiocarcinoma Research Center, Khon Kaen University, Khon Kaen 40002, Thailand

^g Cholangiocarcinoma Screening and Care Program (CASCAP), Khon Kaen University, Khon Kaen 40002, Thailand

ARTICLE INFO

Article history:

Received 17 August 2015

Received in revised form 29 October 2015

Accepted 30 November 2015

Available online xxxxx

Keywords:

Opisthorchis viverrini

Inflammation

Oxidative stress

L-type amino acid transporter 1

Cholangiocarcinoma

PI3K/AKT signaling

ABSTRACT

L-type amino acid transporter 1 (LAT1) is highly expressed in various human cancers, including cholangiocarcinoma (CCA), the most common cancer in Northeast Thailand. Chronic inflammation and oxidative stress induced by liver fluke, *Opisthorchis viverrini*, infection has been recognized as the major cause of CCA in this area. We show here that an increased expression of LAT1 and its co-functional protein CD98 are found during carcinogenesis induced by Ov in hamster CCA tissues. We also demonstrate that oxidative stress induced by H₂O₂ is time-dependent and dramatically activates LAT1 and CD98 expression in immortal cholangiocytes (MMNK1). In addition, H₂O₂ treatment increased LAT1 and CD98 expression, as well as an activated form of AKT and mTOR in MMNK1 and CCA cell lines (KKU-M055 and KKU-M213). We also show that suppression of PI3K/AKT pathway activity with a dual PI3K/mTOR inhibitor, BEZ235, causes a reduction in LAT1 and CD98 expression in KKU-M055 and KKU-M213 in parallel with a reduction of activated AKT and mTOR. Interestingly, high expression of LAT1 in human CCA tissues is a significant prognostic factor for shorter survival. Taken together, our data show that LAT1 expression is significantly associated with CCA progression and cholangiocarcinogenesis induced by oxidative stress. Moreover, the expression of LAT1 and CD98 in CCA is possibly regulated by the PI3K/AKT signaling pathway.

© 2015 Elsevier Ireland Ltd. All rights reserved.

1. Introduction

Cholangiocarcinoma (CCA) is a devastating cancer arising from bile duct epithelial cells. It is characterized as a very poor prognosis and a poor response to current therapies [1]. CCA is the most common cancer in Northeastern Thailand [2]. Epidemiological and experimental evidence strongly implicate the carcinogenic liver fluke, *Opisthorchis viverrini* (Ov), as the etiological agent inducing CCA development in Thailand [3–5]. An oxidative stress condition due to overproduction of ROS and RNS during chronic inflammation caused by Ov infection is considered to play important roles in DNA, lipid, and protein damage leading to cholangiocarcinogenesis [3,6–8]. In hamsters, Ov-induced CCA tissues show altered gene expression. Among these genes, PRKAR1A, the type

1A regulatory subunit of protein kinase A (PKA), is significantly involved in CCA carcinogenesis [9] and represents a target for CCA therapy [10]. Furthermore, Dokduang et al. have shown that multiple kinase signaling pathways, including the PI3K/AKT, Wnt/β-catenin, JAK/STAT, and MAPK signaling pathways are predominately activated in CCA tissues and cell lines [11]. Moreover, we recently demonstrated that upregulation of the PI3K/AKT pathway occurred during Ov-induced cholangiocarcinogenesis [12], and that suppressing PI3K/AKT pathway activity with the specific inhibitor BEZ235 can inhibit CCA growth [13].

Amino acid transporters are commonly unregulated in tumor cells for their supply of amino acids to support massive protein synthesis for continuous growth and proliferation [14,15]. Among several amino acid transporters expressed in tumor cells, the L-type amino acid transporter 1 (LAT1) is frequently observed [16]. LAT1 requires covalent association with co-functional protein CD98 for its functional expression on the plasma membrane [16,17]. Beside the plasma membrane,

* Corresponding author at: Department of Biochemistry, Faculty of Medicine, Khon Kaen University, Khon Kaen 40002, Thailand.

E-mail address: watloi@yahoo.com (W. Loilome).

many studies have demonstrated that LAT1 positive staining is observed in cytoplasm of cancer cells, such as glioma [18,19], pancreatic cancer [20], and lung cancer [21]. This may represent an intracellular pool of LAT1 while LAT1 expression on plasma membranes may represent its function.

Recently, there have been reports which demonstrated that high expression of LAT1 is a promising prognostic marker to predict patient survival [22–26]. It is well known that LAT1 plays an important role not only as a prognostic marker but also in cancer treatment. Furthermore, the LAT1-specific inhibitor JPH203 (KYT0353) inhibited tumor growth both *in vitro* and *in vivo* models [27–29]. In addition, suppressed LAT1 activity can inhibit CCA cell growth, migration, and invasion [23, 30]. To date, however, there have been no reports about LAT1 in cholangiocarcinogenesis. We therefore examined the expression of LAT1 and its co-functional protein CD98 in Ov-induced CCA in a hamster model, as well as in human CCA tissues. Moreover, the molecular mechanisms by which LAT1 and CD98 upregulated under oxidative stress were explored.

2. Materials and methods

2.1. Animals and tumor induction

Experiments in the animal model used in this study were conducted and performed according to the guidelines of the National Committee of Animal Ethics and the protocol was approved by the Animal Ethics Committee of the Faculty of Medicine, Khon Kaen University, Thailand (#AE002/2002). The induction of CCA in male hamsters was performed using a combination treatment with Ov metacercariae infection and *N*-nitrosodimethylamine (NDMA), as in previous studies [9]. Male Syrian golden hamsters ranging from 6 to 8 weeks were used in this study. The hamsters were divided into 2 groups: Group 1 was untreated and served as the control group; Group 2 was fed 50 Ov metacercariae by intragastric intubation combined with oral administration of 12.5 ppm NDMA (Sigma, St. Louis, MO, USA) for 8 weeks. Hamsters were housed under conventional conditions, fed stock diet, and were given water ad libitum. Animals were sacrificed on days 14, 30, 90, and 180 after treatment. Hamster liver tissue was collected and fixed in 10% neutral buffered formalin and embedded in paraffin according to standard techniques. Samples were used for histological and immunohistochemistry staining.

2.2. Human CCA tissue microarrays

The human CCA tissue microarrays contained a total 178 cases. The samples studied were collected from CCA patients admitted to surgical wards of Srinagarind Hospital, Khon Kaen University. The protocol for the collection and study was approved by the Ethics Committee for Human Research, Khon Kaen University (#HE521209). Informed consent was obtained from individual patients. The 4- μ m-thick sections of human CCA tissues used in tissue arrays (TMAs) were constructed by the Department of Pathology, Faculty of Medicine, Khon Kaen University, Thailand.

2.3. Cell lines and culture

Human CCA cell lines including KKK-M055 and KKK-M213 were established at Khon Kaen University Liver Fluke and Cholangiocarcinoma Research Center from CCA patients living in the *O. viverrini* endemic area of northeast Thailand [31]. An immortalized human cholangiocyte cell line (MMNK1) was used in this study as a representative of normal cells as previously described [32]. All cell lines were cultured in Ham's F-12 medium (Gibco/BRL, Grand Island, NY, USA) supplemented with 44 mM NaHCO₃, penicillin (100 units/ml), streptomycin (100 mg/ml), and 10% fetal bovine serum in a humidified atmosphere containing 5% CO₂.

2.4. Antibodies and inhibitor

Antibodies against AKT (#9272), phospho-AKT (#9271), and mTOR (#2983) were purchased from Cell Signaling Technology (Danvers, MA, USA). An antibody against phospho-mTOR (ab109268) was purchased from Abcam (Abcam, Cambridge, UK) and antibody against CD98 was purchased from Santa Cruz Biotechnology (Santa Cruz, CA, USA). LAT1 antibody was kindly provided by Dr. H. Endou (J-Pharma Co., Ltd., Tokyo, Japan). Anti- β -actin antibody was purchased from Sigma-Aldrich (St. Louis, MO, USA).

The dual PI3K/mTOR inhibitor, NVP-BEZ235, was kindly supplied by Novartis Pharma AG (Basel, Switzerland). The stock hydrogen peroxide, H₂O₂ (30%), was purchased from Merck (Darmstadt, Germany).

2.5. Immunohistochemistry staining

Immunohistochemistry (IHC) was performed to identify the expression of LAT1 and CD98 in CCA samples. Briefly, the sections of CCA tissues were de-paraffinized and rehydrated through a gradient of ethanol. Following antigen retrieval and elimination of endogenous peroxidase, slides were blocked with 10% skimmed milk in PBS for 1 h. Samples were then incubated with the primary antibody against the designed target proteins at 4 °C. After washing with PBST, sections were incubated with peroxidase conjugated Envision™ secondary antibody (DAKO, Denmark) for 1 h. After washing, peroxidase-labeled polymer, 0.1% diaminobenzidine tetrahydrochloride solution was used for the signal development, followed by counterstaining with hematoxylin, dried and mounted. The stained sections were observed under a light microscope using high magnification $\times 200$ and $\times 400$ (Axioscope A1, Carl Zeiss, Jena, Germany).

Expression of LAT1 and CD98 in human CCA tissues was assessed as described in a previous study [13]. Briefly, the grading of staining depended on staining intensity and frequency in the tumor area. The staining intensity was scored as follows: 0, negative; +1, weak expression; +2, moderate expression; +3, strong expression. The frequency of staining was divided as follows: 0, negative; +1, 1–25%; +2, 26–50%; +3, >50%. Staining scores were calculated by multiplying intensities and frequencies in each case which were classified into two groups: low expression levels with scores <4 and high expression levels with scores ≥ 4 .

2.6. Western blot analysis

To study the effect of H₂O₂ or NVP-BEZ235 on LAT1 and CD98 as well as PI3K/AKT signaling pathway, the cells were treated with H₂O₂ or NVP-BEZ235 with untreated cells being used as controls. The experiments have been done in the serum containing cultured media. Cells were then lysed with the RIPA lysis buffer and the lysate was centrifuged at 4 °C and 12,000 rpm for 15 min. Whole cell lysates were electrophoresed on 10% SDS-PAGE. Proteins from the gel were transferred to polyvinylidene difluoride membranes (Millipore, Bedford, USA). Membranes were blocked in buffer 5% skimmed milk in TBS at room temperature for 1 h and incubated overnight with primary antibody at 4 °C. After blocking, the membranes were washed three times with TBST for 5 min and then incubated with horseradish peroxidase-conjugated secondary antibody (Santa Cruz Biotechnology, CA, USA) at room temperature for 1 h. Membranes were again washed three times in TBST and developed using ECL Prime Western blotting Detection System (GE Healthcare Bio-Science, UK). The immunoblot and intensity were analyzed by the ImageQuant™ analysis system (GE Healthcare Bio-Science, UK). Human β -actin was used as a loading control. The western blotting for each cell line was done in two independent experiments.

2.7. Statistical analysis

Statistical analyses were performed by using SPSS software version 17 (IBM Corporation, NY, USA). Pearson's correlation coefficient was calculated for the correlation between IHC scores of each protein in CCA tissues. The cumulative survival after tumor removal was calculated according to the Kaplan–Meier method, with a log-rank test. Cox proportional hazard analysis was used to assess survival data. Factors significant in univariate analyses were further examined by multivariable analysis. $P < 0.05$ was considered statistically significant.

3. Results

3.1. Histopathological changes of Ov-induced cholangiocarcinogenesis in hamster liver tissues

The liver tissues of hamster were collected at different times following treatment with Ov plus NDMA. No pathological changes were observed in the control group, whereas hyperplastic lesions, precancerous lesions and carcinomas were observed at 30, 90, and 180 days post-infection (p.i.), respectively [9].

3.2. Increase expression of LAT1 and CD98 in hamster liver tissues during CCA development

The expression patterns of LAT1 and CD98 during carcinogenesis of Ov-induced hamster CCA are shown in Fig. 1A. Positively stained signals of LAT1 and CD98 were observed in both cytoplasm and membrane of bile duct epithelial cells. A faint positive staining for LAT1 and CD98 was also seen in normal bile ducts of the untreated group. In the Ov plus NDMA-treated groups, the intensity of LAT1 and CD98 positively stained cells increased in a time-dependent manner during cholangiocarcinogenesis with the highest positive signal being seen when CCA was fully developed (180 days p.i.). Moreover, our results also revealed the expression of LAT1 and CD98 in the inflammatory cells. Thus, oxidative stress caused by Ov infection can induce LAT1 and CD98 expression in cholangiocytes.

3.3. Increased LAT1 and CD98 expression induced by H₂O₂-induced oxidative stress condition via a PI3K/AKT signaling pathway

To prove whether the increased expression of LAT1 and CD98 was a response to oxidative stress, we next determined the time course of the increase in LAT1 and CD98 expression in immortalized cholangiocytes subjected to oxidative stress induced by H₂O₂ with increasing incubation time. MMNK1 cells were exposed to 200 μ M of H₂O₂ for 0–48 h. Our results reveal that the treatment of MMNK1 cells with H₂O₂ at the indicated concentration can induce LAT1 and CD98 expression in a time-dependent manner as shown in Fig. 1B. We then showed that upregulation of LAT1 and CD98, as well as an increased activation of PI3K/AKT signaling pathway, demonstrated by an increase of p-AKT and p-mTOR levels, occurred under the oxidative stress induced by H₂O₂ in both MMNK1 and CCA cells (Fig. 2). Moreover, a decrease in the expression of LAT1 and CD98 protein, as well as a reduction p-AKT and p-mTOR, was seen in the BEZ235, the specific dual PI3K/mTOR inhibitor treated CCA cell lines (Fig. 3).

3.4. High LAT1 and CD98 expression in human CCA is associated with a poor prognosis

To determine whether the increased expression of LAT1 and CD98 has a significant biological meaning in human cholangiocarcinoma, we examined the expression of LAT1 and CD98 proteins in 178 human CCA tissues. The age of the patients ranged from 26 to 76 years (median = 57 years). Among all patients, 69% (122 cases) were male and

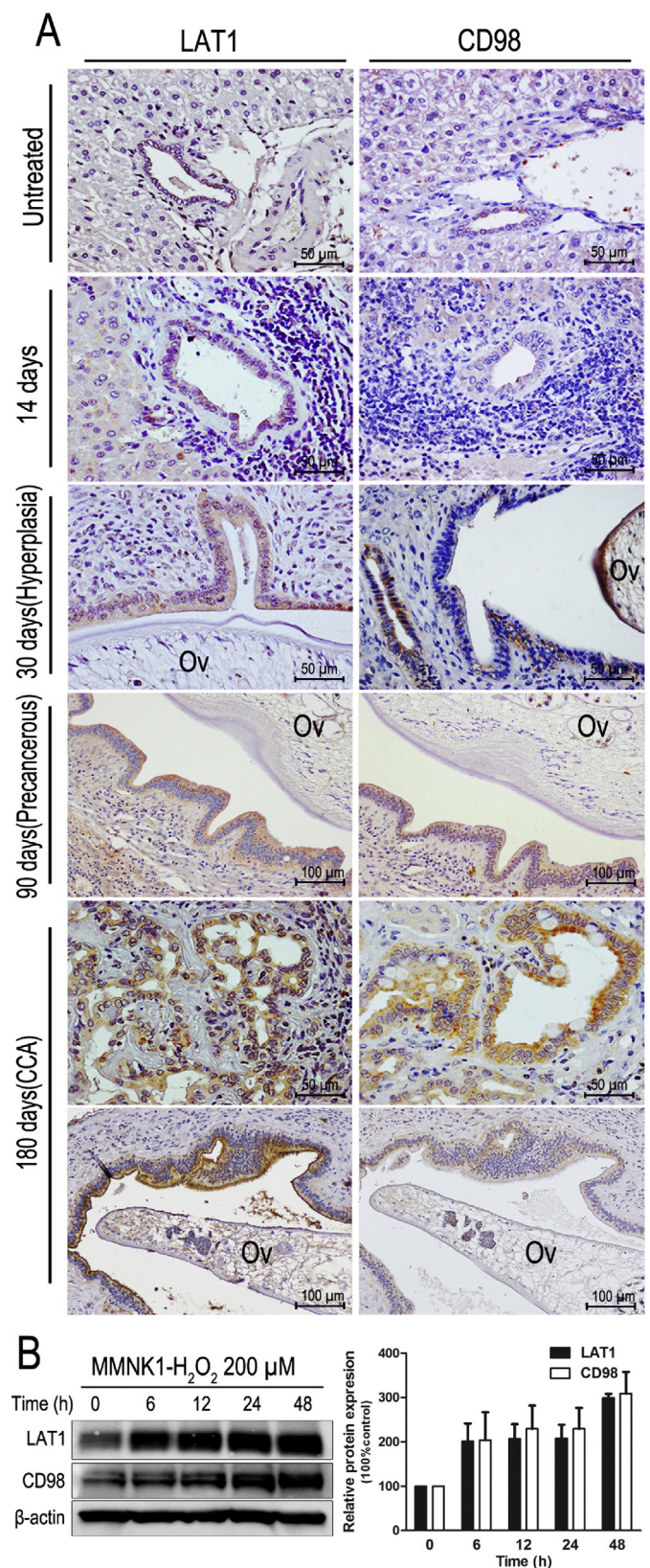


Fig. 1. Expression of LAT1 and CD98 during cholangiocarcinogenesis. (A) Immunohistochemical staining of LAT1 and CD98 in hamster liver tissues at 14, 30, 90, and 180 days post-treatment compared with an untreated group, magnification $\times 200$ and $\times 400$. (B) MMNK1 cells were treated with 200 μ M of H₂O₂ for 0, 6, 12, 24, and 48 h, then expression of LAT1 and CD98 was analyzed by Western blotting. Bar graphs show mean \pm S.E.M. of densitometry values of LAT1 and CD98 and present as % of control.

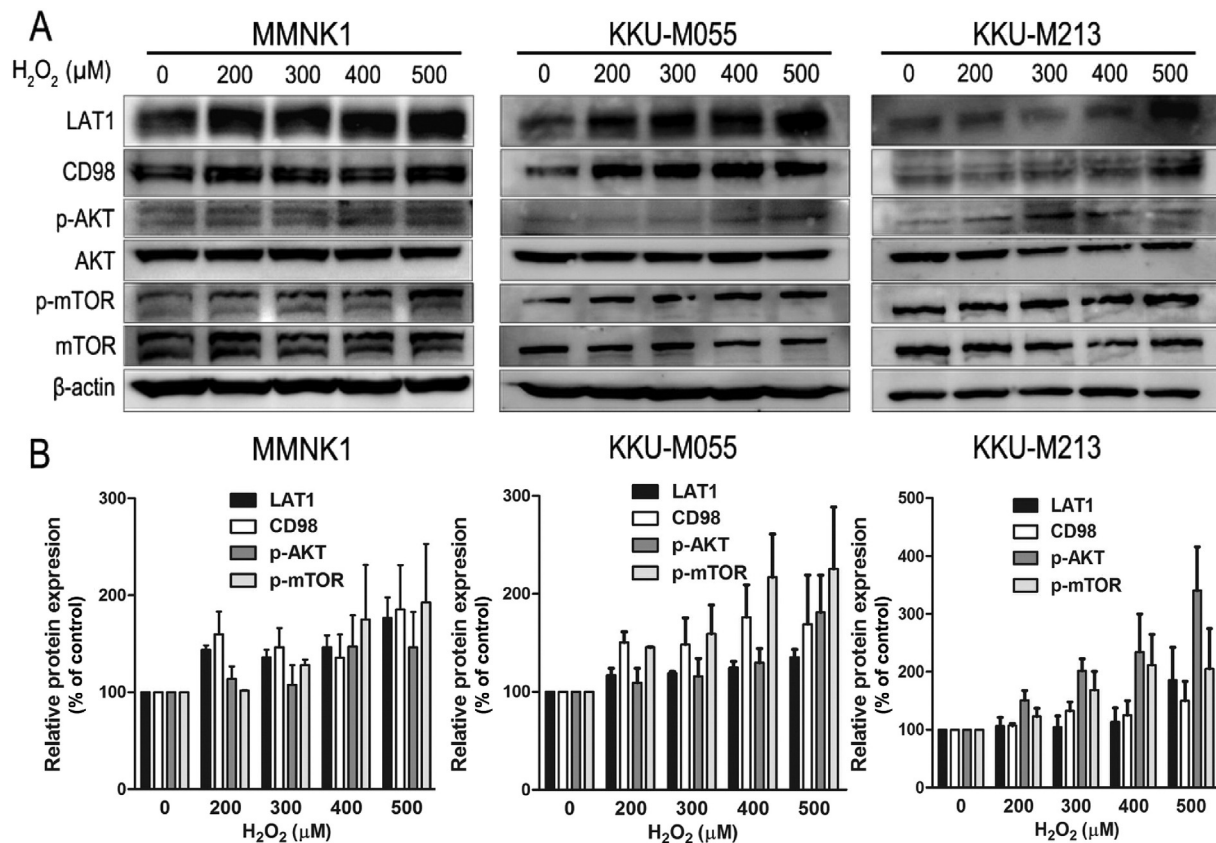


Fig. 2. Oxidative stress induced by H_2O_2 activates LAT1 and CD98 expression along with PI3K/AKT activation in CCA. (A) The indicated cells were treated with H_2O_2 at 0, 200, 300, 400, and 500 μM for 24 h. Then total lysates were extracted and analyzed by Western blotting using the indicated antibodies. (B) Bar graphs show mean \pm S.E.M. of densitometry values of protein bands and present as % of control.

31% (56 cases) were female, resulting in a male-to-female ratio of 2.2:1. All patients had advanced-stage cancer with 58% (104 cases) presenting with metastasis. The histological types were classified as papillary type CCA with 35% (63 cases) and non-papillary type CCA with 65% (115 cases).

The results of immunohistochemical staining revealed the expression of LAT1 and CD98 in both the cytoplasm and plasma membranes of positively stained cells. Normal bile duct epithelia showed no or weak positive staining of LAT1 and CD98, while an increased expression was observed in CCA cells (Fig. 4A). We found that LAT1 was positive in 86% (153 cases). This could be divided into high expression in 56% (100 cases) and low expression in 30% (53 cases). Negative LAT1 was found in 14% (25 cases). In addition, CD98 was positive in 95% (170 cases), divided into high expression in 62% (111 cases) and low expression in 33% (59 cases). Negative CD98 expression was found in 5% (8 cases).

Co-expression of LAT1 with CD98 was found in 83% (147 cases). LAT1 positive and CD98 negative expressions were observed in 3% (6 cases), whereas LAT1 negative and CD98 positive were identified in 13% (23 cases). Two cases (1%) were negative for both proteins. High expression of LAT1 with CD98 was observed in 39% (70 cases). Low expression of LAT1 with CD98 was found in 20% (35 cases). High expression of LAT1 with low or negative CD98 was seen in 17% (30 cases). High expression of CD98 with low or negative LAT1 was identified in 23% (41 cases). LAT1 expression score was positively correlated with CD98 ($P = 0.017$, Table 1).

3.5. The high LAT1 expression is correlated with a short survival of CCA patients

Increased levels of LAT1 or CD98 were not associated with age, gender, histological type, and tumor metastasis (data not shown).

The log-rank analysis indicated that a positive and high expression of LAT1 was significantly correlated with shorter patient survival ($P = 0.002$ and $P < 0.001$, Fig. 4B and C). However, no difference was found between the expression of CD98 and survival (data not shown). Interestingly, patients positive for both LAT1 and CD98 (147 cases, 83%), as well as those having a high expression of both LAT1 and CD98 (70 cases, 39%), had a significantly shorter survival time than patients without these characteristics ($P = 0.001$ and $P < 0.001$, Fig. 4D and E).

According to the results of our univariate analysis, LAT1 positive, high LAT1 expression, positive both LAT1 and CD98, as well as high expression both LAT1 and CD98 with gender were prognostic in CCA patients (Table 2). The subsequent multivariable analysis confirmed that high LAT1 expression ($P = 0.002$) and gender ($P = 0.048$) were independently prognostic of survival in these patients (Table 2). CCA patients who had a high LAT1 expression had a 2.1-fold higher risk of death than the patients whose tumors were negative or had a low expression of LAT1.

4. Discussion

Several studies have demonstrated that the expression of LAT1 is closely linked to the several types of cancer [16,17]. Moreover, increased LAT1 expression is involved in cancer cell proliferation and progression, leading to a poor prognosis for various cancers [22–26]. Interestingly, there is strong evidence supporting the hypothesis that overexpression of LAT1 in tumor cells might be used as a tumor diagnostic marker detected by positron emission tomography (PET) imaging [33–35]. Previous studies have demonstrated that a novel LAT1 inhibitor, JPH203, can inhibit tumor growth in human colon cancer cells [27] and leukemic cells [29] in both *in vitro* and *in vivo* models. Moreover, JPH203 can

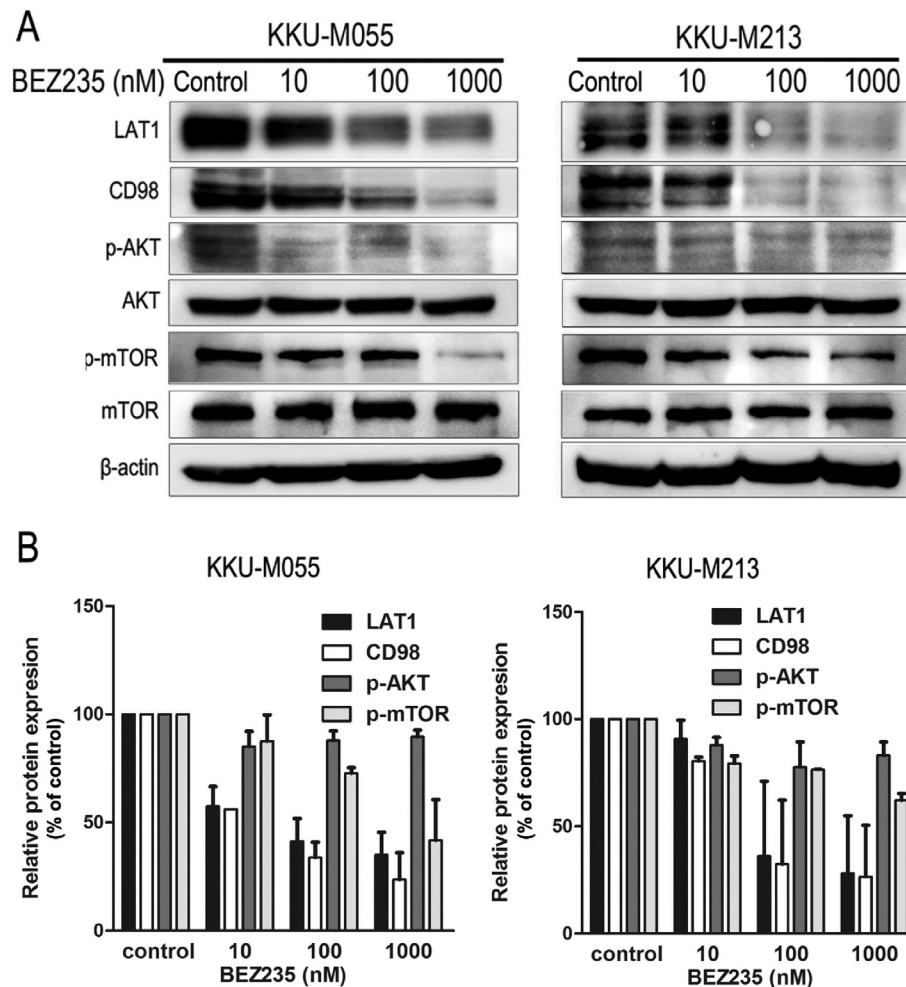


Fig. 3. Suppression of the PI3K/AKT signaling pathway decreased LAT1 and CD98 expression. (A) The indicated cells were treated with BEZ2325 for 48 h at 10, 100, and 1000 nM an 0.1% DMSO was used as control. Results were analyzed by immunoblotting. (B) Bar graphs show mean \pm S.E.M. of densitometry values of protein bands and present as % of control.

induce apoptosis in a model of human oral cancer [28] and leukemia [29], indicating that targeting LAT1 may be clinically useful as a cancer treatment.

Only three studies have reported roles of LAT1 in CCA. The first two demonstrated that increased LAT1 expression predicts a poor prognosis in CCA patients [23,36]. The third showed that targeted knockdown of LAT1 can inhibit leucine uptake and is concomitant with reduced cell migration and invasion in KKKU-M213 CCA cell [30]. However, there was no evidence of LAT1 expression during CCA carcinogenesis.

In the current work, we demonstrated that the expression LAT1 and its co-functional protein CD98 were increased during carcinogenesis processes in Ov-induced hamster CCA tissues. Thus, oxidative stress caused by Ov infection might be responsible for this event. LAT1 expression is regulated by the c-Myc gene [37], which is a proto-oncogene and upregulated by ROS treatment in a model of H₂O₂-treated melanoma cells [38]. In addition, c-Myc expression is upregulated in CCA and appears to be a tumor diagnostic marker [39]. Therefore, upregulation of LAT1 and CD98 caused by oxidative stress during chronic Ov infection may be regulated by the c-Myc gene.

Additionally, we then demonstrated for the first time that oxidative stress induced by H₂O₂ dramatically activates LAT1 and CD98 expression in a time-dependent way in immortal cholangiocyte (MMNK1) via the PI3K/AKT signaling pathway. These results provide more information that is helpful in explaining the molecular mechanisms by which Ov-induced CCA develops. Chronic inflammation caused by Ov infection leads to the overproduction and accumulation of reactive oxygen and reactive nitrogen radicals in inflamed target cells [6,40].

Moreover, increased levels of these radicals have the potential to damage DNA, proteins, lipids, and alter gene expression, all of which can contribute to cellular carcinogenesis [4,6–9]. Repeated cycles of cell damage and compensatory cell proliferation promote the development of tumor cells. LAT1 and its partner CD98 can supply the amino acids needed to support massive protein synthesis for continuous growth and proliferation [14,15]. Interestingly, the increase of LAT1 and CD98 is probably regulated by a PI3K/AKT signaling pathway which is also overactivated during Ov-infection-associated CCA tumorigenesis [12]. Additionally, the expression of LAT1 is closely correlated with p-AKT and p-mTOR, which is the key downstream elements in PI3K/AKT signaling [41,42]. Moreover, mTOR is an upstream regulator of LAT1 in a model of insulin-treated mouse myoblast cell line [43].

Furthermore, we report the expression of LAT1 and CD98 in human CCA tissues from endemic areas of Ov infection. The increase of LAT1 and CD98 expression in human CCA might be regulated by PI3K/AKT signaling for which the overactivation of a particular pathway has been previously reported [11,13]. Interestingly, high expression of LAT1 in human CCA tissue was a significant prognostic factor for shorter survival. Our results conform to previous reports in which the high expression of LAT1 was significantly associated with a shorter survival in cancer patients [23,36]. The results from multivariate analysis confirmed that LAT1 expression is an independent prognostic factor for predicting shorter survival. The result from multivariate analysis also indicated that male gender is an independent risk factor for poor prognosis. The number of male patients is 2.2-fold that of female patients, and male gender is a risk factor for CCA [44].

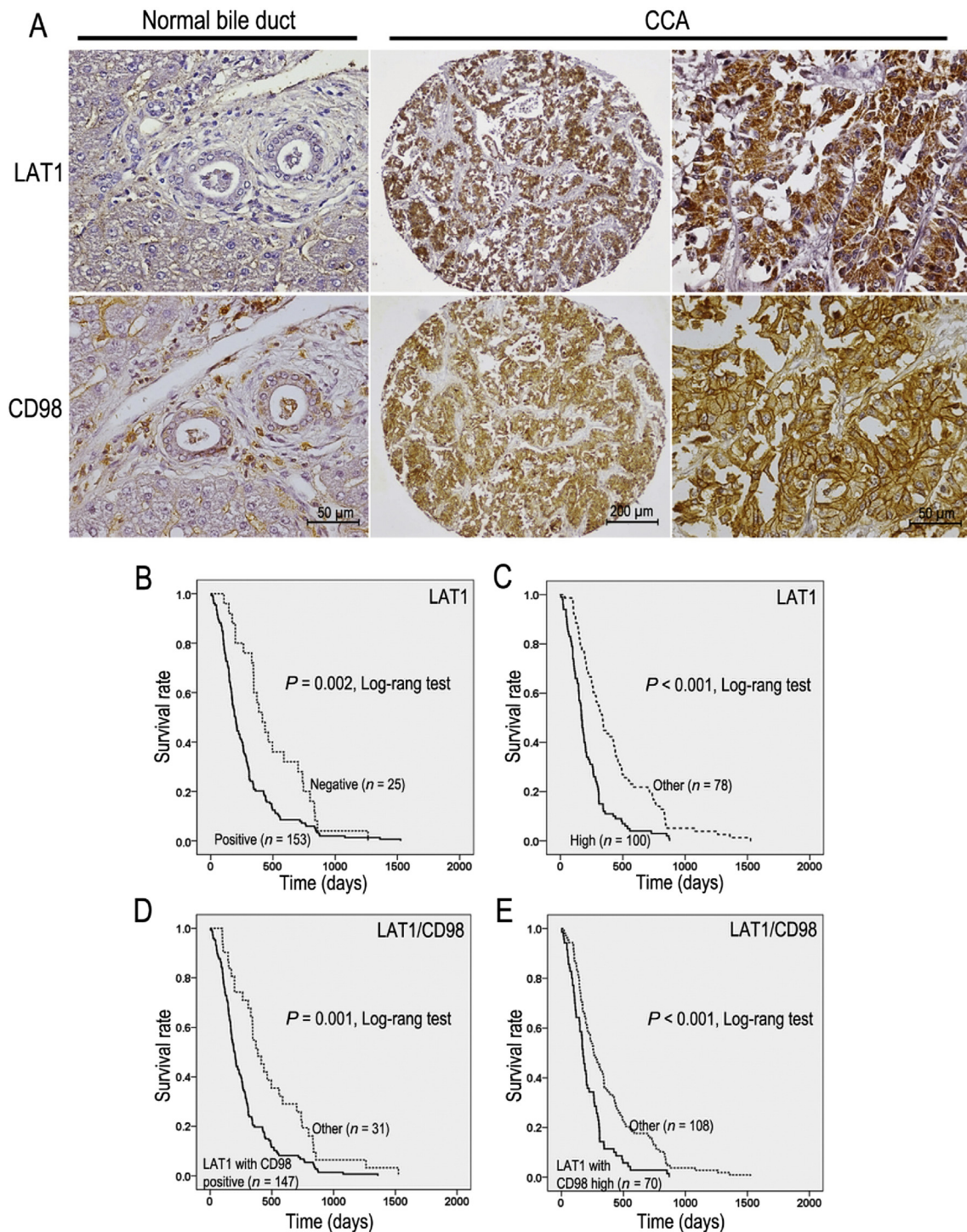


Fig. 4. Expression of LAT1 and CD98 in human CCA tissue. (A) Representative immunohistochemical staining of LAT1 and CD98 in normal bile duct, magnification $\times 400$ and human CCA tissue microarray, magnification $\times 100$ and $\times 400$, respectively. (B) and (C) Kaplan–Meier curve of CCA patients with positive LAT1 and high LAT1 expression, respectively. (D) and (E) Kaplan–Meier curve of CCA patients with co-expression of positive LAT1 and CD98 and high expression of LAT1 and CD98 in human CCA patients, respectively.

Table 1
Correlation coefficient between IHC scores of LAT1 and CD98 in human CCA tissues microarray (TMA).

		LAT1
CD98	Correlation coefficient	0.179
	P	0.017*

* Correlation is significant at the 0.05 level (2-tailed).

In the present study, we also demonstrated the significant positive correlation between the expression levels of LAT1 with its functional protein partner CD98, indicating that CD98 is essential for the functional expression of LAT1. Unfortunately, there was no significant correlation between CD98 and patient survival as previously reported in some types of cancer, such as lung cancer and oral cancer [45–47].

In summary, we demonstrate that oxidative stress during chronic Ov infection can induce LAT1 and CD98 expression in a CCA model. This is

Table 2

Multivariate analysis of clinicopathological variables for survival by a Cox proportional hazards regression model.

Variable (No. patients)	Univariate			Multivariate		
	Hazard ratio	95% CI	P	Hazard ratio	95% CI	P
LAT1						
Negative (25)	1			1		
Positive (153)	1.909	1.245–2.926	0.003*	0.889	0.329–2.379	0.809
LAT1						
Other (78)	1			1		
High (100)	2.241	1.644–3.054	<0.001*	2.103	1.329–3.327	0.002*
CD98						
Negative (8)	1					
Positive (170)	1.562	0.724–3.368	0.255			
CD98						
Other (67)	1					
High (111)	1.151	0.848–1.564	0.367			
LAT1/CD98						
Other (31)	1			1		
Positive/Positive (147)	1.998	1.341–2.976	0.001*	1.542	0.612–3.884	0.358
LAT1/CD98						
Other (108)	1			1		
High/High (70)	1.854	1.359–2.531	<0.001*	0.881	0.567–1.369	0.573
Age (years)						
<57 (89)	1					
>57 (89)	1.099	0.811–1.489	0.542			
Gender						
Female (56)	1			1		
Male (122)	1.488	1.077–2.055	0.016*	1.400	1.003–1.955	0.048*
Histological types						
Papillary (63)	1					
Non-papillary (115)	1.131	0.830–1.541	0.435			
Metastasis						
No (74)	1					
Yes (104)	1.304	0.962–1.766	0.087			

* P value equal to or less than 0.05 was considered statistically significant.

likely to be regulated by the PI3K/AKT signaling pathway. Moreover, high LAT1 expression can be used as a prognostic marker for CCA progression. Further study to explore whether LAT1 can be used as a potential target for the CCA therapy needs to be carried out.

Acknowledgements

This research was supported by The Invitation Research Grant (grant number I57235 and I57305), the Liver Fluke and Cholangiocarcinoma Research Center (LFCRC) (LFCRC04/2556) to SY; Faculty of Medicine Khon Kaen University and the grant of the Higher Education Research Promotion and National Research University Project of Thailand, Office of the Higher Education Commission (NRU582004), through the Health Cluster (SHEP-GMS), Khon Kaen University to WL. The authors are deeply grateful to Dr. Hitoshi Endou (J-Pharma Co., Ltd.) for providing us with the anti-LAT1 antibody. We are grateful to Novartis for providing us with NVP-BE2235 to complete this work. We also thank Professor Trevor N. Petney for editing the MS via Publication Clinic KKU, Thailand.

References

- [1] B. Blechacz, G.J. Gores, Cholangiocarcinoma: advances in pathogenesis, diagnosis, and treatment, *Hepatology* 48 (2008) 308–321.
- [2] V. Vatanasapt, S. Sriamporn, P. Vatanasapt, Cancer control in Thailand, *Jpn. J. Clin. Oncol.* 32 (Suppl.) (2002) S82–S91.
- [3] P. Yongvanit, S. Pinlaor, H. Bartsch, Oxidative and nitrate DNA damage: key events in opisthorchiasis-induced carcinogenesis, *Parasitol. Int.* 61 (2012) 130–135.
- [4] H. Ohshima, H. Bartsch, Chronic infections and inflammatory processes as cancer risk factors: possible role of nitric oxide in carcinogenesis, *Mutat. Res.* 305 (1994) 253–264.
- [5] W. Thamavit, N. Bhamarapravati, S. Sahaphong, S. Vajrasthira, S. Angsubhakorn, Effects of dimethylnitrosamine on induction of cholangiocarcinoma in *Opisthorchis viverrini*-infected Syrian golden hamsters, *Cancer Res.* 38 (1978) 4634–4639.
- [6] S. Pinlaor, N. Ma, Y. Hiraku, P. Yongvanit, R. Semba, S. Oikawa, et al., Repeated infection with *Opisthorchis viverrini* induces accumulation of 8-nitroguanine and 8-oxo-7,8-dihydro-2'-deoxyguanine in the bile duct of hamsters via inducible nitric oxide synthase, *Carcinogenesis* 25 (2004) 1535–1542.
- [7] S. Dechakhamphu, S. Pinlaor, P. Sitthithaworn, H. Bartsch, P. Yongvanit, Accumulation of miscoding etheno-DNA adducts and highly expressed DNA repair during liver fluke-induced cholangiocarcinogenesis in hamsters, *Mutat. Res.* 691 (2010) 9–16.
- [8] R. Thanan, S. Oikawa, P. Yongvanit, Y. Hiraku, N. Ma, S. Pinlaor, et al., Inflammation-induced protein carbonylation contributes to poor prognosis for cholangiocarcinoma, *Free Radic. Biol. Med.* 52 (2012) 1465–1472.
- [9] W. Loilome, P. Yongvanit, C. Wongkham, N. Tepsiri, B. Sripa, P. Sitthithaworn, et al., Altered gene expression in *Opisthorchis viverrini*-associated cholangiocarcinoma in hamster model, *Mol. Carcinog.* 45 (2006) 279–287.
- [10] W. Loilome, S. Juntana, N. Namwat, V. Bhudhisawasdi, A. Puapairoj, B. Sripa, et al., PRKAR1A is overexpressed and represents a possible therapeutic target in human cholangiocarcinoma, *Int. J. Cancer* 129 (2011) 34–44.
- [11] H. Dokduang, S. Juntana, A. Techasen, N. Namwat, P. Yongvanit, N. Khuntikeo, et al., Survey of activated kinase proteins reveals potential targets for cholangiocarcinoma treatment, *Tumour Biol.* (2013).
- [12] S. Yothaisong, M. Thane, N. Namwat, P. Yongvanit, T. Boonmars, A. Puapairoj, et al., *Opisthorchis viverrini* infection activates the PI3K/AKT/PTEN and Wnt/beta-catenin signaling pathways in a cholangiocarcinogenesis model, *Asian Pac. J. Cancer Prev.* 15 (2014) 10463–10468.
- [13] S. Yothaisong, H. Dokduang, A. Techasen, N. Namwat, P. Yongvanit, V. Bhudhisawasdi, et al., Increased activation of PI3K/AKT signaling pathway is associated with cholangiocarcinoma metastasis and PI3K/mTOR inhibition presents a possible therapeutic strategy, *Tumour Biol.* 34 (2013) 3637–3648.
- [14] H.N. Christensen, Role of amino acid transport and countertransport in nutrition and metabolism, *Physiol. Rev.* 70 (1990) 43–77.
- [15] J.D. McGivan, M. Pastor-Anglada, Regulatory and molecular aspects of mammalian amino acid transport, *Biochem. J.* 299 (Pt 2) (1994) 321–334.
- [16] O. Yanagida, Y. Kanai, A. Chairoungdua, D.K. Kim, H. Segawa, T. Nii, et al., Human L-type amino acid transporter 1 (LAT1): characterization of function and expression in tumor cell lines, *Biochim. Biophys. Acta* 1514 (2001) 291–302.
- [17] Y. Kanai, H. Segawa, K. Miyamoto, H. Uchino, E. Takeda, H. Endou, Expression cloning and characterization of a transporter for large neutral amino acids activated by the heavy chain of 4F2 antigen (CD98), *J. Biol. Chem.* 273 (1998) 23629–23632.
- [18] H. Nawashiro, N. Otani, N. Shinomiya, S. Fukui, H. Ooigawa, K. Shima, et al., L-type amino acid transporter 1 as a potential molecular target in human astrocytic tumors, *Int. J. Cancer* 119 (2006) 484–492.
- [19] Z. Haining, N. Kawai, K. Miyake, M. Okada, S. Okubo, X. Zhang, et al., Relation of LAT1/4F2hc expression with pathological grade, proliferation and angiogenesis in human gliomas, *BMC Clin. Pathol.* 12 (2012) 4.
- [20] K. Kaira, Y. Sunose, K. Arakawa, T. Ogawa, N. Sunaga, K. Shimizu, et al., Prognostic significance of L-type amino-acid transporter 1 expression in surgically resected pancreatic cancer, *Br. J. Cancer* 107 (2012) 632–638.

- [21] K. Takeuchi, S. Ogata, K. Nakanishi, Y. Ozeki, S. Hiroi, S. Tominaga, et al., LAT1 expression in non-small-cell lung carcinomas: analyses by semiquantitative reverse transcription-PCR (237 cases) and immunohistochemistry (295 cases), *Lung Cancer* 68 (2010) 58–65.
- [22] N. Yanagisawa, M. Ichinoe, T. Mikami, N. Nakada, K. Hana, W. Koizumi, et al., High expression of L-type amino acid transporter 1 (LAT1) predicts poor prognosis in pancreatic ductal adenocarcinomas, *J. Clin. Pathol.* 65 (2012) 1019–1023.
- [23] K. Kaira, Y. Sunose, Y. Ohshima, N.S. Ishioka, K. Arakawa, T. Ogawa, et al., Clinical significance of L-type amino acid transporter 1 expression as a prognostic marker and potential of new targeting therapy in biliary tract cancer, *BMC Cancer* 13 (2013) 482.
- [24] J. Li, J. Qiang, S.F. Chen, X. Wang, J. Fu, Y. Chen, The impact of L-type amino acid transporter 1 (LAT1) in human hepatocellular carcinoma, *Tumour Biol.* 34 (2013) 2977–2981.
- [25] A. Isoda, K. Kaira, M. Iwashina, N. Oriuchi, H. Tominaga, S. Nagamori, et al., Expression of L-type amino acid transporter 1 (LAT1) as a prognostic and therapeutic indicator in multiple myeloma, *Cancer Sci.* 105 (2014) 1496–1502.
- [26] M. Toyoda, K. Kaira, Y. Ohshima, N.S. Ishioka, M. Shino, K. Sakakura, et al., Prognostic significance of amino-acid transporter expression (LAT1, ASCT2, and xCT) in surgically resected tongue cancer, *Br. J. Cancer* 110 (2014) 2506–2513.
- [27] K. Oda, N. Hosoda, H. Endo, K. Saito, K. Tsujihara, M. Yamamura, et al., L-type amino acid transporter 1 inhibitors inhibit tumor cell growth, *Cancer Sci.* 101 (2010) 173–179.
- [28] D.W. Yun, S.A. Lee, M.G. Park, J.S. Kim, S.K. Yu, M.R. Park, et al., JPH203, an L-type amino acid transporter 1-selective compound, induces apoptosis of YD-38 human oral cancer cells, *J. Pharmacol. Sci.* 124 (2014) 208–217.
- [29] C. Rosilio, M. Nebout, V. Imbert, E. Griessinger, Z. Neffati, J. Benadiba, et al., L-type amino-acid transporter 1 (LAT1): a therapeutic target supporting growth and survival of T-cell lymphoblastic lymphoma/T-cell acute lymphoblastic leukemia, *Leukemia* 29 (2015) 1253–1266.
- [30] K. Janpipatkul, K. Suksen, S. Borwornpinyo, N. Jearawiriyapaisarn, S. Hongeng, P. Piyachaturawat, et al., Downregulation of LAT1 expression suppresses cholangiocarcinoma cell invasion and migration, *Cell. Signal.* (2014).
- [31] B. Sripa, S. Leungwattananawit, T. Nitta, C. Wongkham, V. Bhudhisawasdi, A. Puapairoj, et al., Establishment and characterization of an opisthorchiasis-associated cholangiocarcinoma cell line (KKU-100), *World J. Gastroenterol.* 11 (2005) 3392–3397.
- [32] M. Maruyama, N. Kobayashi, K.A. Westerman, M. Sakaguchi, J.E. Allain, T. Totsugawa, et al., Establishment of a highly differentiated immortalized human cholangiocyte cell line with SV40T and hTERT, *Transplantation* 77 (2004) 446–451.
- [33] O.F. Ikotun, B.V. Marquez, C. Huang, K. Masuko, M. Daiji, T. Masuko, et al., Imaging the L-type amino acid transporter-1 (LAT1) with Zr-89 immunoPET, *PLoS ONE* 8 (2013), e77476.
- [34] A. Nobusawa, M. Kim, K. Kaira, G. Miyashita, A. Negishi, N. Oriuchi, et al., Diagnostic usefulness of (1)(8)F-FAMT PET and L-type amino acid transporter 1 (LAT1) expression in oral squamous cell carcinoma, *Eur. J. Nucl. Med. Mol. Imaging* 40 (2013) 1692–1700.
- [35] C. Haase, R. Bergmann, F. Fuechtner, A. Hoeppling, J. Pietzsch, L-type amino acid transporters LAT1 and LAT4 in cancer: uptake of 3-O-methyl-6-18F-fluoro-L-dopa in human adenocarcinoma and squamous cell carcinoma in vitro and in vivo, *J. Nucl. Med.* 48 (2007) 2063–2071.
- [36] N. Yanagisawa, K. Hana, N. Nakada, M. Ichinoe, W. Koizumi, H. Endou, et al., High expression of L-type amino acid transporter 1 as a prognostic marker in bile duct adenocarcinomas, *Cancer Med.* 3 (2014) 1246–1255.
- [37] K. Hayashi, P. Jutabha, H. Endou, N. Anzai, c-Myc is crucial for the expression of LAT1 in MIA Paca-2 human pancreatic cancer cells, *Oncol. Rep.* 28 (2012) 862–866.
- [38] G.A. de Souza, L.M. Godoy, V.R. Teixeira, A.H. Otake, A. Sabino, J.C. Rosa, et al., Proteomic and SAGE profiling of murine melanoma progression indicates the reduction of proteins responsible for ROS degradation, *Proteomics* 6 (2006) 1460–1470.
- [39] N. Voravud, C.S. Foster, J.A. Gilbertson, K. Sikora, J. Waxman, Oncogene expression in cholangiocarcinoma and in normal hepatic development, *Hum. Pathol.* 20 (1989) 1163–1168.
- [40] H. Ohshima, T.Y. Bandaletova, I. Brouet, H. Bartsch, G. Kirby, F. Ogunbiyi, et al., Increased nitrosamine and nitrate biosynthesis mediated by nitric oxide synthase induced in hamsters infected with liver fluke (*Opisthorchis viverrini*), *Carcinogenesis* 15 (1994) 271–275.
- [41] K. Kaira, N. Oriuchi, T. Takahashi, K. Nakagawa, Y. Ohde, T. Okumura, et al., L-type amino acid transporter 1 (LAT1) expression in malignant pleural mesothelioma, *Anticancer Res.* 31 (2011) 4075–4082.
- [42] K. Kaira, N. Oriuchi, T. Takahashi, K. Nakagawa, Y. Ohde, T. Okumura, et al., LAT1 expression is closely associated with hypoxic markers and mTOR in resected non-small cell lung cancer, *Am. J. Transl. Res.* 3 (2011) 468–478.
- [43] D.K. Walker, M.J. Drummond, J.M. Dickinson, M.S. Borack, K. Jennings, E. Volpi, et al., Insulin increases mRNA abundance of the amino acid transporter SLC7A5/LAT1 via an mTORC1-dependent mechanism in skeletal muscle cells, *Physiol. Rep.* 2 (2014) e00238.
- [44] T.M. Welzel, B.I. Graubard, H.B. El-Serag, Y.H. Shaib, A.W. Hsing, J.A. Davila, et al., Risk factors for intrahepatic and extrahepatic cholangiocarcinoma in the United States: a population-based case-control study, *Clin. Gastroenterol. Hepatol.* 5 (2007) 1221–1228.
- [45] K. Kaira, N. Oriuchi, H. Imai, K. Shimizu, N. Yanagitani, N. Sunaga, et al., CD98 expression is associated with poor prognosis in resected non-small-cell lung cancer with lymph node metastases, *Ann. Surg. Oncol.* 16 (2009) 3473–3481.
- [46] F. Esteban, F. Ruiz-Cabello, A. Concha, M. Perez Ayala, M. Delgado, F. Garrido, Relationship of 4F2 antigen with local growth and metastatic potential of squamous cell carcinoma of the larynx, *Cancer* 66 (1990) 1493–1498.
- [47] D.K. Kim, S.G. Ahn, J.C. Park, Y. Kanai, H. Endou, J.H. Yoon, Expression of L-type amino acid transporter 1 (LAT1) and 4F2 heavy chain (4F2hc) in oral squamous cell carcinoma and its precursor lesions, *Anticancer Res.* 24 (2004) 1671–1675.

SHORT COMMUNICATION

HOXB9 acts as a negative regulator of activated human T cells in response to amino acid deficiency

Keitaro Hayashi¹, Motoshi Ouchi¹, Hitoshi Endou² and Naohiko Anzai¹

T-cell activation is an energy expenditure process and should be properly controlled in accordance with the availability of nutrients such as amino acids to eliminate wasteful energy consumption. However, the details of response to amino acids insufficiency in activated T cells remain largely unknown. Here we show that homeobox B9 (HOXB9), a member of the homeobox gene family that is known as a morphogenesis regulator, acts as a suppressor of activated human T cells to address amino acid starvation. The expression of HOXB9 was triggered by amino acid deprivation as well as functional inhibition of L-type amino acid transporter 1 (also known as SLC7A5) via activating transcription factor 4 in activated T cells. HOXB9 interfered the activities of NF- κ B, NFAT and AP-1 but not retinoic acid receptor-related orphan receptor, resulting in attenuation of the production of selective cytokines in activated T cells. Thus, the morphogenetic gene plays an unexpected role in the regulation of cellular metabolism with changes in the nutrition status in human T cells.

Immunology and Cell Biology (2016) **00**, 1–6. doi:10.1038/icb.2016.13

Recent studies have made it increasingly evident that many cells have certain systems to cope with nutrient starvation.^{1,2} The availability of nutrients is constantly being monitored and once cells have figured out that the amount of the source for cellular metabolism is less than that needed, they initiate a stress response to suppress energy consumption processes, which is safeguard against nutrient deficiency. Mammalian target of rapamycin, a serine/threonine kinase, is one of the representative nutrient sensors, which promotes protein synthesis and cell cycle progression and inhibits autophagy induction provided that nutrients are plentiful.^{3–5} Another major sensor for intracellular nutrients is general control non-derepressible 2 (GCN2).^{6,7} Deprivation of amino acids activates GCN2, which promotes the expression of activating transcription factor 4 (ATF4),⁸ a transcription factor that regulates the expression of special genes responsible for adaptation to an amino acid shortage.^{9,10}

Activated T cells aggressively proliferate and produce various cytokines, which require increased cellular metabolism. It is necessary for activated T cells to take a greater amount of nutrients to satisfy the increased cellular metabolism. Indeed, full activation of T-cells induces the expression of L-type amino acid transporter 1 (LAT1, also known as SLC7A5), a transporter with the capability to intake essential amino acids efficiently in humans and mice.^{11–13} On the other hand, it is also evident that T cells willingly block further activation when LAT1 function is inhibited or amino acids are deprived.^{12,14} However, it is not entirely clear how the systems monitoring nutrient availability in activated T cells ultimately suppress the immunological reaction when amino acids become deprived.

In this study, we characterized HOXB9, a member of the homeobox gene family, as a negative regulator of activated T cells in response to

LAT1 dysfunction and amino acid starvation. The HOX family encodes a transcription factor that has a DNA binding motif called homeodomain and has been demonstrated to be critical for normal morphogenesis, especially for normal segment formation.^{15–17} Although recent studies have shown that some HOX genes including HOXB9 have substantial roles in cancers,^{18–20} the involvement of HOX genes in stress response for nutrient starvation has not been investigated.

We demonstrated that HOX protein contributes to the optimization of immune reactions when activated T cells encounter an amino acid insufficiency. Our surprising finding that the morphogenetic gene plays an unrealized role in stress response to amino acid starvation in activated T cells may provide a new insight into the mechanism of the nutrient sensing system to control intracellular metabolism depending on nutrient conditions.

RESULTS

Induction of HOXB9 expression by amino acid deficiency

Our previous study using a microarray assay demonstrated that inhibition of LAT1 in activated human primary T cells induces expression of a number of genes.¹² One of those genes is HOXB9. By using real time PCR (RT-PCR), we initially confirmed the induction of HOXB9 expression by JPH203, a LAT1-specific inhibitor, in purified human blood T-cells stimulated with anti-CD3, CD28 antibodies (Figure 1a). Facilitated expression of HOXB9 was also observed by activation of human T cells cultured in a medium in which essential amino acids were deprived (Figure 1b). We also found that previously activated human T-cells promote HOXB9 expression by removal of essential amino acids (Figure 1c), suggesting that both

¹Department of Pharmacology and Toxicology, Dokkyo Medical University School of Medicine, Tochigi, Japan and ²J-Pharma Co, Ltd, Kanagawa, Japan
Correspondence: Dr N Anzai, Department of Pharmacology and Toxicology, Dokkyo Medical University School of Medicine, 880 Kitakobayashi, Mibu 321-0293, Japan.
E-mail: anzai@dokkyomed.ac.jp

Received 25 August 2015; revised 22 January 2016; accepted 23 January 2016

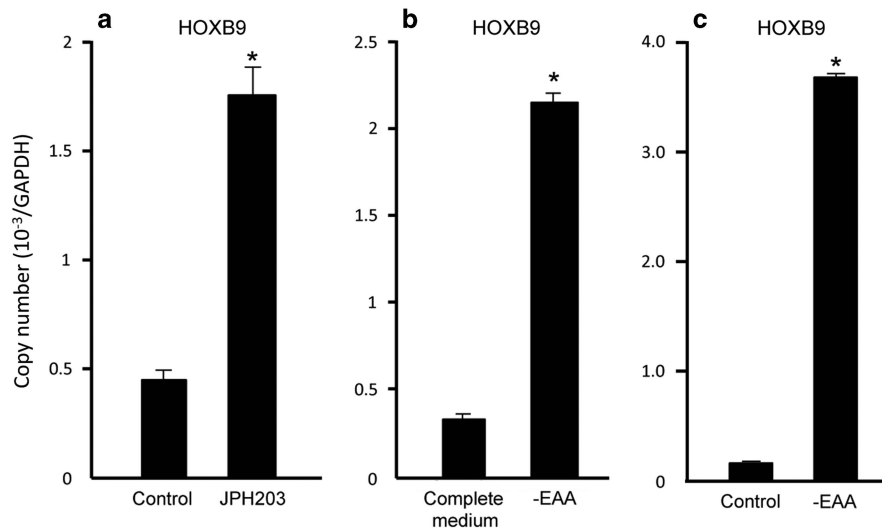


Figure 1 Induction of HOXB9 expression by amino acid starvation in activated T cells. (a and b) Freshly isolated human CD4⁺ T cells were activated by anti-CD3/CD28 in the presence of JPH203 (5 μM) (a) or without essential amino acids (-EAA) (b) for 3 days. HOXB9 expression was measured by RT-PCR. The relative copy number of HOXB9 to one copy of GAPDH was shown. (c) Freshly isolated human CD4⁺ T cells were activated by anti-CD3/CD28 in a normal medium for 5 days and further cultured in the medium with or without essential amino acids for 3 days. HOXB9 expression was measured by RT-PCR. The relative copy number of HOXB9 to one copy of GAPDH was shown. Data are representative of three separate experiments. Data are expressed as the mean ± s.d. **P* < 0.01.

primary and effector T-cells trigger HOXB9 expression as a response to amino acid starvation. In contrast, we could not detect the HOXB9 messenger RNA (mRNA) in freshly isolated T cells, suggesting that HOXB9 is not expressed unless T cells are activated.

Taken together, these results indicate that HOXB9 expression is primed in response to amino acid starvation in activated human T cells.

HOXB9 inhibits T-cell function

We hypothesized that induction of HOXB9 expression by a LAT1 defect or deprivation of amino acids might have special significance in regulation of T-cell metabolism as a stress response to amino acid starvation. To test this hypothesis, we analyzed the function of HOXB9 in T cells. Human primary T cells were transfected with a HOXB9 expression vector and stimulated with anti-CD3 and anti-CD28 antibodies. The amounts of IFN γ , IL-2, IL-4 and IL-17 produced were then determined. Overexpression of HOXB9 significantly reduced the productions of IFN γ , IL-2 and IL-4 (Figure 2a). Interestingly, however, IL-17 production was not significantly changed by HOXB9.

We also found that knockdown of HOXB9 by small interfering RNA (siRNA) in T cells that were activated without essential amino acids slightly increased the productions of IFN γ , IL-2 and IL-4, although deprivation of essential amino acids decreased IL-17 production below measurable limits (Figure 2b).

These results indicate that HOXB9 acts as a negative regulator of production of selective cytokines in activated human T cells, which could contribute to the repression of cellular metabolism in response to a lack of amino acids.

HOXB9 inhibits AP-1, and NFAT and NF- κ B activities but not ROR activity

We next investigated in more detail the basis for interference of cytokine production by HOXB9 in T cells. NFAT, AP-1 and NF- κ B are representative transcription factors that positively regulate the

production of cytokines after T-cell activation.²¹ We therefore investigated the influence of HOXB9 on NFAT, AP-1 and NF- κ B functions. Construct harboring the promoter including the binding sequence of each transcription factors in front of luciferase gene were transfected with a HOXB9 expression vector into Jurkat T cells, and the cells were activated by PMA/Ionomycin to activate the pathway from TCR/co-stimulation. As shown in Figure 3, HOXB9 significantly inhibited NFAT, AP-1 and NF- κ B activities.

As HOXB9 did not impair the production of IL-17 in human T cells, we also examined the effect of HOXB9 on the activity of retinoic acid receptor-related orphan receptor (ROR), which is a critical transcription factor for IL-17 expression.²² HOXB9 increased the expression of a luciferase gene placed behind the ROR binding element to a small extent (Figure 3), suggesting that HOXB9 slightly augments ROR activity, which might explain why HOXB9 does not suppress the production of IL-17 in activated T cells.

Taken together, these results suggest that HOXB9 acts as a potent negative regulator of activated human T cells in response to amino acid starvation by selective inhibition of transcriptional factors that are important for cytokine production.

Induction of HOXB9 expression is mediated by ATF4

We further investigated the mechanism of the induction of HOXB9 expression. GCN2 is one of the major sensors of amino acid shortage in various cells. Amino acids starvation increases uncharged transfer RNAs, which activate GCN2 and the downstream signal ATF4 transcription factor, leading to gene expression that is responsible for amino acid starvation. Indeed, ATF4 phosphorylation, which activates its transcription activity,²³ was enhanced by JPH203 in T cells (Figure 4a). ATF4 recognizes the consensus DNA binding sequence composed of (A/G/T)TT(G/T/A)CATCA.²⁴ We located the complete ATF4 consensus binding sequence (5'-ATTGCATCA-3') at 334 bp upstream of HOXB9 translation initiation site in the human genome. This fact prompted us to examine the involvement of ATF4 in the regulation of HOXB9 expression. We transfected ATF4 siRNA

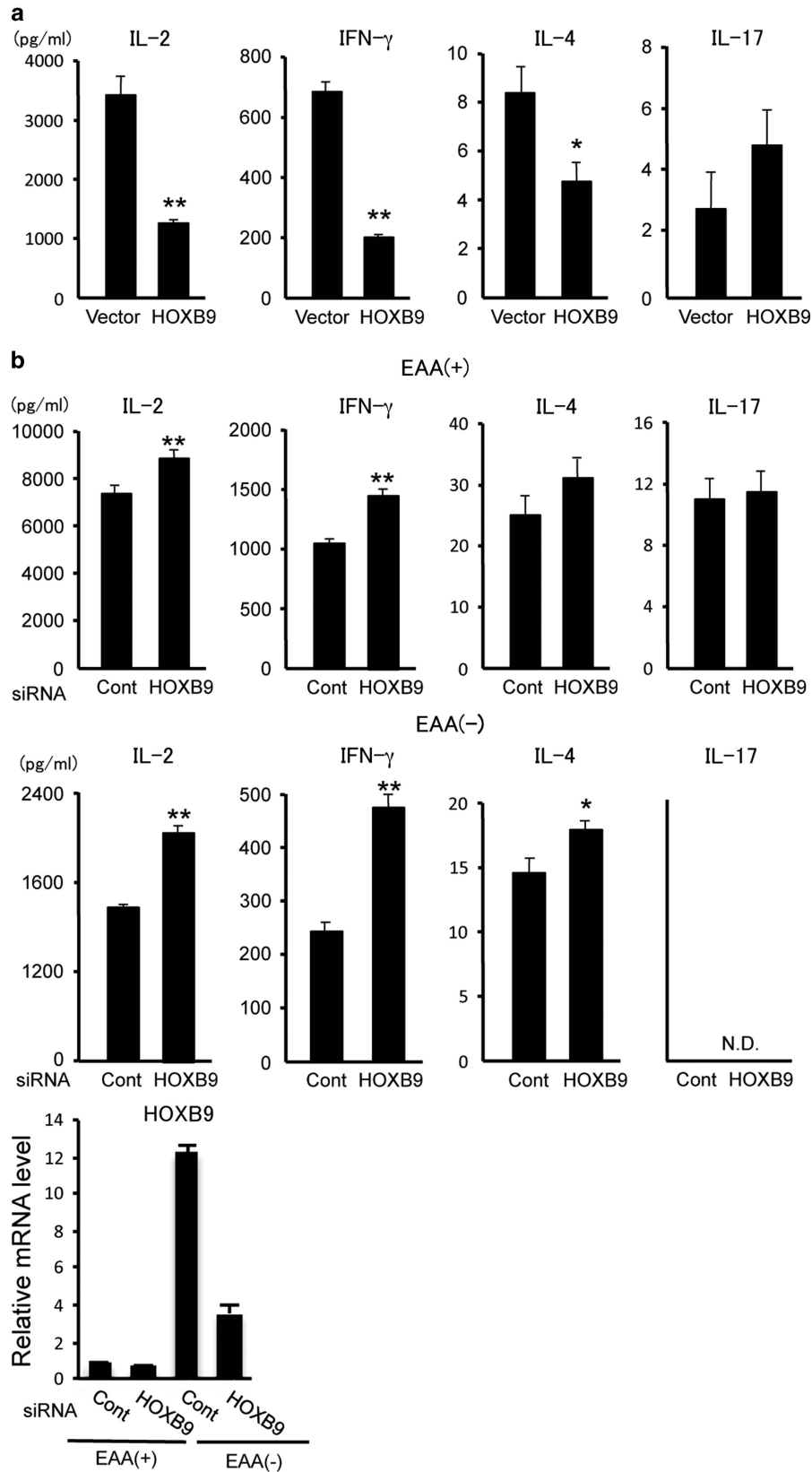


Figure 2 Effect of HOXB9 on T-cell activation. (a) Freshly isolated human CD4⁺ T cells were transfected with a HOXB9 expression vector and activated for 3 days. The concentrations of cytokines in the culture medium were determined. (b) Effect of HOXB9 siRNA on cytokine production. Freshly isolated human CD4⁺ T cells were transfected with HOXB9 siRNA or control siRNA and activated for 3 days with (EAA(+)) or without (EAA(-)) essential amino acids. The concentrations of cytokines in the culture medium were determined. ND, not detected. Data are representative of two separate experiments. Data are expressed as the mean \pm s.d. * P < 0.05, ** P < 0.01.

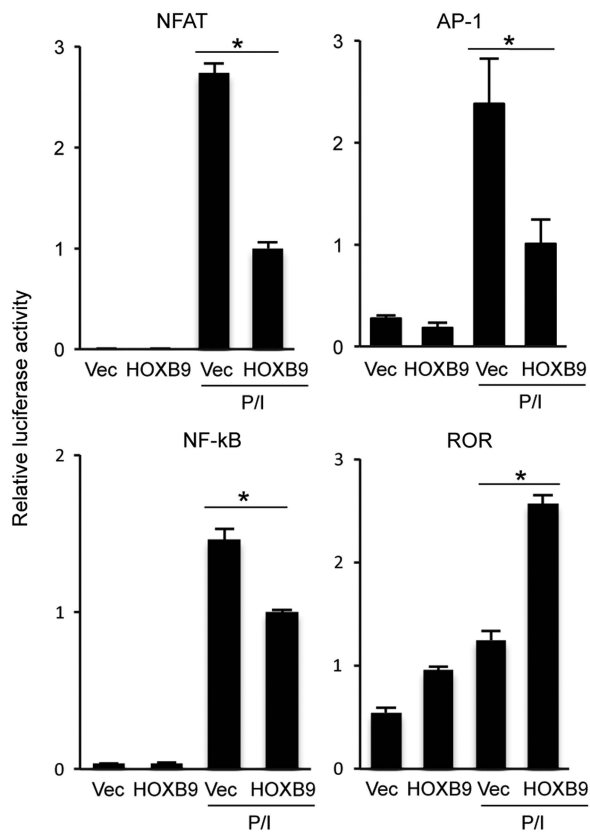


Figure 3 Effect of HOXB9 on activities of NFAT, AP-1, NF-κB and ROR. NFAT-, AP1-, NF-κB- or ROR-luc construct was transfected with empty vector (Vec) or the HOXB9 expression vector into Jurkat T cells. The cells were treated with PMA and Ionomycin (P/I) for 7 h. Luciferase activity was measured and normalized with activity of pRL-TK-luc. Data are representative of two separate experiments. Data are expressed as the mean \pm s.d. * $P < 0.01$.

into human primary T cells and stimulated the cells with anti-CD3/CD28 antibody and analyzed the HOXB9 expression. ATF4 siRNA functioned successfully in a substantial decrease in the expression level of ATF4 (Figure 4b). HOXB9 expression was drastically suppressed by ATF4 siRNA in essential amino acid-starved T cells (Figure 4b). These results indicate that the induction of HOXB9 expression on amino acid starvation in activated T cells is mediated by ATF4.

DISCUSSION

Prompt attention to nutrient deficiency is crucial for the survival of activated T cells as, if T cells leave it untreated, they will synthesize aberrant cellular components and exhaust their energy, resulting in cell death. In this study, we identified a new mechanism to address amino acid starvation in activated T cells wherein HOXB9, a factor known to be a morphogenesis regulator, is upregulated by ATF4 and down-modulates the activity of transcription factors that are crucial for cytokine production. These processes enable activated T cells to avoid wasteful consumption of energy and material for prolonged survival under a condition of nutrient scarcity.

The HOX family is composed of 39 genes,²⁵ but little is known about their functions other than functions in morphogenesis and cancer. Our study revealed a novel role of HOX gene; HOXB9 acts as one of the factors to overcome the difficulty following amino acid starvation in T cells.

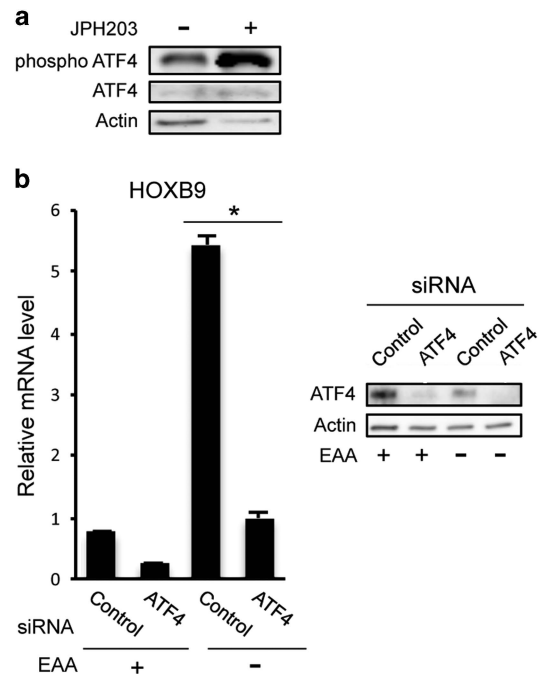


Figure 4 Effect of ATF4 on HOXB9 expression. (a) Promotion of ATF4 phosphorylation by JPH203 in activated CD4⁺ T cells. (b) Freshly isolated human CD4⁺ T cells were transfected with ATF4-specific siRNA or control siRNA and activated in the presence or absence of essential amino acids for 3 days. The expression of HOXB9 was determined by RT-PCR. Data are representative of two separate experiments. Data are expressed as the mean \pm s.d. * $P < 0.01$.

We found that the induction of HOXB9 expression is mediated by ATF4. Although ATF4 is activated by signals from the amino acid sensor GCN2,^{9,10} the target genes of ATF4 are not clear. Our study demonstrating that HOXB9 triggered by ATF4 diminishes the activities of transcription factors for cytokine production provides a new insight into the machinery by which ATF4 enables cellular material and energy to be saved by modulating its target genes in amino acid-deficient T cells.

Of interest is that not all cytokine production was impaired by HOXB9. In this regard, we assume that multiple factors are involved in halting T-cell activity when amino acids are starved. Indeed, we demonstrated that DNA-damage-inducible transcript 3 downshifts global cytokine production in response to amino acid deprivation in activated T cells.¹² The use of a combination of several factors with different characteristics probably provides T cells with most appropriate tuning of cellular metabolism that is suitable for survival in a minimum nutrient environment.

The regulation of preferential cytokine production by HOXB9 raises the possibility about connection between helper T-cells differentiation and HOXB9. We evaluated the expression of HOXB9 in Th1, Th2 and Th17 cells. All cells expressed almost the same level of HOXB9, although Th17 cells cultured with no essential amino acids had a slightly lower HOXB9 expression compared with other lineages (K.H., unpublished data). We also differentiated T-cells transfected with HOXB9 overexpression vector. However, we could not detect any effects of HOXB9 transfection on Th differentiation (K.H., unpublished data). Since T cells cannot maintain a high level of transfected gene expression for long periods with the electroporation method,

another transfection system such as virus infection will be required to resolve this issue.

In conclusion, we uncovered a previously unrecognized mechanism for adaptation to amino acid starvation in activated T cells. Our findings may contribute to an understanding of less well-known eventual targets of pathways monitoring nutrient availability for a downshift of intracellular metabolism in response to changes in nutrient conditions.

METHODS

Cells

Human peripheral blood mononuclear cells were isolated from healthy volunteers by the histopaque centrifugation method (Sigma, St. Louis, MO, USA). The study was approved by the Dokkyo Medical University Bioethics Committee. CD4-positive (CD4⁺) T cells were isolated by Dynabeads untouched human CD4 T cells kit (Invitrogen, Carlsbad, CA, USA). 5 × 10⁵ CD4⁺ T cells were activated by Dynabeads coated with anti-CD3/CD28 (Invitrogen) for the time indicated in RPMI1640 with 10% fetal calf serum. For experiment of essential amino acid starvation, HBSS with glucose (Invitrogen) including vitamin solution (Sigma), MEM non-essential amino acid solution (Invitrogen) and 10% fetal calf serum with or without MEM amino acid solution (Invitrogen) was used. JPH203 was described previously.²⁶

Transfection of human T cells

Pre-designed ATF4-specific siRNA (SI03019345) and its negative control siRNA (1027280) were purchased from Qiagen (Valencia, CA, USA). Pre-designed HOXB9-specific siRNA (s6813) and its control siRNA (negative control) were purchased from Ambion (Austin, TX, USA). siRNA (200 pmol) or plasmid (5 µg) was transfected into peripheral blood mononuclear cells using a nucleofector (Lonza, Basel, Switzerland) with a human T-cell nucleofection kit according to the manufacturer's instructions. CD4⁺ T cells were then purified and activated for 3 days as described above. For cytokine production analysis, the culture supernatant was measured by a cytometric bead array (Becton Dickinson, Franklin Lakes, NJ, USA).

Reporter assay

Jurkat cells were provided by RIKEN Bio-Resource Center (Tsukuba, Japan). The cells were transfected by electroporation as previously described.²⁷ ROR-luciferase (luc) was generated by insertion of ROR element sequence of IL-17 enhancer (5'-GAAAGTTTCTGACCCACTTTAAATCAATTT-3')²² into multi cloning site of pGL4.27 (Promega, Madison, WI, USA). AP-1- and NFAT-luc reporter constructs were described previously.²⁷ NF-κB-luc reporter construct was obtained by inserting NF-κB consensus binding sequence (TTTCCGGGGA) into multi cloning site of pGL4.27 (Promega). Firefly luciferase activity was assessed using a Dual Glo luciferase assay system (Promega) and normalized by the activity of renilla luciferase derived from cotransfected pRL-TK (Promega).

Quantitative RT-PCR

Total RNA was extracted using an RNeasy mini kit (Qiagen). Complementary DNA (cDNA) was synthesized from total RNA using a prime-script RT reagent kit (Takara Bio, Shiga, Japan). RT-PCR was performed with SYBR Premix Ex Taq (Takara Bio). Pre-designed primers for RT-PCR (HA162384 for HOXB9 and HA067812 for GAPDH) were purchased from Takara Bio. ~~The sequences of primers for detection of ATF4 are 5'-CGAATGGCTGGCTGTGGATG-3' and 5'-AGGGCATCCAAGTCGAACCTC-3'.~~

Copy numbers of HOXB9 and GAPDH mRNA were determined using plasmid as a standard.

Plasmid construct

Human HOXB9 cDNA was obtained by the PCR method using cDNA synthesized from human T-cell mRNA as a template. The cDNA fragment was inserted into pcDNA3.

Western blot

For analysis of ATF4 phosphorylation, purified CD4⁺ T cells were stimulated for 1 day in the presence of JPH203 and lysed with 20 mM Tris-HCl (pH 7.5), 150 mM NaCl, 1% Nonidet P-40, 20 mM sodium phosphate, 5 mM sodium pyrophosphate, 1 mM Na₃VO₄, 10 mM NaF, 3 mM β-glycerophosphate and protease inhibitor. After centrifugation at 16 000 g (5 min, 4 °C), the supernatant was used for western blot. For detection of ATF4 in siRNA-transfected T cells, 2 × 10⁴ cells were lysed in sodium dodecyl sulfate sample buffer and boiled. Electrophoresis with sodium dodecyl sulfate–polyacrylamide gel electrophoresis and immunoblotting were performed with a standard protocol. The anti-human phospho ATF4 (Ser245) and anti-human ATF4 (C-20) were purchased from Bioss (Boston, MA, USA) and Santa Cruz Biotechnology (Dallas, TX, USA), respectively.

Statistical analysis

All statistical significance was tested with Student's *t*-test.

CONFLICT OF INTEREST

The authors declare no conflict of interest.

ACKNOWLEDGEMENTS

We thank Dr Amnon Altman at La Jolla Institute for Allergy and Immunology for providing plasmid of AP-1- and NFAT-luciferase reporter constructs.

- 1 Efeyan A, Comb WC, Sabatini DM. Nutrient-sensing mechanisms and pathways. *Nature* 2015; **517**: 302–310.
- 2 Taylor PM. Role of amino acid transporters in amino acid sensing. *Am J Clin Nutr* 2014; **99**: 223S–230S.
- 3 Bar-Peled L, Sabatini DM. Regulation of mTORC1 by amino acids. *Trends Cell Biol* 2014; **24**: 400–406.
- 4 Sengupta S, Peterson TR, Sabatini DM. Regulation of the mTOR complex 1 pathway by nutrients, growth factors, and stress. *Mol Cell* 2010; **40**: 310–322.
- 5 Aramburu J, Ortells MC, Tejedor S, Buxadé M, López-Rodríguez C. Transcriptional regulation of the stress response by mTOR. *Sci Signal* 2014; **7**: re2.
- 6 Sood R, Porter AC, Olsen D, Cavener DR, Wek RC. A mammalian homologue of GCN2 protein kinase important for translational control by phosphorylation of eukaryotic initiation factor-2alpha. *Genetics* 2000; **154**: 787–801.
- 7 Berlanga JJ, Santoyo J, De Haro C. Characterization of a mammalian homolog of the GCN2 eukaryotic initiation factor 2alpha kinase. *Eur J Biochem* 1999; **265**: 754–762.
- 8 Harding HP, Novoa I, Zhang Y, Zeng H, Wek R, Schapira M. Regulated translation initiation controls stress-induced gene expression in mammalian cells. *Mol Cell* 2000; **6**: 1099–1108.
- 9 Castilho BA, Shanmugam R, Silva RC, Ramesh R, Himme BM, Sattlegger E. Keeping the eIF2 alpha kinase Gcn2 in check. *Biophys Acta* 2014; **1843**: 1948–1968.
- 10 Ye J, Kumanova M, Hart LS, Sloane K, Zhang H, De Panis DN *et al*. The GCN2-ATF4 pathway is critical for tumour cell survival and proliferation in response to nutrient deprivation. *EMBO J* 2010; **29**: 2082–2096.
- 11 Morimoto E, Kanai Y, Kim K, Chairoungdua A, Choi HW, Wempe MF *et al*. Establishment and characterization of mammalian cell lines stably expressing human L-type amino acid transporters. *J Pharmacol Sci* 2008; **108**: 505–516.
- 12 Hayashi K, Jutabha P, Endou H, Sagara H, Anzai N. LAT1 is a critical transporter of essential amino acids for immune reactions in activated human T cells. *J Immunol* 2013; **191**: 4080–4085.
- 13 Sinclair LV, Rolf J, Emslie E, Shi YB, Taylor PM, Cantrell DA. Control of amino-acid transport by antigen receptors coordinates the metabolic reprogramming essential for T cell differentiation. *Nat Immunol* 2013; **14**: 500–508.
- 14 Hayashi K, Anzai N. Role of LAT1 in the promotion of amino acid incorporation in activated T cells. *Crit Rev Immunol* 2014; **34**: 467–479.
- 15 Wellik DM. Hox genes and vertebrate axial pattern. *Curr Top Dev Biol* 2009; **88**: 257–278.
- 16 Favier B, Dollé P. Developmental functions of mammalian Hox genes. *Mol Hum Reprod* 1997; **3**: 115–131.
- 17 McGinnis W. Homeobox genes and axial patterning. *Cell* 1992; **68**: 283–302.
- 18 Rawat VP, Humphries RK, Buske C. Beyond Hox: the role of ParaHox genes in normal and malignant hematopoiesis. *Blood* 2012; **120**: 519–527.
- 19 Shah N, Sukumar S. The Hox genes and their roles in oncogenesis. *Nat Rev Cancer* 2010; **10**: 361–371.
- 20 Nguyen DX, Chiang AC, Zhang XH, Kim JY, Kris MG, Ladanyi M *et al*. WNT/TCF signaling through Lef1 and HOXB9 mediates lung adenocarcinoma metastasis. *Cell* 2009; **138**: 51–62.

- 21 Macián F, López-Rodríguez C, Rao A. Partners in transcription: NFAT and AP-1. *Oncogene* 2001; **20**: 2476–2489.
- 22 Yang XO, Pappu BP, Nurieva R, Akimzhanov A, Kang HS, Chung Y *et al*. T helper 17 lineage differentiation is programmed by orphan nuclear receptors ROR alpha and ROR gamma. *Immunity* 2008; **28**: 29–39.
- 23 Ampofo E, Sokolowsky T, Götz C, Montenarh M. Functional interaction of protein kinase CK2 and activating transcription factor 4 (ATF4), a key player in the cellular stress response. *Biochim Biophys Acta* 2013; **1833**: 439–451.
- 24 Kilberg MS, Shan J, Su N. ATF4-dependent transcription mediates signaling of amino acid limitation. *Trends Endocrinol Metab* 2009; **20**: 436–443.
- 25 Quinonez SC, Innis JW. Human HOX gene disorders. *Mol Genet Metab* 2014; **111**: 4–15.
- 26 Oda K, Hosoda N, Endo H, Saito K, Tsujihara K, Yamamura M *et al*. L-type amino acid transporter 1 inhibitors inhibit tumor cell growth. *Cancer Sci* 2010; **101**: 173–179.
- 27 Hayashi K, Altman A. Filamin A is required for T cell activation mediated by protein kinase C-theta. *J Immunol* 2006; **177**: 1721–1728.



Contents lists available at ScienceDirect

Journal of Pharmacological Sciences

journal homepage: www.elsevier.com/locate/jphs

Short communication

LAT1 acts as a crucial transporter of amino acids in human thymic carcinoma cells

Keitaro Hayashi ^a, Promsuk Jutabha ^a, Sumiko Maeda ^b, Yothaisong Supak ^a,
Motoshi Ouchi ^a, Hitoshi Endou ^c, Tomoe Fujita ^a, Masayuki Chida ^b, Naohiko Anzai ^{a, d, *}

^a Department of Pharmacology and Toxicology, Dokkyo Medical University School of Medicine, Shimotsuga, Tochigi 321-0293, Japan

^b Department of General Thoracic Surgery, Dokkyo Medical University School of Medicine, Shimotsuga, Tochigi 321-0293, Japan

^c J-Pharma Co., Ltd., Yokohama, Kanagawa 230-0046, Japan

^d Department of Pharmacology, Chiba University Graduate School of Medicine, Chuo, Chiba 260-8670, Japan

ARTICLE INFO

Article history:

Received 28 March 2016

Received in revised form

27 June 2016

Accepted 11 July 2016

Available online xxx

Keywords:

Thymic carcinoma

Anticancer drug

Transporter

ABSTRACT

L-type amino acid transporter 1 (LAT1, SLC7A5) incorporates essential amino acids into cells. Recent studies have shown that LAT1 is a predominant transporter in various human cancers. However, the function of LAT1 in thymic carcinoma remains unknown. Here we demonstrate that LAT1 is a critical transporter for human thymic carcinoma cells. LAT1 was strongly expressed in human thymic carcinoma tissues. LAT1-specific inhibitor significantly suppressed leucine uptake and growth of Ty82 human thymic carcinoma cell lines, suggesting that thymic carcinoma takes advantage of LAT1 as a quality transporter and that LAT1-specific inhibitor might be clinically beneficial in therapy for thymic carcinoma.

© 2016 The Authors. Production and hosting by Elsevier B.V. on behalf of Japanese Pharmacological Society. This is an open access article under the CC BY-NC-ND license (<http://creativecommons.org/licenses/by-nc-nd/4.0/>).

Thymic carcinomas are rare malignant tumors and are often in an advanced stage when detected (1). Although chemotherapy is the mainstay of treatment for thymic carcinomas, patients frequently show resistance to drugs and more efficacious treatment should therefore be established.

LAT1 is a transporter that incorporates essential amino acids into cells. A unique feature of LAT1 is its extremely high expression in many human cancers (2,3), whereas only a small amount of LAT1 is detected in a healthy body (4,5), though LAT1 still has a clear role in normal tissues (6–8).

A LAT1-specific inhibitor has shown powerful suppressive effects on many cancer cell lines *in vitro* and *in vivo* (9) and is currently under evaluation in a clinical trial of cancer patients. Although a wide range of human cancers express LAT1, little is known about LAT1 in thymic carcinomas. In this study, we investigated the role of LAT1 in human thymic carcinoma.

Ty82 human thymic carcinoma cells were purchased from Japanese Collection of Research Bioresources Cell Bank (Ibaraki). The cells were cultured in RPMI1640 containing 10% FCS. S2 cells stably transfected with empty vector, human LAT1 and LAT2 were described previously (9).

Anti-LAT1 antibody (mouse monoclonal) was kindly provided by J-Pharma (Tokyo).

Anti-β-actin antibody (clone C4) was purchased from Merck Millipore (Darmstadt, Germany).

For human tissue staining, surgically excised thymic carcinoma or thymoma was fixed with formalin, embedded with paraffin, and sliced. The samples were stained with anti-LAT1 antibody and detected by DAB. The study using human tissue was approved by Dokkyo Medical University Bioethics Committee.

For western blot analysis, cells were lysed with lysis buffer (50 mM Tris–HCl pH 7.8, 150 mM NaCl, 5 mM EDTA, 1% Tween-20, 10 mM NaF, 1 mM Na₃VO₄, 3 mM β-glycerophosphate, 5 mM pyrophosphate, protease inhibitor cocktail (Roche Diagnostics, Basel, Switzerland)). Protein amount was determined using BCA Protein Assay Kit (Thermo Fisher Scientific, Waltham, MA, USA). Western blot was performed with 3.5 μg of total protein as described previously (10).

JPH203 was described previously (9).

* Corresponding author. Department of Pharmacology, Chiba University Graduate School of Medicine, 1-8-1, Inohana, Chuo, Chiba 260-8670, Japan. FAX: +81 43 226 2052.

E-mail address: anzai-path@umin.ac.jp (N. Anzai).

Peer review under responsibility of Japanese Pharmacological Society.

<http://dx.doi.org/10.1016/j.jphs.2016.07.006>

1347-8613/© 2016 The Authors. Production and hosting by Elsevier B.V. on behalf of Japanese Pharmacological Society. This is an open access article under the CC BY-NC-ND license (<http://creativecommons.org/licenses/by-nc-nd/4.0/>).

[¹⁴C]-L-leucine uptake was initiated by incubating the cells in HBSS containing 1.0 μM [¹⁴C]-L-leucine (Moravek, Brea, CA, USA) and JPH203 at 37 °C for 1 min. Uptake was terminated by washing the cells 3 times with ice cold HBSS. Cells were lysed with 0.1N NaOH and radioactivity was measured using an LSC-5100 β-scintillation counter (Aloka, Tokyo).

For apoptosis analysis, the cells were stained with annexin V-FITC and propidium iodide (Medical & Biological Laboratories, Nagoya) and analyzed by FACS (Becton Dickinson, Franklin Lakes, New Zealand).

For cell cycle analysis, the cells were initially fixed with 70% ethanol. After washing the cells with PBS, cells were treated with RNase A (100 μg/ml) for 30 min at 37 °C and further incubated with 2 μg/ml of propidium iodide for 10 min at room temperature. Cell cycle was analyzed with FACS.

All statistical significance was tested with Student's t-test by comparing JPH203-treated samples with control sample.

To understand the role of LAT1 in thymic carcinoma, we initially analyzed the expression of LAT1 in human thymic carcinoma tissues. Strong expression of LAT1 was detected in thymic carcinoma

(Fig. 1A). On the other hand, LAT1 was hardly found in thymoma (non-cancer) tissue (Fig. 1A). We next examined LAT1 expression in Ty82 human thymic carcinoma cell line. Ty82 cells expressed LAT1 at a high level (Fig. 1B). These results indicate that LAT1 expression is facilitated in human thymic carcinoma cells.

To investigate the functional significance of LAT1 in thymic carcinoma, we assessed the effects of JPH203, a LAT1-specific inhibitor, on the incorporation of amino acids in Ty82 cells. The cells were incubated with or without JPH203 for 1 min and uptake of [¹⁴C]-labeled L-leucine was analyzed. JPH203 impaired the uptake of leucine in a dose-dependent manner (Fig. 2). These results indicate that LAT1 is crucial transporter of amino acids in Ty82 cells.

We next examined the effect of a LAT1-specific inhibitor on growth of Ty82 cells. The cells were cultured in the presence or absence of JPH203 and the number of cells was counted. The number of Ty82 cells was clearly reduced by JPH203 (Fig. 3A). To determine whether the reduction of Ty82 cells by JPH203 arises from aberrance of the cell cycle or cell death, we first analyzed the survival rate of Ty82 cells treated with JPH203 by annexin V and

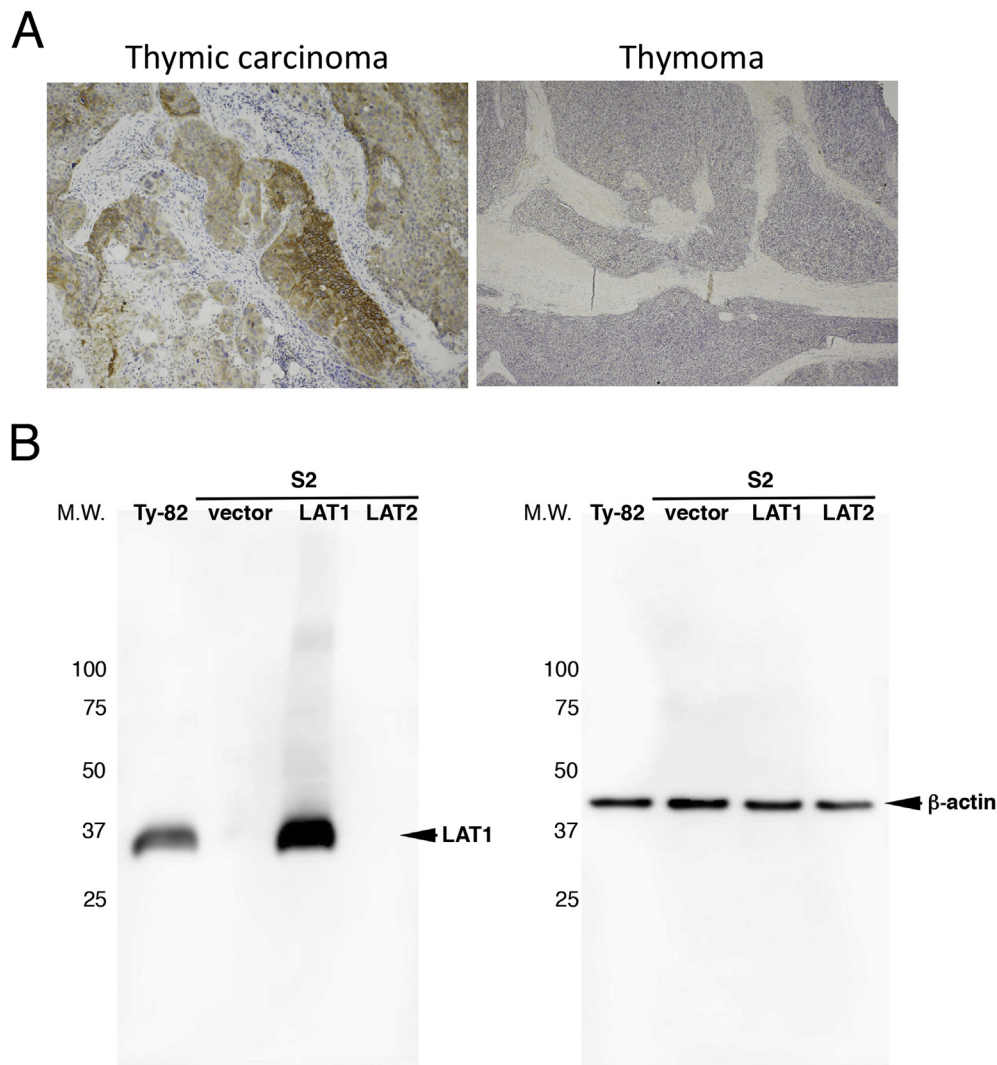


Fig. 1. LAT1 is a critical transporter of amino acids in thymic carcinoma cells. (A) Tissue staining of human thymic carcinoma (left) and thymoma (right) with anti-LAT1 antibody. (B) Ty82 cells were lysed and LAT1 protein was detected by western blot. As controls, lysates from S2 cells stably transfected with an empty vector (negative control), LAT1 (positive control), and LAT2 (negative control) were also used.

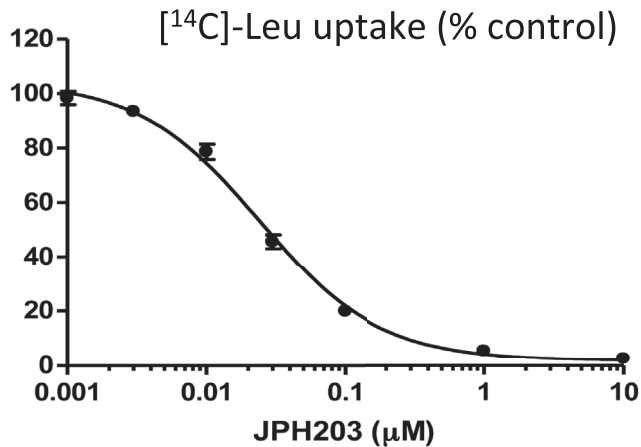


Fig. 2. Impaired incorporation of leucine by JPH203. [^{14}C]-L-leucine and JPH203 were added to Ty82 cells and leucine uptake was analyzed by measuring radioactivity. Data expressed as the mean \pm S.D.

propidium iodide (PI) staining. 100 μM JPH203 increased apoptotic cells (annexin V single positive cells) as well as total dead cells (annexin V positive cells plus PI positive cells) (Fig. 3B), indicating

that a high concentration of JPH203 induces cell death of Ty-82 that is derived from apoptosis. We also found that JPH203 modestly decreased the population of Ty82 cells in S phase and increased the population of cells in G1 phase (Fig. 3C), suggesting that JPH203 prevents progression of the cell cycle from G1 phase to S phase. These results indicate that JPH203 has an anti-proliferative effect on Ty-82 cells that is achieved by both cell death and G1 arrest.

Here we demonstrated that a LAT1-specific inhibitor has the ability to exert anticancer effects against thymic carcinoma cells. Since thymic carcinoma is a relatively infrequent disorder and there has not been sufficient progress in its therapeutic approach, the results of our study could offer an additional and effective treatment option for thymic carcinoma using a LAT1 inhibitor. However, in our study, high concentration of JPH203 was required for the sufficient suppression of Ty-82 cells. In experiments with mice, it appears that the concentration of JPH203 in blood can exceed 100 μM at the point of administration, but immediately drops into single digit (9). This result suggests that it is difficult to maintain a high concentration of JPH203 *in vivo*. Therefore, it is recommended combining JPH203 at low concentration with other anti-cancer drugs to maximize the therapeutic efficacy and minimize adverse effects when JPH203 is used for clinical application.

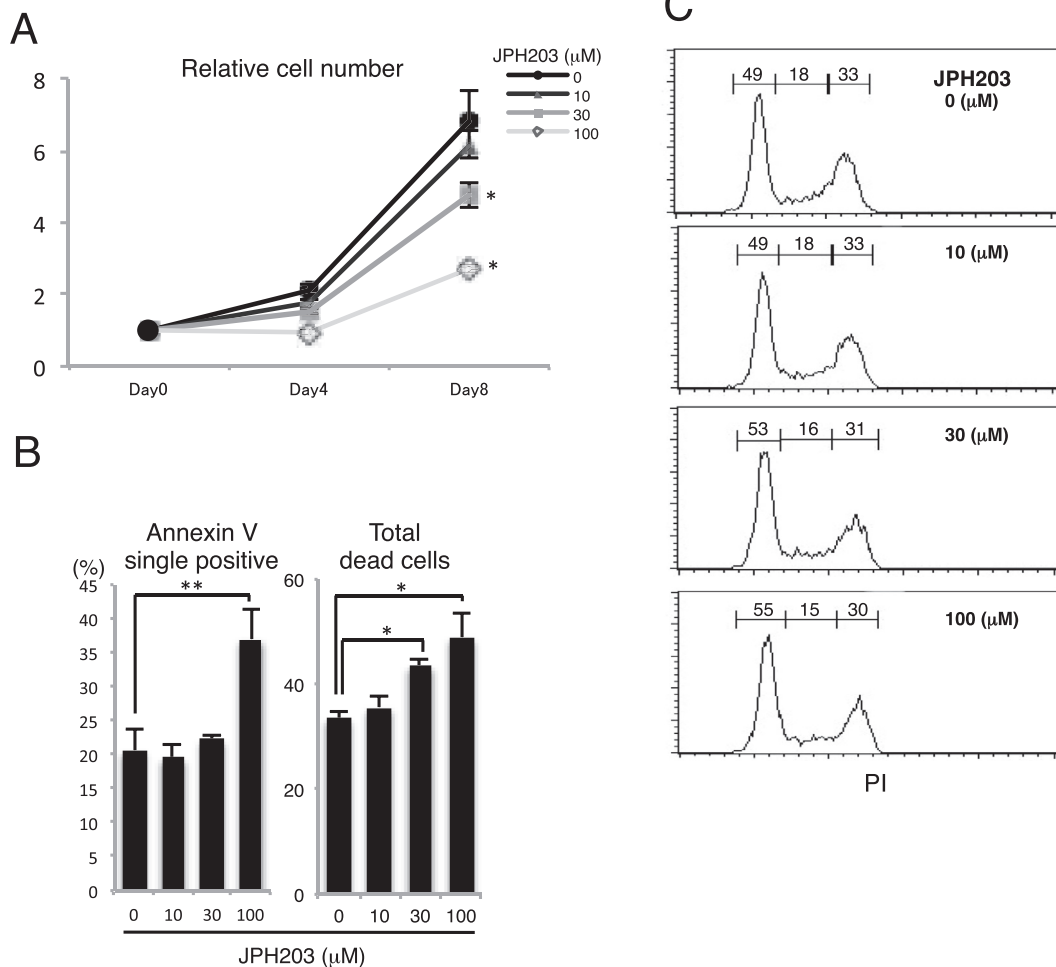


Fig. 3. Effect of JPH203 on growth of Ty82 cells. (A) Cells were cultured with JPH203 for the indicated days. The number of the cells was counted, and relative cell number to day 0 is shown. Data expressed as the mean \pm S.D. * $P < 0.01$. (B) Cells were cultured with JPH203 for 3 days and stained with annexinV and Propidium Iodide (PI). Data expressed as the mean \pm S.D. * $P < 0.01$. ** $P = 0.011$. (C) Cells were cultured with JPH203 for 4 days and the cell cycle was analyzed by staining the cells with PI. The numbers on the top of the histogram indicate the percentages of cells in G1, S and G2 phase from the left.

Conflicts of interest

The authors indicated no potential conflicts of interest.

Acknowledgments

This study was supported by JSPS KAKENHI Grant Number 26670631 and MEXT Program for the Strategic Research Foundation at Private Universities Grant Number S1412001.

References

- (1) Ahmad U, Yao X, Detterbeck F, Huang J, Antonicelli A, Filosso PL, et al. Thymic carcinoma outcomes and prognosis: results of an international analysis. *J Thorac Cardiovasc Surg.* 2015;149:95–100.
- (2) Yanagida O, Kanai Y, Chairoungdua A, Kim DK, Segawa H, Nii T, et al. Human L-type amino acid transporter 1 (LAT1): characterization of function and expression in tumor cell lines. *Biochim Biophys Acta.* 2001;1514:291–302.
- (3) Kanai Y, Segawa H, Miyamoto K, Uchino H, Takeda E, Endou H. Expression cloning and characterization of a transporter for large neutral amino acids activated by the heavy chain of 4F2 antigen (CD98). *J Biol Chem.* 1998;273:23629–23632.
- (4) Kanai Y, Endou H. Heterodimeric amino acid transporters: molecular biology and pathological and pharmacological relevance. *Curr Drug Metab.* 2001;2:339–354.
- (5) Matsuo H, Tsukada S, Nakata T, Chairoungdua A, Kim DK, Cha SH, et al. Expression of a system L neutral amino acid transporter at the blood-brain barrier. *Neuroreport.* 2000;11:3507–3511.
- (6) Hayashi K, Jutabha P, Kamai T, Endou H, Anzai N. LAT1 is a central transporter of essential amino acids in human umbilical vein endothelial cells. *J Pharmacol Sci.* 2014;124:511–513.
- (7) Hayashi K, Ouchi M, Endou H, Anzai N. HOXB9 acts as a negative regulator of activated human T cells in response to amino acid deficiency. *Immunol Cell Biol.* 2016;94:612–617.
- (8) Hayashi K, Anzai N. Role of LAT1 in the promotion of amino acid incorporation in activated T cells. *Crit Rev Immunol.* 2014;34:467–479.
- (9) Oda K, Hosoda N, Endo H, Saito K, Tsujihara K, Yamamura M, et al. L-type amino acid transporter 1 inhibitors inhibit tumor cell growth. *Cancer Sci.* 2010;101:173–179.
- (10) Hayashi K, Jutabha P, Endou H, Anzai N. c-Myc is crucial for the expression of LAT1 in MIA Paca-2 human pancreatic cancer cells. *Oncol Rep.* 2012;28:862–866.

Novel therapeutic approaches targeting L-type amino acid transporters for cancer treatment

Keitaro Hayashi, Naohiko Anzai

Keitaro Hayashi, Naohiko Anzai, Department of Pharmacology and Toxicology, Dokkyo Medical University School of Medicine, Shimotsuga, Tochigi 321-0293, Japan

Naohiko Anzai, Department of Pharmacology, Chiba University Graduate School of Medicine, Chuo, Chiba 260-8670, Japan

Author contributions: Hayashi K wrote the manuscript; Anzai N reviewed the manuscript.

Conflict-of-interest statement: There is no conflict of interest associated with any of the senior author or other coauthors contributed their efforts in this manuscript.

Open-Access: This article is an open-access article which was selected by an in-house editor and fully peer-reviewed by external reviewers. It is distributed in accordance with the Creative Commons Attribution Non Commercial (CC BY-NC 4.0) license, which permits others to distribute, remix, adapt, build upon this work non-commercially, and license their derivative works on different terms, provided the original work is properly cited and the use is non-commercial. See: <http://creativecommons.org/licenses/by-nc/4.0/>

Manuscript source: Invited manuscript

Correspondence to: Keitaro Hayashi, PhD, Associate Professor, Department of Pharmacology and Toxicology, Dokkyo Medical University School of Medicine, 880 Kitakobayashi, Mibu, Shimotsuga, Tochigi 321-0293, Japan. khayashi@dokkyomed.ac.jp
Telephone: +81-282-872128
Fax: +81-282-862915

Received: August 15, 2016
Peer-review started: August 16, 2016
First decision: September 28, 2016
Revised: October 8, 2016
Accepted: November 1, 2016
Article in press: November 2, 2016
Published online: January 15, 2017

Abstract

L-type amino acid transporters (LATs) mainly assist the

uptake of neutral amino acids into cells. Four LATs (LAT1, LAT2, LAT3 and LAT4) have so far been identified. LAT1 (SLC7A5) has been attracting much attention in the field of cancer research since it is commonly up-regulated in various cancers. Basic research has made it increasingly clear that LAT1 plays a predominant role in malignancy. The functional significance of LAT1 in cancer and the potential therapeutic application of the features of LAT1 to cancer management are described in this review.

Key words: LAT1; Amino acid transporter; Molecular target drug; Amino acid starvation response; Signal transduction

© **The Author(s) 2017.** Published by Baishideng Publishing Group Inc. All rights reserved.

Core tip: The discovery of molecules preferentially expressed in cancer cells is extremely valuable for the development of molecular target drugs in cancer therapy. Amino acid transporters have been receiving a great amount of attention as a candidate of such molecular targets. This review summarizes new initiatives for clinical applications of the basic research relative to L-type amino acid transporters, which are commonly expressed in cancers.

Hayashi K, Anzai N. Novel therapeutic approaches targeting L-type amino acid transporters for cancer treatment. *World J Gastrointest Oncol* 2017; 9(1): 21-29 Available from: URL: <http://www.wjgnet.com/1948-5204/full/v9/i1/21.htm> DOI: <http://dx.doi.org/10.4251/wjgo.v9.i1.21>

INTRODUCTION

Cancers consume a huge amount of materials for biochemical reactions, and a continuous supply of sufficient nutrients is essential for their survival. Hydrophilic nutrients are delivered into cells by transporters.

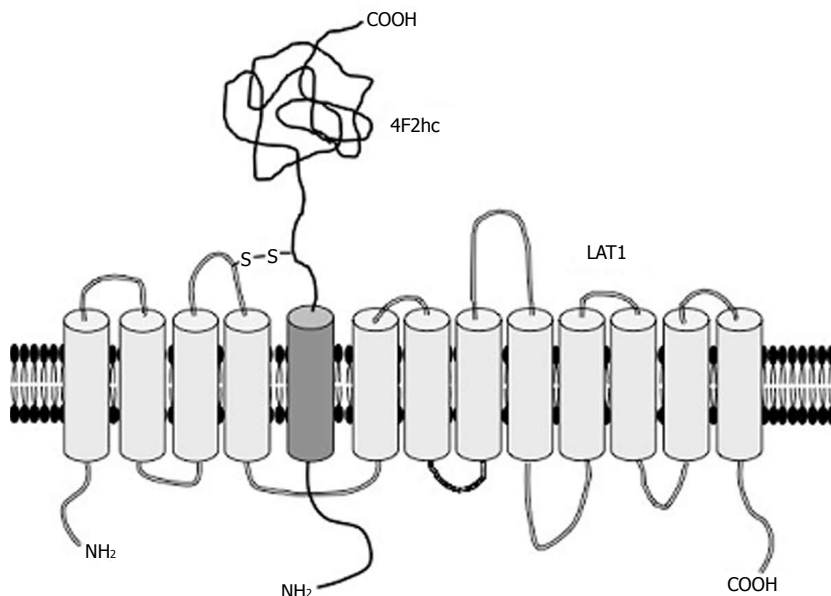


Figure 1 Structure of LAT1. LAT1 is composed of 12 transmembrane helices that are predicted to form a cylindrical conformation penetrating the cellular membrane. LAT1 associates with 4F2hc for stable localization at the cellular membrane. LAT2 is similar in structure to LAT1, whereas LAT3 and LAT4 function independently of 4F2hc.

Recent studies have revealed several transporters preferentially expressed in cancers. Inhibition of cancer specific-nutrient transporters would be a good strategy for cancer management with minimal side effects. Indeed, a therapeutic approach using transporter inhibitors for cancer prevention has been proven to be efficacious in cell lines and animal experiments and is now under evaluation in a clinical trial.

L-TYPE AMINO ACID TRANSPORTERS

Many cells take advantage of transporters to incorporate what is necessary at the time of need. Transporters fall into two broad categories based on ATP dependency for their transport form^[1]. ATP-dependent transporters, known as ATP-binding cassette, hydrolyze ATP to obtain the energy for translocation of their substrates across the membrane (active transport). Transporters with no ATPase, called solute carriers (SLCs), facilitate diffusive transport. Each SLC transporter is named in combination with the family numeral based on the sequence similarity and individual number with letter A between them (*e.g.*, SLC3A2), with a few exceptions. Most of the amino acid transporters were formerly categorized into several groups ("System") on the basis of their substrates and sodium dependency (*e.g.*, System L, which incorporates neutral amino acids without sodium), but they are currently classified into SLCs according to their protein homology.

L-type amino acid transporters (LATs) are categorized as system L transporters. LATs mainly deliver neutral amino acids into cells in a sodium-independent manner. So far, four LATs have been identified.

LAT1 (SLC7A5) was identified as the first LAT by

two groups in 1998^[2,3]. The major substrate of LAT1 is large neutral amino acids as typified by leucine. The expression of LAT1 in normal adults is detected in proliferative zones of gastrointestinal mucosa, testicular sertoli cells, ovarian follicular cells, pancreatic islet cells, and some endothelial cells that serve as a barrier between tissues (blood-brain, blood-retinal and blood-follicle barrier)^[4]. Recent studies revealed a crucial role of LAT1 in activated T cells^[5,6]. As described below, LAT1 expression is commonly up-regulated in various cancers.

LAT2 (SLC7A8) was subsequently isolated on the basis of sequence similarity to LAT1^[7-9]. LAT2 has broader specificity of its substrates including polar uncharged and small neutral amino acids than that of LAT1^[8]. LAT2 is ubiquitously expressed in normal body^[4], though LAT2 knockout mice show a mild phenotype and almost no visible symptoms except aminoaciduria^[10]. Both LAT1 and LAT2 are composed of 12 transmembrane domains that form the pathway of their substrates^[11] (Figure 1). They associate with the heavy glycoprotein subunit 4F2hc (SLC3A2) by sulfur bond^[11]. Although 4F2hc does not seem to have a function to directly transfer the substrates, it makes the localization of its partner LATs more stable at the plasma membrane^[12].

LAT3 (SLC43A1) was isolated by expression cloning from hepatocarcinoma cells^[13]. Sequence analysis revealed that LAT3 was identical to POV1, which was originally identified as a cancer-up-regulated gene^[14,15]. The substrate selectivity of LAT3 was similar to that of LAT1. LAT3 mRNA is expressed in the liver, skeletal muscle, and pancreas^[16]. The physiological role of LAT3 in normal individuals of mammals remains unknown,

but it was shown that LAT3 functions for podocyte development in zebrafish^[17].

LAT3 appears to behave as a critical transporter in several cancers. LAT3 is up-regulated in response to androgen and knockdown of LAT3 expression by RNA interference (RNAi) significantly inhibits the leucine uptake and cell proliferation in human prostate cancer cell lines *in vitro*^[18]. Furthermore, high expression of LAT3 is detected in prostate cancer patients, and stably knockdown of LAT3 by RNAi in human prostate cancer cell lines results in decrease of their growth and metastatic potential with alteration of cell cycle gene expression after xenografts into mice^[19].

LAT4 (SLC43A2) was identified by searching for sequence homology to LAT3^[20]. LAT4 is expressed in the basolateral membrane of the small intestine, kidney proximal tubule and thick ascending limb epithelial cells. LAT4 knockout mice are smaller than their controls and die within 9 d, presumably because of defective amino acid absorption^[21]. Unlike LAT1 and LAT2, LAT3 as well as LAT4 functions independently of heavy chain.

LAT1

LAT1 is the most extensively studied transporter among LATs. The interest in LAT1 is because of its extremely high expression in diverse human cancers. LAT1 was originally cloned from mRNA of C6 glioma cells^[2]. Subsequent studies have shown that LAT1 is highly expressed in many cancer cell lines. Histological analysis with qualitatively enhanced antibodies confirmed potent expression of LAT1 in human cancers in a broad range of tissues. The number of cancer types that were reported to express a high level of LAT1 is well above twenty (Table 1). LAT1 is thus a commonly up-regulated amino acid transporter in multiple human cancers. Furthermore, LAT1 expression level appears to be associated with prognosis of cancer patients. For example, elevated expression of LAT1 correlates with an adverse prognosis in prostate^[22], gastric^[23], and pancreatic cancers^[24], suggesting that higher-grade tumors are more dependent on LAT1. Not only the expression of LAT1 but also the functional significance of LAT1 in cancers has been verified by use of its inhibitors, by knockdown with RNAi and by gene disruption. 2-Aminobicyclo (2,2,1) heptane-2-carboxylic acid (BCH) is an inhibitor of system L transporters. BCH inhibits leucine uptake and strongly suppresses the proliferation of many cancer cells (Table 1). Genetic manipulation confirmed the functional significance of LAT1 in cancer cells. Knockdown of LAT1 with RNAi^[25-29] as well as genetic disruption of *LAT1* by zinc fingers nucleases-mediated gene knockout^[12] in cancer cells reduces leucine uptake and cell proliferation, indicating that LAT1 is a predominant transporter that is essential for growth of cancers. The reason that so many cancers use LAT1 despite the presence of many other amino acid transporters might be that LAT1 has a prominent capability for substrate transport. Indeed,

the affinity of LAT1 for leucine is much higher than that of LAT2^[30], although LAT2 is ubiquitously expressed in the normal body^[4]. Cancers may therefore be more dependent on LAT1 for rapid uptake of sufficient amino acids, whereas normal cells need less amino acid delivery that can be supported by LAT2.

The definite effect of LAT1 on the growth of various cancer cell lines prompted researchers to apply the LAT1 inhibitor in a clinical setting. However, the concentration of BCH required for suppression of cancer growth is extremely high (usually around 10 mmol/L). Moreover, the unselective effect of BCH that inhibits all LATs is another problem, since LATs other than LAT1 are considered to have functions in the normal body. It has been necessary to develop drugs that act on just LAT1 but not other transporters at a low concentration. In 2010, Endo and colleagues designed a new compound named JPH203 ((S)-2-amino-3-(4-((5-amino-2-phenylbenzo[d]oxazol-7-yl) methoxy)-3,5-dichlorophenyl) propanoic acid)^[31]. JPH203 has structural analogy to tyrosine, but it inhibits only LAT1 without affecting any other LATs. JPH203 displayed potent suppressive effects on the growth of cancers *in vitro*^[12,32,33]. Moreover, this compound has the ability to powerfully inhibit the proliferation of tumor cell lines of the colon and leukemia injected into nude mice^[31,33]. Following improvements in its specificity and pharmacological effect, JPH203 is under evaluation in a phase I clinical trial of cancer patients.

CLINICAL APPLICATION OF LAT1

Positron emission tomography

By exploiting the characteristics of LAT1 expression, an approach for the diagnosis of cancers through radiolabeled substrates of LAT1 has been attempted. [¹⁸F] or [¹¹C]-labeled compound administered into the body can be visualized by positron emission tomography (PET)^[34]. Cancers incorporating an isotopically labeled probe can be located by tracing the body with PET. In the past, 2-¹⁸F-fluoro-2-deoxy-d-glucose ([¹⁸F]FDG) was one of the most commonly used probe for diagnosis of cancer with PET. This strategy exploits the characteristic of cancers consuming a huge amount of glucose compared to that consumed by normal cells. Although [¹⁸F]FDG has been of assistance in the clinical diagnosis of many cancers, it sometimes showed false positive results, especially in brain, because even normal brain cells take up a relatively large amount of glucose. To overcome this problem, amino acids have attracted attention as alternative probes to glucose. Representative amino acids or their analogs developed as probes of PET are L-3-[¹⁸F]-fluoro- α -methyl tyrosine ([¹⁸F]FAMT), 6-¹⁸F-fluoro-L-3,4-dihydroxy-phenylalanine (¹⁸F-DOPA), L-[¹¹C-methyl] methionine ([¹¹C]MET) and O-(2-[¹⁸F]fluoroethyl)-L-tyrosine ([¹⁸F]FET). If the compounds are delivered into cells specifically through LAT1, those cells are likely to be cancers. Indeed,

Table 1 Summary of studies for expression and functions of LAT1 in cancers

Cancer	Expression (method of detection)	Inhibition of amino acid uptake by	Growth inhibition by	Ref.
Biliary tract	Immunohistochemistry	BCH	BCH	[71]
Bladder	Northern blot (cell line)	BCH		[72]
Bone	Immunohistochemistry			[73]
Brain	Immunohistochemistry, RT-PCR (cell line), Western blot (tissue, cell line)	BCH	BCH	[74,75]
Breast	Immunohistochemistry, RT-PCR (cell line)	BCH	RNAi, BCH	[29,76-78]
Colon	Western blot (cell line)	Knockout (cell line)	Knockout (cell line) JPH203	[12]
Esophagus	Immunohistochemistry			[79,80]
Hepatocyte	Immunohistochemistry			[81]
Gastrointestine	Immunohistochemistry, Western blot (cell line)		RNAi	[23,45]
Laryngeal	Immunohistochemistry			[82]
Leukemia	RT-PCR (cell line)		BCH, JPH203	[33]
Lung	Immunohistochemistry			[41,83-85]
Melanoma	Immunohistochemistry, Microarray (tissue), Western blot (cell line)	BCH		[86,87]
Myeloma	RT-PCR (cell line)	RNAi		[88]
Neuroendocrine	Immunohistochemistry, RT-PCR (tissue), Western blot (tissue)			[89]
Ovarian	Immunohistochemistry, RT-PCR (cell line), Western blot (tissue, cell line)	BCH	BCH	[47,65,90]
Oral	RT-PCR (cell line)	RNAi	RNAi	[25]
Pancreas	Immunohistochemistry, Western blot (cell line)	RNAi	RNAi	[24,27,91]
Pleura	Immunohistochemistry			[92]
Prostate	Immunohistochemistry, Western blot (cell line)	RNAi, BCH	RNAi, BCH	[18,19,22,28]
Tongue	Immunohistochemistry			[93]
Thymus	Immunohistochemistry, Western blot (cell line)	JPH203	JPH203	[94,95]
Urinary tract	Immunohistochemistry			[96]

RT-PCR: Reverse transcription polymerase chain reaction; BCH: 2-aminobicyclo (2,2,1) heptane-2-carboxylic acid.

[¹⁸F]FAMT images accord well with LAT1 distribution^[35]. Moreover, FAMT is incorporated by LAT1 but not by other amino acid transporters^[35]. Although there is still room for improvement in its specificity, this method is powerful tool for diagnosis of cancers including microcarcinoma.

Boron neutron capture therapy

LAT1 is an attractive molecular target for boron neutron capture therapy (BNCT). BNCT is an anticancer therapy that utilizes high linear energy transfer alpha particles. Particle radiation is produced by fission reaction when irradiated thermal neutrons collide with boron incorporated by a malignant tumor. The traveling distance of particle radiation is limited (5-9 μm), and it therefore disrupts only cancer cells incorporating boron without damage to other cells around target cells^[36,37]. A key component of BNCT success is accumulation of boron specifically in cancer cells. This difficult task could be achieved by the synthesis of a boron compound that is selectively delivered by LAT1. Indeed, p-boronophenylalanine (BPA), a boron compound commonly used in BNCT, is incorporated by LAT1^[38-40], suggesting that LAT1 is an optimal mediator for delivery of boron in BNCT. However, since we cannot still completely rule out the possibility of BPA uptake by other transporters, it is necessary to develop compounds that exhibit strict selectivity to LAT1. BNCT has accomplished certain clinical outcomes so far, but the problem in the

past was that it required a large-scale nuclear reactor to generate neutrons. However, a compact accelerator has been developed as an alternative to a nuclear reactor and it can be installed in a hospital, making BNCT easier to perform. Such technology will expand the applications of BNCT in the future.

LAT1 AND METASTASIS

It has been suggested that LAT1 is involved in cancer metastasis. A number of studies have shown a correlation of increase in LAT1 expression with metastasis of multiple cancers. Lymph node metastasis-positive squamous cell carcinomas express LAT1 whereas there is no positive signal of LAT1 in metastasis-negative cells^[41]. LAT1 mRNA level was significantly higher in renal cell carcinoma with metastasis^[42]. A group of cells with high LAT1 expression showed a larger size of the metastatic lesion of gastric carcinoma^[43]. LAT1 expression in neuroendocrine tumors was significantly associated with lymph node metastasis^[44]. The potency of the functional significance of LAT1 in metastasis has been shown. Knockdown of LAT1 by RNAi inhibited the migration and invasion of gastric cancer^[45] and a cholangiocarcinoma cell line^[46]. BCH inhibited the proliferation and migration of a human epithelial ovarian cancer cell line^[47]. On the basis of these findings, inhibition of LAT1 will be good strategy to prevent metastasis of cancer. However, it remains to

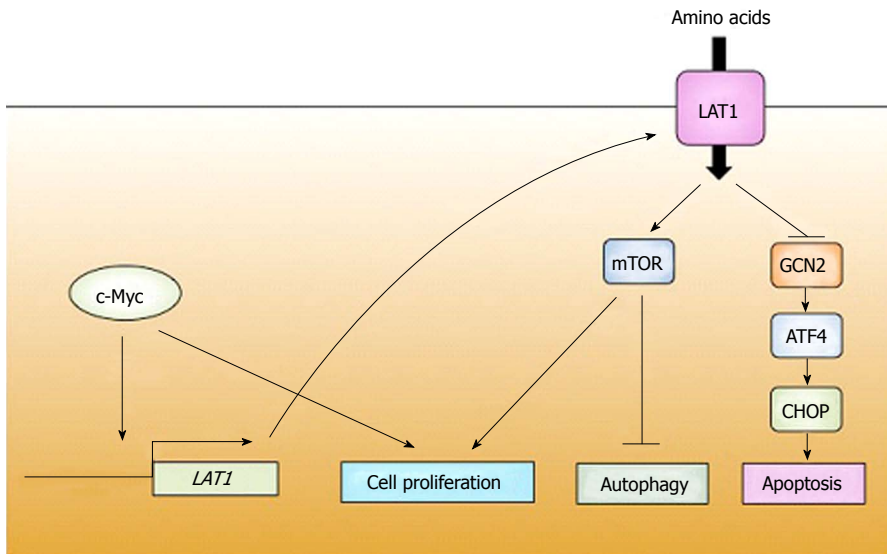


Figure 2 Schematic model of acquisition and monitoring of amino acids in cancer. c-Myc promotes expression of LAT1, which supplies amino acids necessary for growth of cancers. The availability of amino acids is constantly monitored by factors such as mTOR and GCN2. Once amino acid deficiency is detected, cancers suppress their proliferation and, as occasion demands, induce apoptosis. mTOR: Mechanistic target of rapamycin; GCN2: General control non-derepressible 2; ATF4: Activating transcription factor 4; CHOP: C/EBP homologous protein.

be determined whether the metastasis defect is derived from amino acid starvation or from other factors such as an aberrance of adhesion molecules. It would thus be valuable to investigate the relevance of LAT1 and integrin in metastasis, since they form a complex^[48].

MECHANISM OF LAT1 EXPRESSION

Although it remains unknown how LAT1 expression is facilitated in cancers, some possible molecular mechanisms have been proposed. c-Myc, a proto-oncogenic transcription factor, has been demonstrated to be an upstream of LAT1. The expression of c-Myc in normal adults is generally low^[49], but overexpression of c-Myc triggered by some cues such as gene amplification, gene translocation or other gene mutations^[50] is responsible for malignant transformation. Numerous human cancer tissues strongly express c-Myc. Target genes of c-Myc include many factors involved in progression of the cell cycle^[51]. On the other hand, the consensus binding sequence of c-Myc is also located at the *LAT1* promoter^[27]. Moreover, knockdown of c-Myc leads to reduction of LAT1 expression in cancer cell lines^[27]. These results suggest that up-regulation of LAT1 is mediated, at least in part, by c-Myc (Figure 2). Of note is that c-Myc also enhances the metabolic reprogram in cancers by promoting the expression of enzymes of glycolysis and glucose transporter^[52,53]. This is an ingenious strategy of cancers since they can coordinate multiple events required for cell growth by just one factor.

Some other factors appear to regulate LAT1 expression. Hypoxia-inducible factor (Hif) is a critical regulator in response to hypoxia. Hif2 α , an isoform of the Hif family, binds to the *LAT1* promoter and enhances LAT1 expression in renal carcinoma cell

lines^[54]. Artificial manipulation to elevate Hif2 α activity induces LAT1 expression in lung and liver tissues, in which LAT1 expression is usually low^[54]. Aryl hydrocarbon receptor (AHR) is a transcription factor that is activated by interaction with its ligands such as dioxin, and it promotes tumorigenesis^[55]. AHR binds to its consensus binding sequence in *LAT1* and drives LAT1 expression in breast cancer cell lines^[56], suggesting that LAT1 contributes to tumorigenesis induced by an environmental carcinogen. As described previously, T cell activation induces LAT1 expression^[5,6]. Nuclear factor kappa B, AP-1 and nuclear factor of activated T-cells are critical transcription factors that are activated by T cell stimulation and enhance immunological reactions. The expression of LAT1 is prevented by inhibitors of these transcription factors^[5,6]. This means that LAT1 expression is induced by the common regulators that also boost immunological reaction in T cells.

DOWNSTREAM OF LAT1

Ensuring a sufficient supply of nutrients is an issue of vital importance for cancers. The majority of cancers are thought to constantly monitor the availability of amino acids. Starvation of amino acids rapidly induces a stress response that puts a brake on cellular biochemical reactions to avoid wasting energy and materials. The most extensively studied system for monitoring the amino acid availability is mechanistic target of rapamycin (mTOR)^[57], a serine-threonine kinase. Plenty of amino acids maintains mTOR kinase activity, resulting in progression of the cell cycle, protein synthesis, or inhibition of autophagy induction (Figure 2). Some mTOR regulators such as SLC38A9^[58-60], Cellular arginine sensor for mTORC1 (CASTOR1)^[61] and Sestrin2^[62] have

been demonstrated to associate with amino acids to dictate mTOR activity. Dissociation of those interactions caused by amino acid deficiency inactivates mTOR and inverses the reaction of its downstream, resulting in a halt of cancer growth. Growing evidence suggests that LAT1 disruption leads to the inhibition of mTOR. LAT1 inhibition decreases mTOR activity in many cancer cell lines^[28,33,63-65]. These findings suggest that the arrest of cell growth of cancers by a defect of LAT1 is derived from inactivation of mTOR (Figure 2). mTOR inhibitors are being used in practical trials for therapeutic management of several cancers^[66]. Application of JPH203 together with an mTOR inhibitor probably creates a synergistic effect and might be useful for maximizing the benefit of treatment with a low-dose drug, which would help to minimize adverse effects.

General control non-derepressible 2 (GCN2) is another factor for detection of amino acid starvation^[67]. GCN2 is a serine-threonine kinase that is activated by amino acid deficiency. Uncharged tRNAs caused by a decline of amino acid concentration activates GCN2, which eventually induces activity of activating transcription factor 4 (ATF4). ATF4 regulates the expression of genes responsible for coping with amino acid deficiency^[68]. Several studies have shown that dysfunction of LAT1 initiates the GCN2 signal. JPH203 promotes the expression of C/EBP homologous protein [CHOP, also known as DNA damage inducible transcript 3 (DDIT3)], which is up-regulated by ATF4^[68] and probably takes part in apoptosis in leukemia^[33]. Gene disruption of LAT1 in cancer cell lines activates the GCN2-ATF4 cascade^[12]. Activation of ATF4 by LAT1 defect was also shown in cells other than cancer. JPH203 triggers the expression of CHOP^[5,69] and homeobox B9^[70], a novel target of ATF4, in human T cells to repress cytokine production. These findings suggest that GCN2-ATF4 is another critical system for detecting amino acid deficiency evoked by LAT1 inhibition (Figure 2).

CONCLUSION

After the importance of LAT1 in cancer cells had been established, basic studies on LAT1 have progressed with remarkable speed. Better still, research achievements are potentially capable of technical developments for the use of LAT1 as a molecular target in clinical practice. However, although JPH203 is more effective and specific than BCH, it still requires a high concentration for sufficient suppression of the growth of cancers, and wariness of adverse effect persists. Nevertheless, such concerns might be overcome, at least for the time being, by virtue of the proper combinational use of multiple drugs with different action points in cellular metabolism (*e.g.*, mTOR inhibitor). However, further improvements in selectivity of the inhibitor, boron donor of BNCT and PET probe to LAT1 will raise the quality of cancer treatment. Besides, although not to the extent to LAT1, there are several cancers that rely on LAT3

for their growth and development of a LAT3-specific inhibitors is also encouraged. Advances in technologies are expected to resolve such issues.

REFERENCES

- Hediger MA**, Clémenton B, Burrier RE, Bruford EA. The ABCs of membrane transporters in health and disease (SLC series): introduction. *Mol Aspects Med* 2013; **34**: 95-107 [PMID: 23506860 DOI: 10.1016/j.mam.2012.12.009]
- Kanai Y**, Segawa H, Miyamoto Ki, Uchino H, Takeda E, Endou H. Expression cloning and characterization of a transporter for large neutral amino acids activated by the heavy chain of 4F2 antigen (CD98). *J Biol Chem* 1998; **273**: 23629-23632 [PMID: 9726963]
- Mastroberardino L**, Spindler B, Pfeiffer R, Skelly PJ, Loffing J, Shoemaker CB, Verrey F. Amino-acid transport by heterodimers of 4F2hc/CD98 and members of a permease family. *Nature* 1998; **395**: 288-291 [PMID: 9751058 DOI: 10.1038/26246]
- Nakada N**, Mikami T, Hana K, Ichinoe M, Yanagisawa N, Yoshida T, Endou H, Okayasu I. Unique and selective expression of L-amino acid transporter 1 in human tissue as well as being an aspect of oncofetal protein. *Histol Histopathol* 2014; **29**: 217-227 [PMID: 23824658]
- Hayashi K**, Jutabha P, Endou H, Sagara H, Anzai N. LAT1 is a critical transporter of essential amino acids for immune reactions in activated human T cells. *J Immunol* 2013; **191**: 4080-4085 [PMID: 24038088 DOI: 10.4049/jimmunol.1300923]
- Sinclair LV**, Rolf J, Emslie E, Shi YB, Taylor PM, Cantrell DA. Control of amino-acid transport by antigen receptors coordinates the metabolic reprogramming essential for T cell differentiation. *Nat Immunol* 2013; **14**: 500-508 [PMID: 23525088 DOI: 10.1038/ni.2556]
- Rossier G**, Meier C, Bauch C, Summa V, Sordat B, Verrey F, Kühn LC. LAT2, a new basolateral 4F2hc/CD98-associated amino acid transporter of kidney and intestine. *J Biol Chem* 1999; **274**: 34948-34954 [PMID: 10574970]
- Segawa H**, Fukasawa Y, Miyamoto K, Takeda E, Endou H, Kanai Y. Identification and functional characterization of a Na⁺-independent neutral amino acid transporter with broad substrate selectivity. *J Biol Chem* 1999; **274**: 19745-19751 [PMID: 10391916]
- Pineda M**, Fernández E, Torrents D, Estévez R, López C, Camps M, Lloberas J, Zorzano A, Palacin M. Identification of a membrane protein, LAT-2, that Co-expresses with 4F2 heavy chain, an L-type amino acid transport activity with broad specificity for small and large zwitterionic amino acids. *J Biol Chem* 1999; **274**: 19738-19744 [PMID: 10391915]
- Braun D**, Wirth EK, Wohlgemuth F, Reix N, Klein MO, Grüters A, Köhrle J, Schweizer U. Aminoaciduria, but normal thyroid hormone levels and signalling, in mice lacking the amino acid and thyroid hormone transporter Slc7a8. *Biochem J* 2011; **439**: 249-255 [PMID: 21726201 DOI: 10.1042/BJ20110759]
- Verrey F**, Closs EI, Wagner CA, Palacin M, Endou H, Kanai Y. CATs and HATs: the SLC7 family of amino acid transporters. *Pflugers Arch* 2004; **447**: 532-542 [PMID: 14770310 DOI: 10.1007/s00424-003-1086-z]
- Cormerais Y**, Giuliano S, LeFloch R, Front B, Durivault J, Tambuté E, Massard PA, de la Ballina LR, Endou H, Wempe MF, Palacin M, Parks SK, Pouyssegur J. Genetic Disruption of the Multifunctional CD98/LAT1 Complex Demonstrates the Key Role of Essential Amino Acid Transport in the Control of mTORC1 and Tumor Growth. *Cancer Res* 2016; **76**: 4481-4492 [PMID: 27302165 DOI: 10.1158/0008-5472.CAN-15-3376]
- Babu E**, Kanai Y, Chairoungdua A, Kim DK, Iribe Y, Tangtrongsup S, Jutabha P, Li Y, Ahmed N, Sakamoto S, Anzai N, Nagamori S, Endou H. Identification of a novel system L amino acid transporter structurally distinct from heterodimeric amino acid transporters. *J Biol Chem* 2003; **278**: 43838-43845 [PMID: 12930836 DOI: 10.1074/jbc.M305221200]

- 14 **Chuaqui RF**, Englert CR, Strup SE, Vocke CD, Zhuang Z, Duray PH, Bostwick DG, Linehan WM, Liotta LA, Emmert-Buck MR. Identification of a novel transcript up-regulated in a clinically aggressive prostate carcinoma. *Urology* 1997; **50**: 302-307 [PMID: 9255310]
- 15 **Cole KA**, Chuaqui RF, Katz K, Pack S, Zhuang Z, Cole CE, Lyne JC, Linehan WM, Liotta LA, Emmert-Buck MR. cDNA sequencing and analysis of POV1 (PB39): a novel gene up-regulated in prostate cancer. *Genomics* 1998; **51**: 282-287 [PMID: 9722952 DOI: 10.1006/geno.1998.5359]
- 16 **Fukuhara D**, Kanai Y, Chairoungdua A, Babu E, Bessho F, Kawano T, Akimoto Y, Endou H, Yan K. Protein characterization of NA⁺-independent system L amino acid transporter 3 in mice: a potential role in supply of branched-chain amino acids under nutrient starvation. *Am J Pathol* 2007; **170**: 888-898 [PMID: 17322374 DOI: 10.2353/ajpath.2007.060428]
- 17 **Sekine Y**, Nishibori Y, Akimoto Y, Kudo A, Ito N, Fukuhara D, Kurayama R, Higashihara E, Babu E, Kanai Y, Asanuma K, Nagata M, Majumdar A, Tryggvason K, Yan K. Amino acid transporter LAT3 is required for podocyte development and function. *J Am Soc Nephrol* 2009; **20**: 1586-1596 [PMID: 19443642 DOI: 10.1681/ASN.2008070809]
- 18 **Wang Q**, Bailey CG, Ng C, Tiffen J, Thoeng A, Minhas V, Lehman ML, Hendy SC, Buchanan G, Nelson CC, Rasko JE, Holst J. Androgen receptor and nutrient signaling pathways coordinate the demand for increased amino acid transport during prostate cancer progression. *Cancer Res* 2011; **71**: 7525-7536 [PMID: 22007000 DOI: 10.1158/0008-5472.CAN-11-1821]
- 19 **Wang Q**, Tiffen J, Bailey CG, Lehman ML, Ritchie W, Fazli L, Metierre C, Feng YJ, Li E, Gleave M, Buchanan G, Nelson CC, Rasko JE, Holst J. Targeting amino acid transport in metastatic castration-resistant prostate cancer: effects on cell cycle, cell growth, and tumor development. *J Natl Cancer Inst* 2013; **105**: 1463-1473 [PMID: 24052624 DOI: 10.1093/jnci/djt241]
- 20 **Bodoy S**, Martin L, Zorzano A, Palacin M, Estévez R, Bertran J. Identification of LAT4, a novel amino acid transporter with system L activity. *J Biol Chem* 2005; **280**: 12002-12011 [PMID: 15659399 DOI: 10.1074/jbc.M408638200]
- 21 **Guettg A**, Mariotta L, Bock L, Herzog B, Fingerhut R, Camargo SM, Verrey F. Essential amino acid transporter Lat4 (Slc43a2) is required for mouse development. *J Physiol* 2015; **593**: 1273-1289 [PMID: 25480797 DOI: 10.1113/jphysiol.2014.283960]
- 22 **Sakata T**, Ferdous G, Tsuruta T, Satoh T, Baba S, Muto T, Ueno A, Kanai Y, Endou H, Okayasu I. L-type amino-acid transporter 1 as a novel biomarker for high-grade malignancy in prostate cancer. *Pathol Int* 2009; **59**: 7-18 [PMID: 19121087 DOI: 10.1111/j.1440-1827.2008.02319.x]
- 23 **Ichinoe M**, Mikami T, Yoshida T, Igawa I, Tsuruta T, Nakada N, Anzai N, Suzuki Y, Endou H, Okayasu I. High expression of L-type amino-acid transporter 1 (LAT1) in gastric carcinomas: comparison with non-cancerous lesions. *Pathol Int* 2011; **61**: 281-289 [PMID: 21501294 DOI: 10.1111/j.1440-1827.2011.02650.x]
- 24 **Yanagisawa N**, Ichinoe M, Mikami T, Nakada N, Hana K, Koizumi W, Endou H, Okayasu I. High expression of L-type amino acid transporter 1 (LAT1) predicts poor prognosis in pancreatic ductal adenocarcinomas. *J Clin Pathol* 2012; **65**: 1019-1023 [PMID: 22813728 DOI: 10.1136/jclinpath-2012-200826]
- 25 **Kim CH**, Park KJ, Park JR, Kanai Y, Endou H, Park JC, Kim DK. The RNA interference of amino acid transporter LAT1 inhibits the growth of KB human oral cancer cells. *Anticancer Res* 2006; **26**: 2943-2948 [PMID: 16886618]
- 26 **Marshall AD**, van Geldermalsen M, Otte NJ, Anderson LA, Lum T, Vellozzi MA, Zhang BK, Thoeng A, Wang Q, Rasko JE, Holst J. LAT1 is a putative therapeutic target in endometrioid endometrial carcinoma. *Int J Cancer* 2016; **139**: 2529-2539 [PMID: 27486861 DOI: 10.1002/ijc.30371]
- 27 **Hayashi K**, Jutabha P, Endou H, Anzai N. c-Myc is crucial for the expression of LAT1 in MIA Paca-2 human pancreatic cancer cells. *Oncol Rep* 2012; **28**: 862-866 [PMID: 22736142 DOI: 10.3892/or.2012.1878]
- 28 **Xu M**, Sakamoto S, Matsushima J, Kimura T, Ueda T, Mizokami A, Kanai Y, Ichikawa T. Up-Regulation of LAT1 during Antiandrogen Therapy Contributes to Progression in Prostate Cancer Cells. *J Urol* 2016; **195**: 1588-1597 [PMID: 26682754 DOI: 10.1016/j.juro.2015.11.071]
- 29 **Liang Z**, Cho HT, Williams L, Zhu A, Liang K, Huang K, Wu H, Jiang C, Hong S, Crowe R, Goodman MM, Shim H. Potential Biomarker of L-type Amino Acid Transporter 1 in Breast Cancer Progression. *Nucl Med Mol Imaging* 2011; **45**: 93-102 [PMID: 24899987 DOI: 10.1007/s13139-010-0068-2]
- 30 **Morimoto E**, Kanai Y, Kim DK, Chairoungdua A, Choi HW, Wempe MF, Anzai N, Endou H. Establishment and characterization of mammalian cell lines stably expressing human L-type amino acid transporters. *J Pharmacol Sci* 2008; **108**: 505-516 [PMID: 19075510]
- 31 **Oda K**, Hosoda N, Endo H, Saito K, Tsujihara K, Yamamura M, Sakata T, Anzai N, Wempe MF, Kanai Y, Endou H. L-type amino acid transporter 1 inhibitors inhibit tumor cell growth. *Cancer Sci* 2010; **101**: 173-179 [PMID: 19900191 DOI: 10.1111/j.1349-7006.2009.01386.x]
- 32 **Yun DW**, Lee SA, Park MG, Kim JS, Yu SK, Park MR, Kim SG, Oh JS, Kim CS, Kim HJ, Kim JS, Chun HS, Kanai Y, Endou H, Wempe MF, Kim DK. JPH203, an L-type amino acid transporter 1-selective compound, induces apoptosis of YD-38 human oral cancer cells. *J Pharmacol Sci* 2014; **124**: 208-217 [PMID: 24492461]
- 33 **Rosilio C**, Nebout M, Imbert V, Griessinger E, Neffati Z, Benadiba J, Hagenbeek T, Spits H, Reverso J, Ambrosetti D, Michiels JF, Bailly-Maitre B, Endou H, Wempe MF, Peyron JF. L-type amino-acid transporter 1 (LAT1): a therapeutic target supporting growth and survival of T-cell lymphoblastic lymphoma/T-cell acute lymphoblastic leukemia. *Leukemia* 2015; **29**: 1253-1266 [PMID: 25482130 DOI: 10.1038/leu.2014.338]
- 34 **Sharma P**, Mukherjee A. Newer positron emission tomography radiopharmaceuticals for radiotherapy planning: an overview. *Ann Transl Med* 2016; **4**: 53 [PMID: 26904575 DOI: 10.3978/j.issn.2305-5839.2016.01.26]
- 35 **Wei L**, Tominaga H, Ohgaki R, Wiriyaerkmul P, Hagiwara K, Okuda S, Kaira K, Oriuchi N, Nagamori S, Kanai Y. Specific transport of 3-fluoro-l- α -methyl-tyrosine by LAT1 explains its specificity to malignant tumors in imaging. *Cancer Sci* 2016; **107**: 347-352 [PMID: 26749017 DOI: 10.1111/cas.12878]
- 36 **Barth RF**, Coderre JA, Vicente MG, Blue TE. Boron neutron capture therapy of cancer: current status and future prospects. *Clin Cancer Res* 2005; **11**: 3987-4002 [PMID: 15930333 DOI: 10.1158/1078-0432.CCR-05-0035]
- 37 **Das BC**, Thapa P, Karki R, Schinck C, Das S, Kambhampati S, Banerjee SK, Van Veldhuizen P, Verma A, Weiss LM, Evans T. Boron chemicals in diagnosis and therapeutics. *Future Med Chem* 2013; **5**: 653-676 [PMID: 23617429 DOI: 10.4155/fmc.13.38]
- 38 **Detta A**, Cruickshank GS. L-amino acid transporter-1 and boronophenylalanine-based boron neutron capture therapy of human brain tumors. *Cancer Res* 2009; **69**: 2126-2132 [PMID: 19244126 DOI: 10.1158/0008-5472.CAN-08-2345]
- 39 **Yoshimoto M**, Kurihara H, Honda N, Kawai K, Ohe K, Fujii H, Itami J, Arai Y. Predominant contribution of L-type amino acid transporter to 4-borono-2-(18)F-fluoro-phenylalanine uptake in human glioblastoma cells. *Nucl Med Biol* 2013; **40**: 625-629 [PMID: 23557719 DOI: 10.1016/j.nucmedbio.2013.02.010]
- 40 **Wongthai P**, Hagiwara K, Miyoshi Y, Wiriyaerkmul P, Wei L, Ohgaki R, Kato I, Hamase K, Nagamori S, Kanai Y. Boronophenylalanine, a boron delivery agent for boron neutron capture therapy, is transported by ATB0+, LAT1 and LAT2. *Cancer Sci* 2015; **106**: 279-286 [PMID: 25580517 DOI: 10.1111/cas.12602]
- 41 **Kaira K**, Oriuchi N, Imai H, Shimizu K, Yanagitani N, Sunaga N, Hisada T, Tanaka S, Ishizuka T, Kanai Y, Endou H, Nakajima T, Mori M. Prognostic significance of L-type amino acid transporter 1 expression in resectable stage I-III nonsmall cell lung cancer. *Br J Cancer* 2008; **98**: 742-748 [PMID: 18253116 DOI: 10.1038/sj.bjc.6604235]

- 42 **Betsunoh H**, Fukuda T, Anzai N, Nishihara D, Mizuno T, Yuki H, Masuda A, Yamaguchi Y, Abe H, Yashi M, Fukabori Y, Yoshida K, Kamai T. Increased expression of system large amino acid transporter (LAT)-1 mRNA is associated with invasive potential and unfavorable prognosis of human clear cell renal cell carcinoma. *BMC Cancer* 2013; **13**: 509 [PMID: 24168110 DOI: 10.1186/1471-2407-13-509]
- 43 **Ichinoe M**, Yanagisawa N, Mikami T, Hana K, Nakada N, Endou H, Okayasu I, Murakumo Y. L-Type amino acid transporter 1 (LAT1) expression in lymph node metastasis of gastric carcinoma: Its correlation with size of metastatic lesion and Ki-67 labeling. *Pathol Res Pract* 2015; **211**: 533-538 [PMID: 25908107 DOI: 10.1016/j.prp.2015.03.007]
- 44 **Kaira K**, Oriuchi N, Imai H, Shimizu K, Yanagitani N, Sunaga N, Hisada T, Kawashima O, Iijima H, Ishizuka T, Kanai Y, Endou H, Nakajima T, Mori M. Expression of L-type amino acid transporter 1 (LAT1) in neuroendocrine tumors of the lung. *Pathol Res Pract* 2008; **204**: 553-561 [PMID: 18440724 DOI: 10.1016/j.prp.2008.02.003]
- 45 **Shi L**, Luo W, Huang W, Huang S, Huang G. Downregulation of L-type amino acid transporter 1 expression inhibits the growth, migration and invasion of gastric cancer cells. *Oncol Lett* 2013; **6**: 106-112 [PMID: 23946786 DOI: 10.3892/ol.2013.1342]
- 46 **Janpipatkul K**, Suksen K, Borwornpinoy S, Jearawiriyapaisarn N, Hongeng S, Piyachaturawat P, Chairoungdua A. Downregulation of LAT1 expression suppresses cholangiocarcinoma cell invasion and migration. *Cell Signal* 2014; **26**: 1668-1679 [PMID: 24726839 DOI: 10.1016/j.cellsig.2014.04.002]
- 47 **Kaji M**, Kabir-Salmani M, Anzai N, Jin CJ, Akimoto Y, Horita A, Sakamoto A, Kanai Y, Sakurai H, Iwashita M. Properties of L-type amino acid transporter 1 in epidermal ovarian cancer. *Int J Gynecol Cancer* 2010; **20**: 329-336 [PMID: 20375792 DOI: 10.1111/IGC.0b013e3181d28e13]
- 48 **Zent R**, Fenczik CA, Calderwood DA, Liu S, Dellos M, Ginsberg MH. Class- and splice variant-specific association of CD98 with integrin beta cytoplasmic domains. *J Biol Chem* 2000; **275**: 5059-5064 [PMID: 10671548]
- 49 **Wierstra I**, Alves J. The c-myc promoter: still MysterY and challenge. *Adv Cancer Res* 2008; **99**: 113-333 [PMID: 18037408 DOI: 10.1016/S0065-230X(07)99004-1]
- 50 **Vita M**, Henriksson M. The Myc oncoprotein as a therapeutic target for human cancer. *Semin Cancer Biol* 2006; **16**: 318-330 [PMID: 16934487 DOI: 10.1016/j.semcancer.2006.07.015]
- 51 **Kress TR**, Sabò A, Amati B. MYC: connecting selective transcriptional control to global RNA production. *Nat Rev Cancer* 2015; **15**: 593-607 [PMID: 26383138 DOI: 10.1038/nrc3984]
- 52 **Kim JW**, Zeller KI, Wang Y, Jegga AG, Aronow BJ, O'Donnell KA, Dang CV. Evaluation of myc E-box phylogenetic footprints in glycolytic genes by chromatin immunoprecipitation assays. *Mol Cell Biol* 2004; **24**: 5923-5936 [PMID: 15199147 DOI: 10.1128/MCB.24.13.5923-5936.2004]
- 53 **Osthus RC**, Shim H, Kim S, Li Q, Reddy R, Mukherjee M, Xu Y, Wonsley D, Lee LA, Dang CV. Deregulation of glucose transporter 1 and glycolytic gene expression by c-Myc. *J Biol Chem* 2000; **275**: 21797-21800 [PMID: 10823814 DOI: 10.1074/jbc.C000023200]
- 54 **Elorza A**, Soro-Arnáiz I, Meléndez-Rodríguez F, Rodríguez-Vaello V, Marsboom G, de Cárcer G, Acosta-Iborra B, Albacete-Albacete L, Ordóñez A, Serrano-Oviedo L, Giménez-Bachs JM, Vara-Vega A, Salinas A, Sánchez-Prieto R, Martín del Río R, Sánchez-Madrid F, Malumbres M, Landázuri MO, Aragonés J. HIF2 α acts as an mTORC1 activator through the amino acid carrier SLC7A5. *Mol Cell* 2012; **48**: 681-691 [PMID: 23103253 DOI: 10.1016/j.molcel.2012.09.017]
- 55 **Murray IA**, Patterson AD, Perdew GH. Aryl hydrocarbon receptor ligands in cancer: friend and foe. *Nat Rev Cancer* 2014; **14**: 801-814 [PMID: 25568920 DOI: 10.1038/nrc3846]
- 56 **Tomblin JK**, Arthur S, Primerano DA, Chaudhry AR, Fan J, Denvir J, Salisbury TB. Aryl hydrocarbon receptor (AHR) regulation of L-Type Amino Acid Transporter 1 (LAT-1) expression in MCF-7 and MDA-MB-231 breast cancer cells. *Biochem Pharmacol* 2016; **106**: 94-103 [PMID: 26944194 DOI: 10.1016/j.bcp.2016.02.020]
- 57 **Goberdhan DC**, Wilson C, Harris AL. Amino Acid Sensing by mTORC1: Intracellular Transporters Mark the Spot. *Cell Metab* 2016; **23**: 580-589 [PMID: 27076075 DOI: 10.1016/j.cmet.2016.03.013]
- 58 **Rebsamen M**, Pochini L, Stasyk T, de Araújo ME, Galluccio M, Kandasamy RK, Snijder B, Fauster A, Rudashevskaya EL, Bruckner M, Scorzoni S, Filipek PA, Huber KV, Bigenzahn JW, Heinz LX, Kraft C, Bennett KL, Indiveri C, Huber LA, Superti-Furga G. SLC38A9 is a component of the lysosomal amino acid sensing machinery that controls mTORC1. *Nature* 2015; **519**: 477-481 [PMID: 25561175 DOI: 10.1038/nature14107]
- 59 **Wang S**, Tsun ZY, Wolfson RL, Shen K, Wyant GA, Plovianich ME, Yuan ED, Jones SD, Chantranupong L, Comb W, Wang T, Bar-Peled L, Zoncu R, Straub C, Kim C, Park J, Sabatini BL, Sabatini DM. Metabolism. Lysosomal amino acid transporter SLC38A9 signals arginine sufficiency to mTORC1. *Science* 2015; **347**: 188-194 [PMID: 25567906 DOI: 10.1126/science.1257132]
- 60 **Jung J**, Genau HM, Behrends C. Amino Acid-Dependent mTORC1 Regulation by the Lysosomal Membrane Protein SLC38A9. *Mol Cell Biol* 2015; **35**: 2479-2494 [PMID: 25963655 DOI: 10.1128/MCB.00125-15]
- 61 **Chantranupong L**, Scaria SM, Saxton RA, Gygi MP, Shen K, Wyant GA, Wang T, Harper JW, Gygi SP, Sabatini DM. The CASTOR Proteins Are Arginine Sensors for the mTORC1 Pathway. *Cell* 2016; **165**: 153-164 [PMID: 26972053 DOI: 10.1016/j.cell.2016.02.035]
- 62 **Wolfson RL**, Chantranupong L, Saxton RA, Shen K, Scaria SM, Cantor JR, Sabatini DM. Sestrin2 is a leucine sensor for the mTORC1 pathway. *Science* 2016; **351**: 43-48 [PMID: 26449471 DOI: 10.1126/science.aab2674]
- 63 **He B**, Zhang N, Zhao R. Dexamethasone Downregulates SLC7A5 Expression and Promotes Cell Cycle Arrest, Autophagy and Apoptosis in BeWo Cells. *J Cell Physiol* 2016; **231**: 233-242 [PMID: 26094588 DOI: 10.1002/jcp.25076]
- 64 **Imai H**, Kaira K, Oriuchi N, Shimizu K, Tominaga H, Yanagitani N, Sunaga N, Ishizuka T, Nagamori S, Promchan K, Nakajima T, Yamamoto N, Mori M, Kanai Y. Inhibition of L-type amino acid transporter 1 has antitumor activity in non-small cell lung cancer. *Anticancer Res* 2010; **30**: 4819-4828 [PMID: 21187458]
- 65 **Fan X**, Ross DD, Arakawa H, Ganapathy V, Tamai I, Nakanishi T. Impact of system L amino acid transporter 1 (LAT1) on proliferation of human ovarian cancer cells: a possible target for combination therapy with anti-proliferative aminopeptidase inhibitors. *Biochem Pharmacol* 2010; **80**: 811-818 [PMID: 20510678 DOI: 10.1016/j.bcp.2010.05.021]
- 66 **Rodrik-Outmezguine VS**, Okaniwa M, Yao Z, Novotny CJ, McWhirter C, Banaji A, Won H, Wong W, Berger M, de Stanchina E, Barratt DG, Cosulich S, Klinowska T, Rosen N, Shokat KM. Overcoming mTOR resistance mutations with a new-generation mTOR inhibitor. *Nature* 2016; **534**: 272-276 [PMID: 27279227 DOI: 10.1038/nature17963]
- 67 **Castilho BA**, Shanmugam R, Silva RC, Ramesh R, Himme BM, Sattlegger E. Keeping the eIF2 alpha kinase Gcn2 in check. *Biochim Biophys Acta* 2014; **1843**: 1948-1968 [PMID: 24732012 DOI: 10.1016/j.bbamcr.2014.04.006]
- 68 **Kilberg MS**, Shan J, Su N. ATF4-dependent transcription mediates signaling of amino acid limitation. *Trends Endocrinol Metab* 2009; **20**: 436-443 [PMID: 19800252 DOI: 10.1016/j.tem.2009.05.008]
- 69 **Hayashi K**, Anzai N. Role of LAT1 in the promotion of amino acid incorporation in activated T cells. *Crit Rev Immunol* 2014; **34**: 467-479 [PMID: 25597310]
- 70 **Hayashi K**, Ouchi M, Endou H, Anzai N. HOXB9 acts as a negative regulator of activated human T cells in response to amino acid deficiency. *Immunol Cell Biol* 2016; **94**: 612-617 [PMID: 26926958 DOI: 10.1038/icc.2016.13]
- 71 **Kaira K**, Sunose Y, Ohshima Y, Ishioka NS, Arakawa K, Ogawa T, Sunaga N, Shimizu K, Tominaga H, Oriuchi N, Itoh H, Nagamori S, Kanai Y, Yamaguchi A, Segawa A, Ide M, Mori M, Oyama T, Takeyoshi I. Clinical significance of L-type amino acid transporter 1 expression as a prognostic marker and potential of new targeting therapy in biliary tract cancer. *BMC Cancer* 2013; **13**: 482 [PMID:

- 24131658 DOI: 10.1186/1471-2407-13-482]
- 72 **Kim DK**, Kanai Y, Choi HW, Tangtrongsup S, Chairoungdua A, Babu E, Tachampa K, Anzai N, Iribe Y, Endou H. Characterization of the system L amino acid transporter in T24 human bladder carcinoma cells. *Biochim Biophys Acta* 2002; **1565**: 112-121 [PMID: 12225859]
- 73 **Koshi H**, Sano T, Handa T, Yanagawa T, Saitou K, Nagamori S, Kanai Y, Takagishi K, Oyama T. L-type amino acid transporter-1 and CD98 expression in bone and soft tissue tumors. *Pathol Int* 2015; **65**: 460-467 [PMID: 26134029 DOI: 10.1111/pin.12323]
- 74 **Kobayashi K**, Ohnishi A, Promsuk J, Shimizu S, Kanai Y, Shiokawa Y, Nagane M. Enhanced tumor growth elicited by L-type amino acid transporter 1 in human malignant glioma cells. *Neurosurgery* 2008; **62**: 493-503; discussion 503-504 [PMID: 18382329 DOI: 10.1227/01.neu.0000316018.51292.19]
- 75 **Haining Z**, Kawai N, Miyake K, Okada M, Okubo S, Zhang X, Fei Z, Tamiya T. Relation of LAT1/4F2hc expression with pathological grade, proliferation and angiogenesis in human gliomas. *BMC Clin Pathol* 2012; **12**: 4 [PMID: 22373026 DOI: 10.1186/1472-6890-12-4]
- 76 **Shennan DB**, Thomson J, Gow IF, Travers MT, Barber MC. L-leucine transport in human breast cancer cells (MCF-7 and MDA-MB-231): kinetics, regulation by estrogen and molecular identity of the transporter. *Biochim Biophys Acta* 2004; **1664**: 206-216 [PMID: 15328053 DOI: 10.1016/j.bbame.2004.05.008]
- 77 **Shennan DB**, Thomson J, Barber MC, Travers MT. Functional and molecular characteristics of system L in human breast cancer cells. *Biochim Biophys Acta* 2003; **1611**: 81-90 [PMID: 12659948]
- 78 **Furuya M**, Horiguchi J, Nakajima H, Kanai Y, Oyama T. Correlation of L-type amino acid transporter 1 and CD98 expression with triple negative breast cancer prognosis. *Cancer Sci* 2012; **103**: 382-389 [PMID: 22077314 DOI: 10.1111/j.1349-7006.2011.02151.x]
- 79 **Kobayashi H**, Ishii Y, Takayama T. Expression of L-type amino acid transporter 1 (LAT1) in esophageal carcinoma. *J Surg Oncol* 2005; **90**: 233-238 [PMID: 15906366 DOI: 10.1002/jso.20257]
- 80 **Honjo H**, Kaira K, Miyazaki T, Yokobori T, Kanai Y, Nagamori S, Oyama T, Asao T, Kuwano H. Clinicopathological significance of LAT1 and ASCT2 in patients with surgically resected esophageal squamous cell carcinoma. *J Surg Oncol* 2016; **113**: 381-389 [PMID: 26936531 DOI: 10.1002/jso.24160]
- 81 **Namikawa M**, Kakizaki S, Kaira K, Tojima H, Yamazaki Y, Horiguchi N, Sato K, Oriuchi N, Tominaga H, Sunose Y, Nagamori S, Kanai Y, Oyama T, Takeyoshi I, Yamada M. Expression of amino acid transporters (LAT1, ASCT2 and xCT) as clinical significance in hepatocellular carcinoma. *Hepatol Res* 2014 Oct 9; Epub ahead of print [PMID: 25297701 DOI: 10.1111/hepr.12431]
- 82 **Nikkuni O**, Kaira K, Toyoda M, Shino M, Sakakura K, Takahashi K, Tominaga H, Oriuchi N, Suzuki M, Iijima M, Asao T, Nishiyama M, Nagamori S, Kanai Y, Oyama T, Chikamatsu K. Expression of Amino Acid Transporters (LAT1 and ASCT2) in Patients with Stage III/IV Laryngeal Squamous Cell Carcinoma. *Pathol Oncol Res* 2015; **21**: 1175-1181 [PMID: 26024742 DOI: 10.1007/s12253-015-9954-3]
- 83 **Imai H**, Kaira K, Oriuchi N, Yanagitani N, Sunaga N, Ishizuka T, Kanai Y, Endou H, Nakajima T, Mori M. L-type amino acid transporter 1 expression is a prognostic marker in patients with surgically resected stage I non-small cell lung cancer. *Histopathology* 2009; **54**: 804-813 [PMID: 19635099 DOI: 10.1111/j.1365-2559.2009.03300.x]
- 84 **Kaira K**, Oriuchi N, Imai H, Shimizu K, Yanagitani N, Sunaga N, Hisada T, Ishizuka T, Kanai Y, Endou H, Nakajima T, Mori M. Prognostic significance of L-type amino acid transporter 1 (LAT1) and 4F2 heavy chain (CD98) expression in early stage squamous cell carcinoma of the lung. *Cancer Sci* 2009; **100**: 248-254 [PMID: 19068093 DOI: 10.1111/j.1349-7006.2008.01029.x]
- 85 **Kaira K**, Oriuchi N, Imai H, Shimizu K, Yanagitani N, Sunaga N, Hisada T, Kawashima O, Kamide Y, Ishizuka T, Kanai Y, Nakajima T, Mori M. Prognostic significance of L-type amino acid transporter 1 (LAT1) and 4F2 heavy chain (CD98) expression in surgically resectable stage III non-small cell lung cancer. *Exp Ther Med* 2010; **1**: 799-808 [PMID: 22993604 DOI: 10.3892/etm.2010.117]
- 86 **Shimizu A**, Kaira K, Kato M, Yasuda M, Takahashi A, Tominaga H, Oriuchi N, Nagamori S, Kanai Y, Oyama T, Asao T, Ishikawa O. Prognostic significance of L-type amino acid transporter 1 (LAT1) expression in cutaneous melanoma. *Melanoma Res* 2015; **25**: 399-405 [PMID: 26237765 DOI: 10.1097/CMR.000000000000181]
- 87 **Wang Q**, Beaumont KA, Otte NJ, Font J, Bailey CG, van Geldermalsen M, Sharp DM, Tiffen JC, Ryan RM, Jormakka M, Haass NK, Rasko JE, Holst J. Targeting glutamine transport to suppress melanoma cell growth. *Int J Cancer* 2014; **135**: 1060-1071 [PMID: 24531984 DOI: 10.1002/ijc.28749]
- 88 **Kühne A**, Tzvetkov MV, Hagos Y, Lage H, Burckhardt G, Brockmüller J. Influx and efflux transport as determinants of melphalan cytotoxicity: Resistance to melphalan in MDR1 over-expressing tumor cell lines. *Biochem Pharmacol* 2009; **78**: 45-53 [PMID: 19447222 DOI: 10.1016/j.bcp.2009.03.026]
- 89 **Barollo S**, Bertazza L, Watutantrige-Fernando S, Censi S, Cavedon E, Galuppini F, Pennelli G, Fassina A, Citton M, Rubin B, Pezzani R, Benna C, Opocher G, Iacobone M, Mian C. Overexpression of L-Type Amino Acid Transporter 1 (LAT1) and 2 (LAT2): Novel Markers of Neuroendocrine Tumors. *PLoS One* 2016; **11**: e0156044 [PMID: 27224648 DOI: 10.1371/journal.pone.0156044]
- 90 **Kaira K**, Nakamura K, Hirakawa T, Imai H, Tominaga H, Oriuchi N, Nagamori S, Kanai Y, Tsukamoto N, Oyama T, Asao T, Minegishi T. Prognostic significance of L-type amino acid transporter 1 (LAT1) expression in patients with ovarian tumors. *Am J Transl Res* 2015; **7**: 1161-1171 [PMID: 26279759]
- 91 **Kaira K**, Sunose Y, Arakawa K, Ogawa T, Sunaga N, Shimizu K, Tominaga H, Oriuchi N, Itoh H, Nagamori S, Kanai Y, Segawa A, Furuya M, Mori M, Oyama T, Takeyoshi I. Prognostic significance of L-type amino-acid transporter 1 expression in surgically resected pancreatic cancer. *Br J Cancer* 2012; **107**: 632-638 [PMID: 22805328 DOI: 10.1038/bjc.2012.310]
- 92 **Kaira K**, Oriuchi N, Takahashi T, Nakagawa K, Ohde Y, Okumura T, Murakami H, Shukuya T, Kenmotsu H, Naito T, Kanai Y, Endo M, Kondo H, Nakajima T, Yamamoto N. L-type amino acid transporter 1 (LAT1) expression in malignant pleural mesothelioma. *Anticancer Res* 2011; **31**: 4075-4082 [PMID: 22199264]
- 93 **Toyoda M**, Kaira K, Ohshima Y, Ishioka NS, Shino M, Sakakura K, Takayasu Y, Takahashi K, Tominaga H, Oriuchi N, Nagamori S, Kanai Y, Oyama T, Chikamatsu K. Prognostic significance of amino-acid transporter expression (LAT1, ASCT2, and xCT) in surgically resected tongue cancer. *Br J Cancer* 2014; **110**: 2506-2513 [PMID: 24762957 DOI: 10.1038/bjc.2014.178]
- 94 **Kaira K**, Oriuchi N, Imai H, Shimizu K, Yanagitani N, Sunaga N, Hisada T, Ishizuka T, Kanai Y, Endou H, Nakajima T, Mori M. L-type amino acid transporter 1 (LAT1) is frequently expressed in thymic carcinomas but is absent in thymomas. *J Surg Oncol* 2009; **99**: 433-438 [PMID: 19347882 DOI: 10.1002/jso.21277]
- 95 **Hayashi K**, Jutabha P, Maeda S, Supak Y, Ouchi M, Endou H, Fujita T, Chida M, Anzai N. LAT1 acts as a crucial transporter of amino acids in human thymic carcinoma cells. *J Pharmacol Sci* 2016; **132**: 201-204 [PMID: 27567475 DOI: 10.1016/j.jphs.2016.07.006]
- 96 **Nakanishi K**, Ogata S, Matsuo H, Kanai Y, Endou H, Hiroi S, Tominaga S, Aida S, Kasamatsu H, Kawai T. Expression of LAT1 predicts risk of progression of transitional cell carcinoma of the upper urinary tract. *Virchows Arch* 2007; **451**: 681-690 [PMID: 17622555 DOI: 10.1007/s00428-007-0457-9]

P- Reviewer: Bugaj AM, Camacho J, Song JJ **S- Editor:** Ji FF

L- Editor: A **E- Editor:** Wu HL





Published by **Baishideng Publishing Group Inc**

8226 Regency Drive, Pleasanton, CA 94588, USA

Telephone: +1-925-223-8242

Fax: +1-925-223-8243

E-mail: bpgoffice@wjgnet.com

Help Desk: <http://www.wjgnet.com/esps/helpdesk.aspx>

<http://www.wjgnet.com>



Matrix-assisted laser desorption/ionization imaging mass spectrometry reveals changes of phospholipid distribution in induced pluripotent stem cell colony differentiation

Yasuo Shimizu¹ · Motoyasu Satou² · Keitaro Hayashi³ · Yusuke Nakamura¹ · Mio Fujimaki¹ · Yasuhiro Horibata² · Hiromi Ando² · Taiji Watanabe¹ · Taichi Shiobara¹ · Kazuyuki Chibana¹ · Akihiro Takemasa¹ · Hiroyuki Sugimoto² · Naohiko Anzai^{3,4} · Yoshiki Ishii¹

Received: 8 July 2016 / Revised: 29 September 2016 / Accepted: 6 October 2016 / Published online: 4 November 2016
© Springer-Verlag Berlin Heidelberg 2016

Abstract Induced pluripotent stem cells (iPSCs) are opening up new possibilities for medicine. Understanding the regulation of iPSC biology is important when attempting to apply these cells to disease models or therapy. Changes of lipid metabolism in iPSCs were investigated by matrix-assisted laser desorption/ionization time-of-flight imaging mass spectrometry (MALDI-TOF-IMS). Analysis revealed changes of the intensity and distribution of peaks at m/z 782.5 and 798.5 in iPSC colonies during spontaneous differentiation. Two phosphatidylcholines (PCs) were identified: $C_{44}H_{81}NO_8P$, PC(36:4)[M+H]⁺ at m/z 782.5 and $C_{42}H_{82}NO_8P$, PC(34:1)[M+K]⁺ at m/z 798.5. The intensity of PC(36:4) showed an inverse relation between undifferentiated and

differentiated iPSC colonies. PC(34:1) displayed a diffuse distribution in undifferentiated iPSC colonies, while it showed a concentric distribution in differentiated iPSC colonies, and was localized at the border of the differentiated and undifferentiated areas or the border between undifferentiated iPSC and feeder cells. These findings suggested that the distribution of lipids changes during the growth and differentiation of iPSCs and that MALDI-TOF-IMS was useful for analyzing these changes. PC(36:4) might play a role in maintaining pluripotency, while PC(34:1) might play a role in the differentiation and spread of iPSCs.

Keywords iPS · Phospholipids · Phosphatidylcholine · MALDI · Imaging · Differentiation

Electronic supplementary material The online version of this article (doi:10.1007/s00216-016-0015-x) contains supplementary material, which is available to authorized users.

✉ Yasuo Shimizu
yasuo-s@dokkyomed.ac.jp

- ¹ Department of Pulmonary Medicine and Clinical Immunology, Dokkyo Medical University School of Medicine, 880 Kitakobayashi, Mibu, Tochigi 321-0293, Japan
- ² Department of Biochemistry, Dokkyo Medical University School of Medicine, 880 Kitakobayashi, Mibu, Tochigi 321-0293, Japan
- ³ Department of Pharmacology and Toxicology, Dokkyo Medical University School of Medicine, 880 Kitakobayashi, Mibu, Tochigi 321-0293, Japan
- ⁴ Department of Pharmacology, Chiba University Graduate School of Medicine, 1-8-1 Inohana, Chuo, Chiba 260-8670, Japan

Introduction

Induced pluripotent stem cells (iPSCs) are expected to have various medical uses in the future, such as for the construction of disease models and for cell therapy [1]. For medical application, however, several points need to be considered before medical application can be achieved, including methods of regulating iPSC functions such as differentiation, cell purity, and the biological products [2, 3]. Therefore, to apply and optimize iPSC technology for medical uses, better elucidation of iPSC biology is required.

Lipid metabolism influences numerous cellular processes, including growth, proliferation, differentiation, and motility [4]. Phosphocholines (Pcho), which were precursors of phosphatidylcholine (PC) or polyunsaturated PCs, have been reported to be abundant in embryonic stem cells and iPSCs compared to mature cells [5, 6].

Matrix-assisted laser desorption/ionization (MALDI) imaging mass spectrometry (IMS) is a technique that can be used to identify substances by their molecular signatures. In particular, MALDI with time-of-flight/time-of-flight IMS (MALDI-TOF/TOF-IMS) is useful for the analysis of numerous biomolecules by collecting hundreds of mass peaks [7]. Imaging analysis enables in situ analysis that distinguishes the undifferentiated from the differentiated regions of cell cultures.

As an iPSC colony grows larger, spontaneous differentiation is initiated from the central region of the colony. In colonies of pluripotent stem cells, the differentiated cells show obvious morphological changes and form typical flat squamous epithelium [8], so the differentiated area is apparently different from the surrounding undifferentiated area of the colony.

In the present study, an IMS method was developed to enable simultaneous mass spectrometry in situ analysis of differentiated and undifferentiated iPSC colonies in culture. Previously, preparation of different cell culture dishes with undifferentiated or differentiated iPSCs and extraction of lipids from each culture were required. However, we considered that it might not be necessary to prepare separate differentiated and undifferentiated cell cultures and also might not be necessary to add cytokines or special media to obtain differentiated cells. Therefore, we employed MALDI-TOF-IMS to identify changes of lipids during spontaneous differentiation of iPSC colonies in the present study.

Materials and methods

Cell culture

The mouse embryonic fibroblast cell line SNL 76/7 (SNL cells; ECACC) was cultured on gelatin-coated culture dishes in D-MEM (Nacalai Tesque, Japan) with 10 % fetal bovine serum and 1 % penicillin/streptomycin (Invitrogen, USA) as feeder cells. A human iPSC cell line (409B2) was obtained from RIKEN BRC through the Project for Realization of Regenerative Medicine and National Bio-Resource Project of NEXT, Japan. The iPSCs were established with episomal plasmid vectors using pCXLE-hOCT3/4-shp53, pCXLE-hSox2-Klf4, and pCLXE-hLmyc-Lin28, as reported previously [9]. The iPSCs were transferred onto SNL cell feeder layers and cultured in standard human embryonic stem cell medium (ReproCELL, Japan) containing 4 ng/ml basic fibroblast growth factor (Wako, Japan). For MALDI analysis, SNL cells were cultured on gelatin- and indium/tin oxide-coated (ITO) glass slides (Sigma-Aldrich, USA) in a 10-cm culture dish. Then, iPSCs were transferred onto the SNL cell layers and cultured for 6 days. On day 6, the culture dish was placed on ice and the slides were removed from the dish and washed

three in times cold saline. Then, the slides were placed in an ITO-coated glass cassette for MALDI analysis. Differentiated and undifferentiated areas of the colony were identified by microscopic examination (Olympus CK30, Japan) and marked on the reverse side of the glass slide, which was immediately frozen at -80°C .

Immunocytochemistry

Immunocytochemistry was performed according to the method reported previously [10]. iPSCs grown on ITO-coated glass slides were fixed for 10 min at room temperature with PBS containing 4 % paraformaldehyde. After washing with pure water, the cells were stained for alkaline phosphatase (ALP) by using a Leukocyte Alkaline Phosphatase kit (Sigma, England). To stain cells for stage-specific embryonic antigen-4 (SSEA-4), iPSCs were first treated with PBS containing 5 % normal goat serum (Funakoshi, Japan), followed by incubation with mouse anti-human SSEA-4 antibody (Santa Cruz, USA) as the primary antibody and Alexa488-conjugated goat anti-mouse IgG (Invitrogen) as the secondary antibody. Then, the nuclei were stained with 4',6-diamidino-2-phenylindole (DAPI; Invitrogen).

Matrix-assisted laser desorption/ionization time-of-flight imaging mass spectrometry

MALDI-TOF/TOF-IMS was performed with an iMScopeTRIO® (Shimadzu, Japan) equipped with a 355-nm Nd:YAG laser [7]. ITO-coated glass slides with cultured cells were thawed to room temperature just before MS analysis, and dried samples were automatically and homogeneously coated with a matrix (2-hydroxy-5-methoxybenzoic acid, DHB) using an iMLayer® (Shimadzu). Mass spectrometry data were acquired in positive ion mode in the mass range m/z 500–1000. The laser beam diameter was set at 5 μm , and the mass resolving power was 10,000 at m/z 1000 used in MS and MS/MS scans. During culture, parts of the iPSC colonies show spontaneous differentiation. To find lipids with a different distribution between the differentiated and undifferentiated areas of the iPSC colonies, screening of various m/z distributions was performed by IMS analysis. The steps in the analysis were as follows: First, MS analysis was performed for the entire iPSC colony (both differentiated and undifferentiated colonies) on the ITO glass slide. Principal component analysis (PCA) was performed as unsupervised multivariate analysis, and hierarchical clustering analysis (HCA) of image patterns was done with iMScopeTRIO® software. Then, IMS analysis was performed on undifferentiated areas in the undifferentiated iPSC colonies and on differentiated areas in the differentiated iPSC colonies. A total of 16 areas ($n = 16$) in each group from another four cell culture samples were analyzed; the data were processed with

iMScopeTRIO® software. Next, comparing the overall and focal analyses, common target m/z in both differentiated and undifferentiated iPSC colonies were determined, followed by MS/MS analysis of the peaks at target m/z values. The target m/z was determined after elimination of m/z peaks derived from DHB (matrix). Target m/z was further confirmed by reversed-phase ultra-high-pressure liquid chromatography (UHPLC) MS/MS analysis. The IMS and MS/MS analysis data were compared with the Lipid MAP (<http://www.lipidmaps.org/>) and LipidBlast and NIST MS/MS libraries (<http://fiehnlab.ucdavis.edu/projects/LipidBlast>), as previously reported [11, 12]. Mass accuracy tolerance used in database searches was 0.3 Da. To compare the intensity of the target lipids in the differentiated and undifferentiated areas of the differentiated iPSC colonies, imaging analysis was performed after setting regions of interest (ROIs).

Reversed-phase ultra-high-pressure liquid chromatography (UHPLC)-MS/MS analysis

Lipids were analyzed by reversed-phase UHPLC using an Acquity UPLC BEH C18 column (1.7 μm , 2.1×50 mm; Waters, Milford, MA, USA) coupled to a 5500 QTRAP mass spectrometer (Sciex Inc., Framingham, MA, USA). A binary gradient consisting of solvent A (1:1:3 acetonitrile/methanol/water containing 5 mM ammonium acetate) and solvent B (2-propanol containing 5 mM ammonium acetate) was used. The gradient profile was as follows: 0–1 min, 95 % A; 1–9 min, 5–95 % B linear gradient; and 9–13 min, 95 % B. The flow rate was 0.3 ml/min and the column temperature was 40 °C. The instrument was operated with the following settings: source voltage of 5000 kV, GS1 40, GS2 40, CUR 30, TEM 300, and CAD gas HIGH. Phosphocholine-containing phospholipids were monitored by precursor ion scan of m/z 184.

Extraction of lipids

After washing three times in cold saline, iPSC colonies grown on feeder cells were harvested with a cell scraper, and all of the cells were collected (including differentiated and undifferentiated iPSC and SNL cells). After sonication of the cells, lipids were extracted by the Bligh–Dyer method [13]. Samples were immediately stored at -80 °C after sealing under nitrogen. To confirm the lipids identified in the cell samples, lipid extracts with DHB solution (DHB dissolved in 50 % CH_3CN and 1 % trifluoroacetic acid) were spotted onto stainless steel slides for MS/MS analysis by MALDI-TOF/TOF.

Statistical analysis

PCA was done for the cumulative contribution ratio of PC > 80 % in each image and the contribution of PC value to each group > mean PC value of each image. HCA was

performed on the basis of the Euclidean distance and the method of Ward. PCA, HCA, and generation of dendrograms were performed by using iMScopeTrio® software. Differences in the relative intensity of the target m/z values between the differentiated and undifferentiated areas of colonies were determined by using Statview software (version 5.0; Abacus Concepts, Inc., Berkeley, CA).

Results and discussion

Confirmation of undifferentiated and differentiated areas in iPSC colonies by immunocytochemistry

Because the iPSC colonies grew outwards, the central zone of each colony underwent differentiation before the peripheral region. To distinguish the differentiated and undifferentiated areas of the iPSC colonies, ALP and SSEA-4 staining was performed on day 6 after passaging the cells. ALP and SSEA-4 were positive in the undifferentiated iPSC colonies and in the undifferentiated areas of the differentiated iPSC colonies (Fig. 1a–e). In the central zone of the differentiated iPSC colonies, there were only a few SSEA-4-positive cells. DAPI staining was densely positive in the undifferentiated iPSC colonies and the undifferentiated areas of the differentiated iPSC colonies, but was also positive in the differentiated areas (Fig. 1f–h). From these findings, the differentiated and undifferentiated iPSC colonies were confirmed as reported previously [10].

MS analysis of entire colonies

MS analysis of entire colonies showed differences of the relative intensity of various m/z peaks between the differentiated and undifferentiated iPSC colonies (Fig. 1i–l). The signal intensity of the top 100 peaks was screened for entire colonies. Representative spectra are shown in Fig. 1, including peaks derived from DHB and from SNL cells located at the periphery of the iPSC colonies. Thus, peaks showing high intensities did not necessarily reflect the distribution of lipids in the differentiated or undifferentiated iPSC colonies. PCA based on two-dimensional image patterns identified 28 groups in the undifferentiated iPSC colonies and 30 groups in the differentiated iPSC colonies (see Electronic supplementary material (ESM) Figs. S1 and S2 and Tables S1 and S2). Although several peaks overlapped in several PCA groups, most of the groups identified in undifferentiated iPSCs also showed a high intensity in SNL cells localized at the borders of the iPSC colonies, while several PCA groups showed a higher intensity in the undifferentiated iPSC areas than in the SNL cell areas. In differentiated iPSC colonies, most of the PCA groups showed a similar

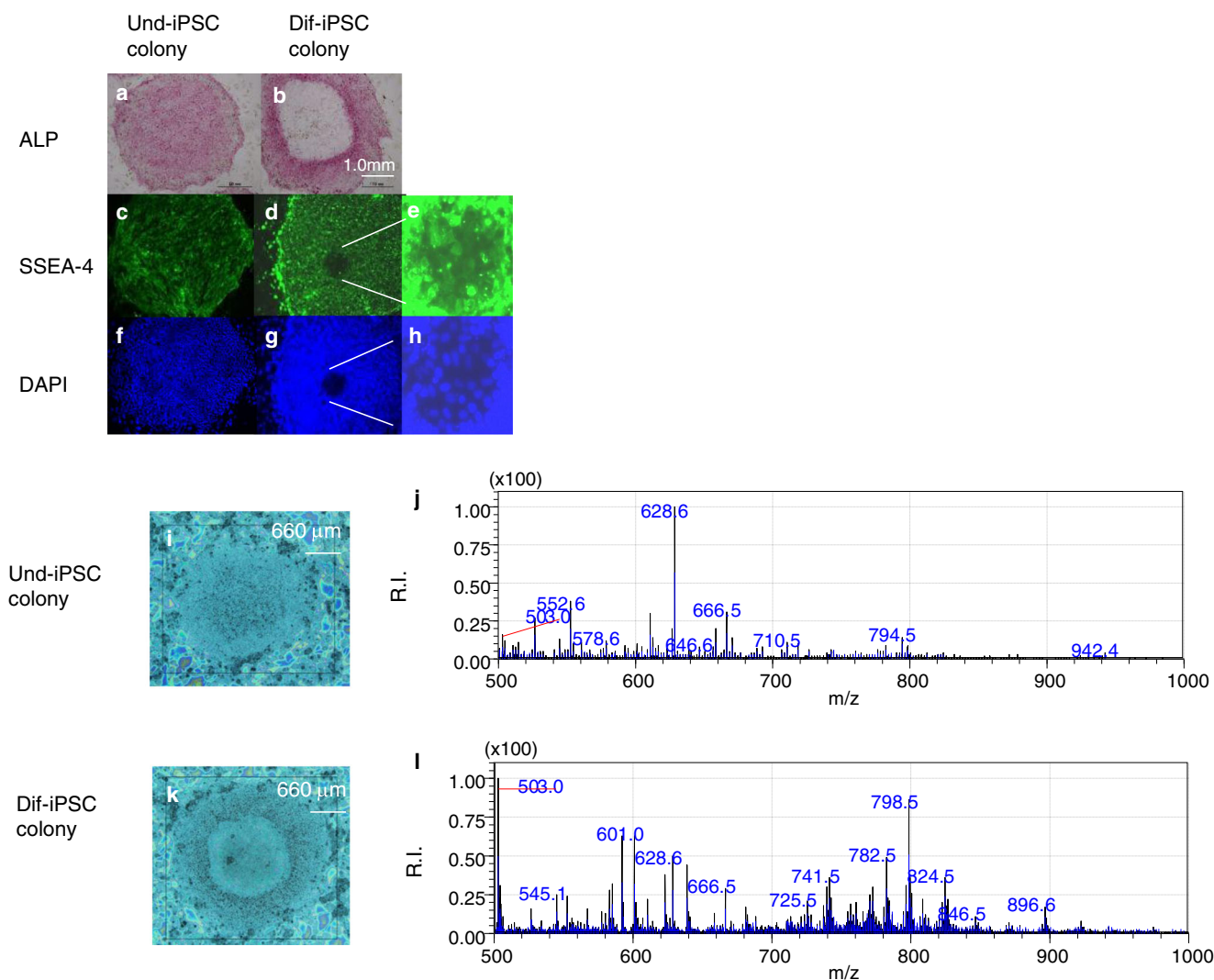


Fig. 1 Confirmation of undifferentiated (*und-*) and differentiated (*dif-*) iPSC colonies by immunocytochemistry and MS analysis of the entire iPSC colonies. Alkaline phosphatase (*ALP*) and stage-specific embryonic antigen-4 (*SSEA-4*) were positive in both undifferentiated iPSC colonies and the undifferentiated zone of differentiated iPSC colonies (**a–d**). *Scale bar* indicates 1.0 mm. At higher magnification, there were several *SSEA-4*-positive cells in the central zone of differentiated iPSC colonies (**e**). Staining for 4',6-diamidino-2-phenylindole (*DAPI*) was strongly positive

in undifferentiated areas (**f, g**), but also positive in the central zones of differentiated iPSC colonies at higher magnification (**h**). Squamous epithelial cells differentiated from iPSC were observed at the center of differentiated iPSC colonies (**h**). Microscopic images and spectra obtained by MS analysis of entire colonies are shown for undifferentiated iPSC colonies (**i, j**) and differentiated iPSC colonies (**k, l**). *Scale bar* indicates 660 μm (**i, k**). The spectra of differentiated and undifferentiated iPSC colonies (**j, l**) showed different *m/z* peak patterns. *R.I.* relative intensity

high intensity in both the SNL cell areas and differentiated areas, but several PCA groups formed concentric circles in the differentiated iPSC colonies. In the next step, HCA showed four clusters in the undifferentiated iPSC colonies (Fig. 2a) and nine clusters in the differentiated iPSC colonies (Fig. 2b). In the undifferentiated iPSC colonies, the high-intensity area of cluster 1 corresponded with the undifferentiated cells. Cluster 1 clearly showed a different distribution from cluster 4, which corresponded with the SNL cells. In the differentiated iPSC colonies, cluster 1 showed a high intensity in the differentiated

zone, while cluster 9 showed a high intensity in the undifferentiated area (the *m/z* peaks belonging to cluster 4 in the undifferentiated iPSCs and cluster 9 in the differentiated iPSC colonies are shown in ESM Fig. S3 and Table S3, plus Fig. S4 and Table S4, respectively). Both cluster 1 at *m/z* 798.5 in the undifferentiated iPSC colonies (Fig. 2a) and cluster 9 at *m/z* 798.5 (Fig. 2b) had the same *m/z* value, but different distributions in the undifferentiated area, and both areas were morphologically and immunologically associated with undifferentiated features. Further, dendrograms of the HCA clusters

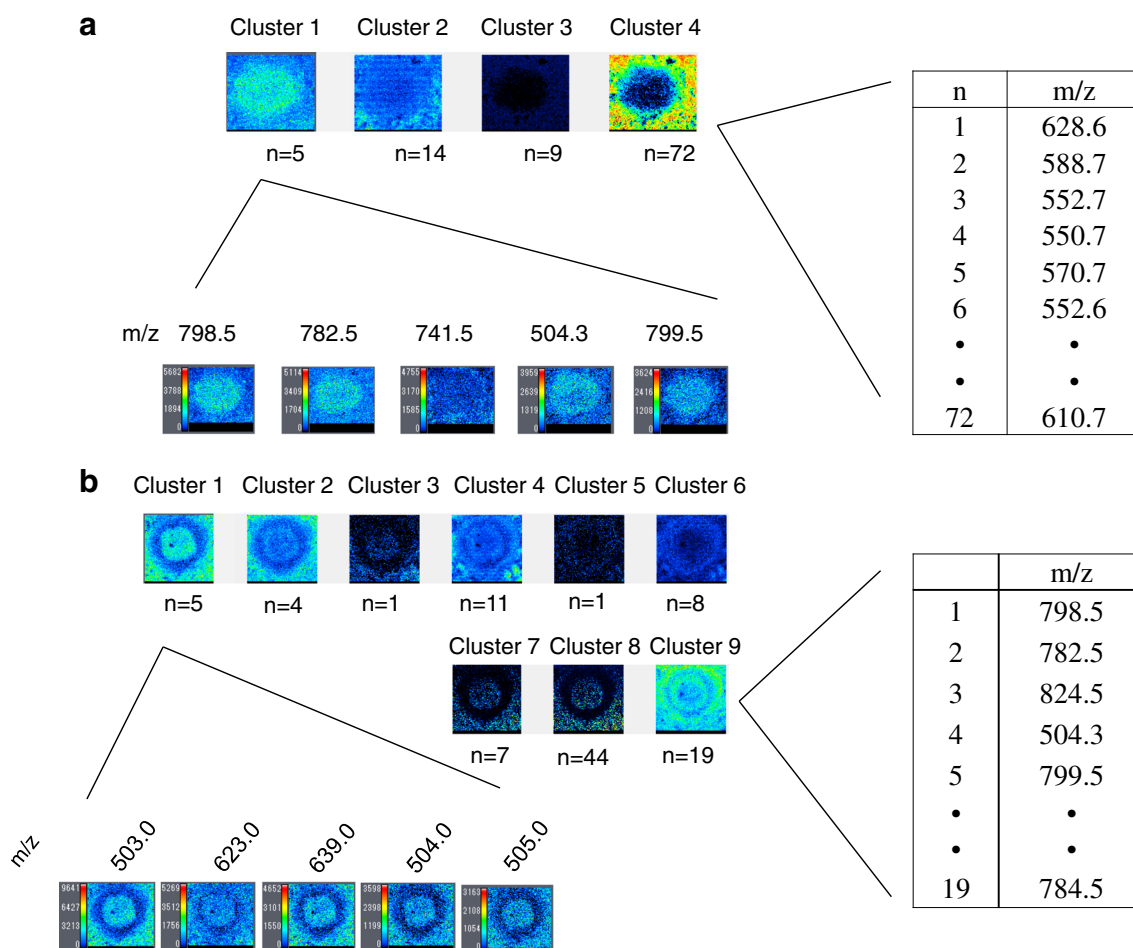


Fig. 2 HCA analysis showed four clusters in undifferentiated iPSC colonies (**a**). The top 100 high-intensity m/z peaks were assigned to HCA clusters. Cluster 1 showed high-intensity m/z peaks in undifferentiated iPSC ($n = 4$), while cluster 4 showed high-intensity m/z peaks in SNL cells ($n = 72$). Note that SNL cells were localized around the undifferentiated iPSC colonies. Images and m/z peaks of cluster 4 are shown in ESM

Fig. S3 and Table S3. HCA analysis showed nine clusters in differentiated iPSC colonies (**b**). Cluster 1 had high-intensity m/z peaks in the differentiated zone and SNL cell area ($n = 5$), while cluster 9 showed high-intensity m/z peaks in the undifferentiated rather than the differentiated areas ($n = 19$). Images and m/z peaks of cluster 9 are shown in ESM Fig. S4 and Table S4

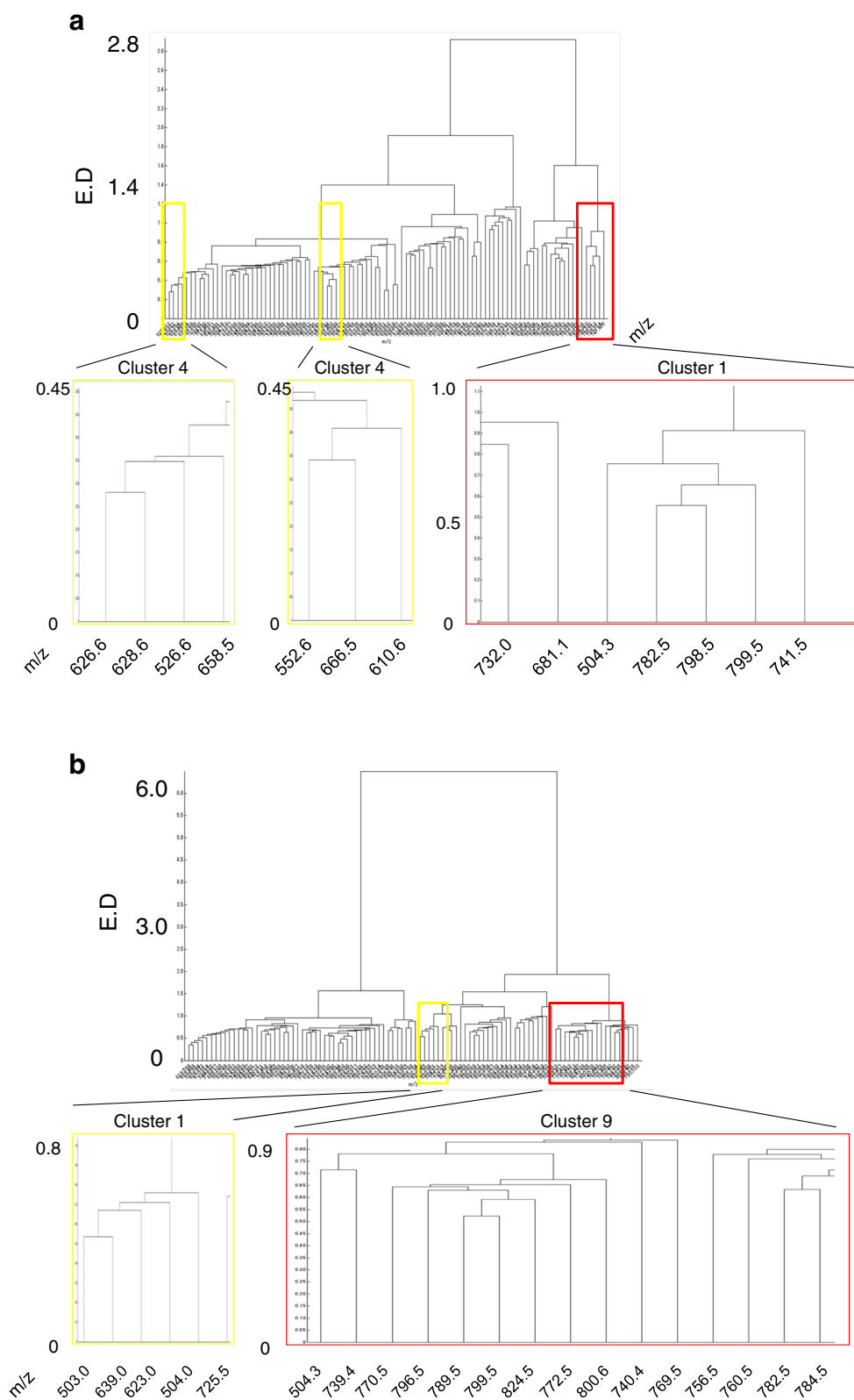
demonstrated that the m/z peaks of clusters 1 and 4 in the undifferentiated iPSC colonies (Fig. 3a) or clusters 1 and 9 in the differentiated iPSC colonies (Fig. 3b) formed separate trees.

Localized IMS and MS/MS analyses

Analysis of the entire of colonies demonstrated the distribution of various lipids, but this analysis included data for DHB and SNL cells. Therefore, to exclude these background data, analysis of localized areas was done as the next step (Fig. 4a–f). Focused MS analysis was done by focusing on the undifferentiated areas in the undifferentiated iPSC colonies and on the differentiated areas in the differentiated iPSC colonies. In the previous step of screening entire colonies, the peaks of DHB and SNL cells had been included, so the range had been broadly set as the top 100 m/z peaks based on intensity. In the step of focused analysis, the range had been set as the top 50

m/z peaks based on intensity in order to find major abundant lipids. MS analysis on focused areas showed high intensities of the peaks, such as m/z 503.0, 601.0, 638.9, 772.5, 782.5, 798.5, and 824.5 in the undifferentiated iPSC colonies ($n = 16$), while the peaks such as m/z 503.0, 580.1, 601.0, and 681.0 were high, and m/z 782.5 and 798.5 also appeared in the differentiated iPSC colonies ($n = 16$; Fig. 4b, d). High-intensity peaks derived from DHB were found at m/z 545.0, 580.1, 585.0, 681.0, and 721.0 (Fig. 4f). From the results of the analysis of the entire colonies and the localized analysis, candidate target peaks were selected as follows. First, the m/z peaks derived from DHB were excluded from the peaks of the undifferentiated and differentiated iPSC colonies. Second, peaks common to the undifferentiated and differentiated iPSC colonies in the localized analysis were selected (ESM Fig. S5). Third, peaks common to the analysis of entire colonies and to localized analysis were determined. Finally, six peaks at m/z 503.0, 578.6, 623.0, 638.9, 782.5, and 798.5 were

Fig. 3 Dendrograms of HCA clusters showed that the m/z peaks in clusters 1 and 4 from undifferentiated iPSC colonies (**a**) and the m/z peaks in clusters 1 and 9 from differentiated iPSC colonies (**b**) belonged to separate trees. *E.D* Euclidian distance



selected (Fig. 5a, b). When the six peaks were subjected to MS/MS analysis by MALDI-TOF-IMS, two precursor ions of m/z 782.5 and 798.5 were matched to be PCs by lipid database

search (Figs. 5a, b and 6a–h). Fragment ions of m/z 782.5 (Fig. 6b, f) and 798.5 (Fig. 6d, h) also matched to each PC(36:4) or PC(34:1) for m/z 782.5 and PC(34:1) for m/z

Fig. 4 MS analysis of localized areas (a–f). MS analysis focused on the area inside the *black square* (a, c, and e). Scale bar indicates 660 μm (a, c, and e). High-intensity peaks at *m/z* 503.0, 601.0, 638.9, 772.5, 782.5, 798.5, and 824.5 were found in undifferentiated iPSC colonies (b) (*n* = 16), while peaks at *m/z* 503.0, 580.1, 601.0, and 681.0 were high, and also *m/z* 782.5 and 798.5, and were in differentiated iPSC colonies (d) (*n* = 16). High-intensity peaks for DHB were detected at *m/z* 545.0, 580.1, 585.0, 681.0, and 721.0 (f)

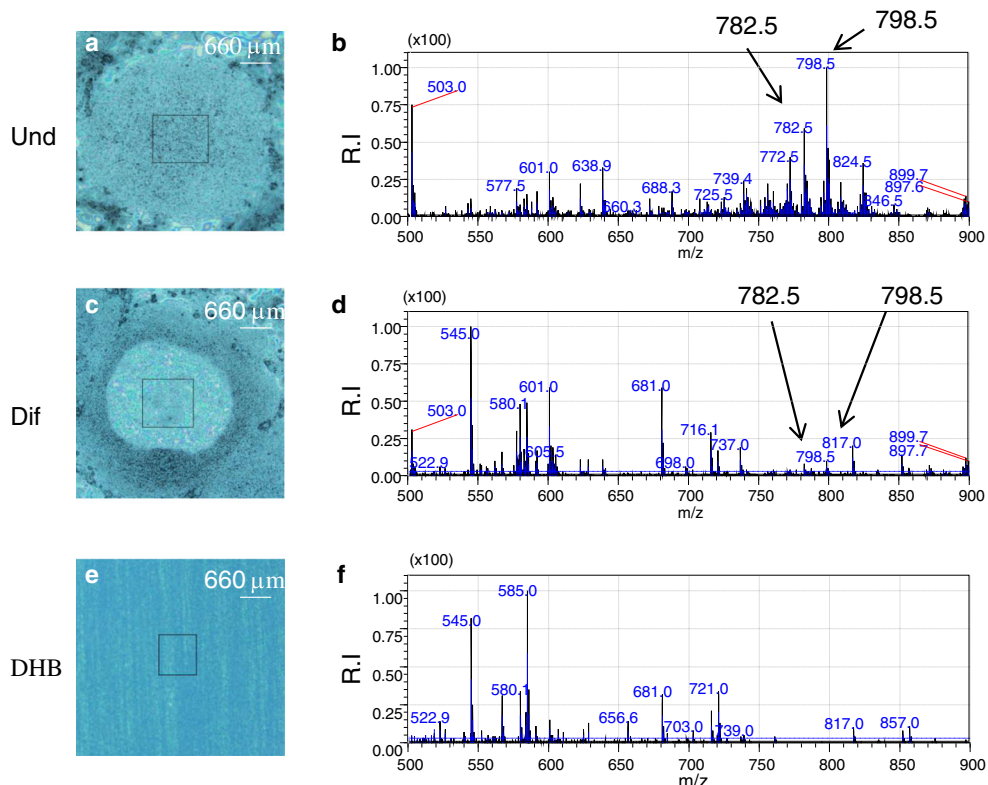
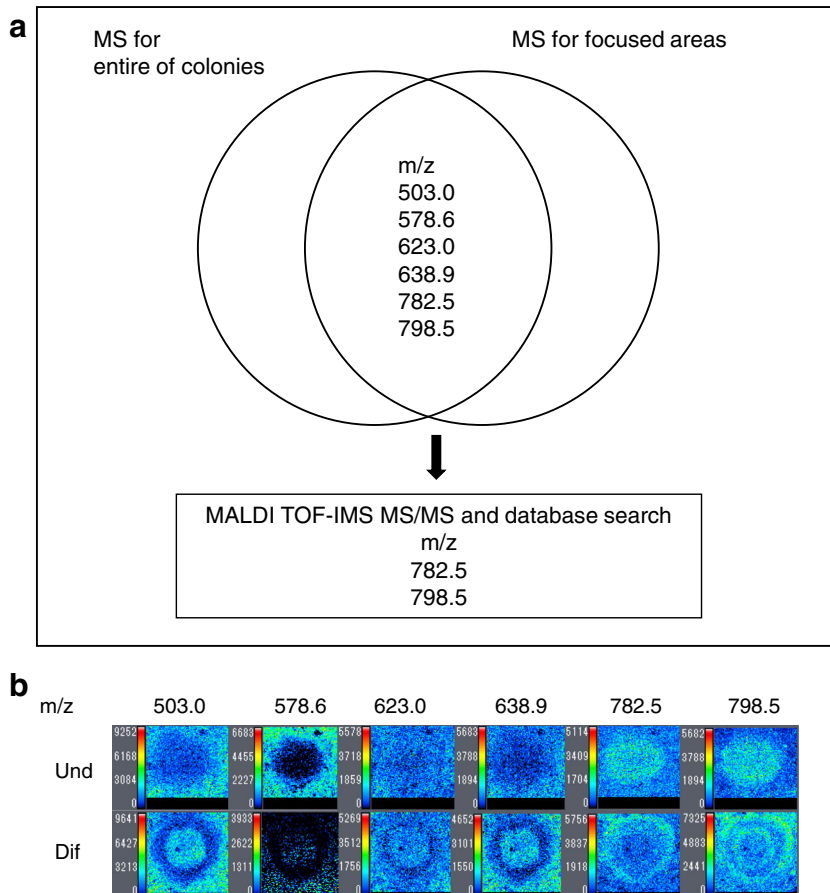


Fig. 5 a Selection of candidate *m/z* peaks. Six peaks were common to the analysis of entire colonies and to localized analysis, and two peaks of *m/z* 782.5 and 798.5 were matched to database. b Summary of candidate target *m/z* peaks for the analysis of entire colonies and for localized analysis. Images of undifferentiated and differentiated iPSC colonies corresponding with the target peaks are shown



798.5, according to previous reports [11, 12]. The identity of the other four m/z peaks could not be determined because parental ions could not be found, although several fragment ions were obtained by MS/MS analysis. Precursor ions m/z 782.5 was more abundant in the undifferentiated iPSC colonies than in SNL cells localized at around the colonies (Fig. 6a) and was also more abundant in the undifferentiated areas than in the differentiated areas of the differentiated iPSC colonies (Fig. 6e). Precursor ion m/z 798.5 was also more abundant in the undifferentiated iPSC colonies than in SNL cells (Fig. 6c), while it was distributed in concentric circles in the differentiated iPSC colonies (Fig. 6g). To confirm PCs obtained from MALDI-TOF-IMS, MS/MS analysis was performed using lipid extract in the next steps.

MS/MS analysis of lipid extracts from cell culture dishes, including undifferentiated iPSC colonies, differentiated iPSC colonies, and SNL feeder cells

To confirm the existence of the m/z fragments, MS/MS by MALDI-TOF analysis was performed again using droplets of lipid extracts from the whole culture dish of a day 6 iPSC culture. The differentiated iPSC colonies accounted for 49.9 ± 11.7 % of all iPSC colonies in 6-cm culture dishes ($n=4$). Fragment m/z peaks of the peaks at m/z 782.5 and 798.5 could be obtained, but there were numerous background peaks (see ESM Fig. S6; a representative m/z peak list is shown in Table S5). From these results, UHPLC-MS/MS analysis was done on lipid extracts on the next further step. Lipid extracts from the whole culture dish of a day 3 iPSC culture (undifferentiated extracts) and day 8 iPSC culture (differentiated extracts) were subjected to this

analysis. Extracts from undifferentiated iPSC colonies accounting for less than about 10 % of the undifferentiated colonies of all iPSC cultures (undifferentiated extracts) and extracts from differentiated colonies accounting for more than 80 % of the differentiated colonies of the iPSC culture (differentiated extracts) were subjected. Phosphocholine-containing phospholipids were monitored by precursor ion scan of m/z 184. From both samples, the peak at m/z 184.1, which was a phosphocholine ion, was obtained by UHPLC MS/MS analysis on precursor ions m/z 782.5 (ESM Fig. S7a, c) and 798.5 (ESM Fig. S7b, d). To identify target PCs, product ion data obtained by both MALDI-TOF-IMS and UHPLC were collected. From the precursor ion at m/z 798.5, the product ions at m/z 739.4, 615.5, and 184.1 were detected. The difference between the m/z values represents neutral losses (NLs) corresponding to 59 Da from m/z 798.5 to 739.5 and NLs corresponding to 124 Da from m/z 739.5 to 615.5. NLs of 59 and 124 Da are known PC species of trimethylamine $[N(CH_3)_3]$ and cyclophosphane ring $[(CH_2)_2PO_4H]$, respectively [12, 14, 15]. According to a database research, the peak at m/z 798.5 was identified as $(C_{42}H_{82}NO_8P, PC(34:1)[M+K]^+)$. For the precursor ion at m/z 782.5, the product ions at m/z 723.4, 599.5, and 184.1 were detected. The difference between the m/z values represents NLs corresponding to 59 Da from m/z 782.5 to 723.4 and NLS corresponding to 124 Da from m/z 723.4 to 599.5. According to a database research, peaks at m/z 782.5 were $(C_{44}H_{81}NO_8P, PC(36:4)[M+H]^+)$ or $(C_{42}H_{82}NO_8P, PC(34:1)[M+Na]^+)$. Therefore, images for differentiated colonies were compared between m/z peaks 782.5 and 798.5

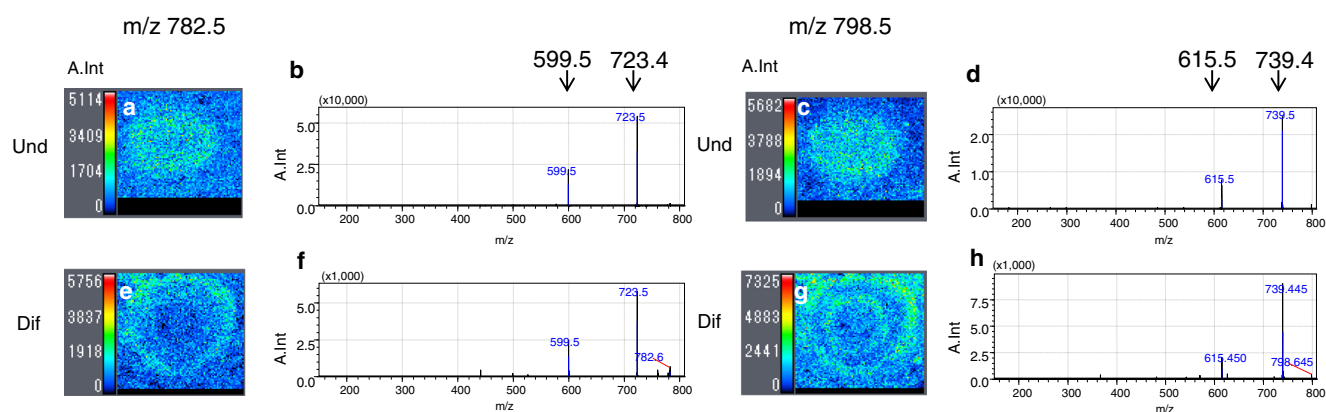


Fig. 6 Lipids showing different distributions in undifferentiated and differentiated iPSC colonies. When the six peaks were subjected to MS/MS analysis by MALDI-TOF-IMS, two precursor ions of m/z 782.5 and 798.5 were matched to be PCs by database search. The peak at m/z 782.5 showed an inverse pattern between undifferentiated and differentiated iPSC colonies (a, e). The peak at m/z 798.5 showed a diffuse distribution in undifferentiated iPSC colonies, but a concentric pattern in

differentiated iPSC colonies (c, g). Fragment ion spectra obtained by localized MS/MS analysis are shown (b, d, f, h). Fragment ion peaks obtained by MS/MS analysis of the peak at m/z 782.5 were found at m/z 599.5 and 723.4 in both undifferentiated (b) and differentiated (f) iPSCs, while fragment ion peaks obtained from the peak at m/z 798.5 were detected at m/z 615.4 and 739.4 in both undifferentiated (d) and differentiated (h) iPSCs

Table 1 Summary of the identified lipids

Molecular formula	Matched lipids	MS-observed m/z		Theoretical m/z	MS/MS fragments
		Entire colony	Focused area		
C ₄₄ H ₈₁ NO ₈ P	PC(36:4)[M+H] ⁺	782.5	782.5	782.569	184/599.5/723.4/782.5
C ₄₂ H ₈₂ NO ₈ P	PC(34:1)[M+K] ⁺	798.5	798.5	798.541	184/615.5/739.4/798.5

(Fig. 6e, g). These images indicated different PC distribution patterns between 782.5 and 798.5; nevertheless, the analysis was done on the same differentiated iPSC colony. If m/z 782.5 is PC(34:1)[M+Na]⁺, the images of m/z 782.5 and 798.5 (PC(34:1)[M+K]⁺) are possibly the same; however, the images indicated different patterns between m/z 782.5 and 798.5 in the same differentiated colony. Then, we concluded that m/z 782.5 was (C₄₄H₈₁NO₈P, PC(36:4)[M+H]⁺). Taken together, these findings confirmed the presence of two distinct lipids, which were at m/z 782.5 (C₄₄H₈₁NO₈P, PC(36:4)[M+H]⁺) and at m/z 798.5 (C₄₂H₈₂NO₈P, PC(34:1)[M+K]⁺) (Table 1). The relative intensity of PC(36:4), which was m/z 782.5, was significantly higher in the undifferentiated areas (77.5 ± 18.2) than in the differentiated areas (32.4 ± 14.7) of the differentiated iPSC colonies shown in Fig. 6e ($n = 6$, $p = 0.0008$).

It has been reported that PC(36:4) was the major lipid showing elevation in murine embryonic stem cells and murine iPSCs compared with murine fibroblasts [6]. An increase of unsaturated PCs, such as PC(36:4), PC(38:6), and PC(38:4), was reported previously, and it was speculated that changes of PC saturation might alter cell membrane fluidity in relation to phenotypic changes of stem cells [5, 6]. PC(34:1) has been reported in various human cancers, such as breast, colorectal, esophageal, lung, gastric, thyroid, and liver cancer [11, 16]. PC(34:1) is also widely distributed in the rat brain [7], while its level is reduced in ischemic areas [14]. For regenerating an organ, MALDI-IMS revealed that multiple PCs were distributed in regenerating mouse liver. Interestingly, most of the PCs increased, such as PC(1-acyl 34:1)[M+Na]⁺, PC(1-acyl 34:1)[M+K]⁺, PC(1-acyl 34:2)[M+Na]⁺, and PC(1-acyl 34:1)[M+K]⁺, but PC(1-acyl 36:4) was not changed. PC(1-acyl 40:6) and PC(1-acyl 40:8) decreased in the regenerating liver [17]. From these reports, PC(34:1) may be abundant in cells with high proliferative activity and metabolism, while it is decreased in low or stable metabolic states. PC localization during cell differentiation was reported. MALDI imaging analysis for the characterization of lipid markers of chondrogenic differentiation by mesenchymal stem cells (MSCs) revealed that PCs and Pcho were more abundant in the peripheral zone of micromasses composed by MSCs on day 14 of differentiation, while those lipids were distributed diffusely in micromasses in the early stage of differentiation on day 2 [18]. In the present study, PC(34:1) was distributed in

concentric circles, with a high intensity at the border between the differentiated area (center of the colony) and the undifferentiated area of iPSC colonies, as well as at the border between the undifferentiated area of iPSCs and the SNL cells (Fig. 6g). Therefore, PC(34:1) may play a role in the differentiation of iPSCs or the invasion of these cells into tissues.

Conclusion

Lipid metabolism changes during the differentiation of iPSC cells. This is the first report about the spatial distribution of lipids in iPSC colonies. MALDI-TOF-IMS revealed differences in the distribution of PCs in iPSC colonies, and the distribution of peaks at m/z 782.5 and 798.5 changed during the differentiation of iPSC colonies. PC(36:4) and PC(34:1) may be associated with iPSC cell differentiation, but further analysis is needed to elucidate the functional significance of these lipids.

Acknowledgments This work was partly supported by a grant-in-aid for the MEXT KAKENHI Grant, Japan (S1412001) and JSPS KAKENHI Grant, Japan (16K09553). The authors are grateful to Isao Asaka [Center for iPSC Cell Research and Application (CiRA), Kyoto University] for advice on iPSC culture and to Satomi Tateno, Mio Maekawa, and Sachiko Nakadate (Department of Pharmacology and Toxicology, Dokkyo Medical University) for assistance with iMScope analysis, as well as Akiko Horigane (Department of Pulmonary Medicine and Clinical Immunology) for assistance with cell culture.

Compliance with ethical standards

Conflict of interest The authors declare that they have no conflict of interests.

References

- Inoue H, Nagata N, Kurokawa H, Yamanaka S. iPSC cells: a game changer for future medicine. *EMBO J*. 2014;33:409–17.
- Hayakawa T, Aoi T, Umezawa A, Ozawa K, Sato Y, Sawa Y, et al. A study on ensuring the quality and safety of pharmaceuticals and medical devices derived from the processing of autologous human somatic stem cells. *Regen Ther*. 2015;2:57–69.
- French A, Bravery C, Smith J, Chandra A, Archibald A, Gold JD, et al. Enabling consistency in pluripotent stem cell-derived products for research and development and clinical applications through material standards. *Stem Cells Transl Med*. 2015;4:217–23.

4. Santos CR, Schulze A. Lipid metabolism in cancer. *FEBS J*. 2012;279:2610–23.
5. Yanes O, Clark J, Wong DM, Patti GJ, Sánchez-Ruiz A, Benton HP, et al. Metabolic oxidation regulates embryonic stem cell differentiation. *Nat Chem Biol*. 2010;6:411–7.
6. Meissen JK, Yuen BT, Kind T, Riggs JW, Barupal DK, Knoepfler PS, et al. Induced pluripotent stem cells show metabolomic differences to embryonic stem cells in polyunsaturated phosphatidylcholines and primary metabolism. *PLoS One*. 2012;7:e46770.
7. Setou M, Kurabe N. Mass microscopy: high-resolution imaging mass spectrometry. *J Electron Microsc (Tokyo)*. 2011;60:47–56.
8. Malchenko S, Xie J, de Fatima BM, Vanin EF, Bhattacharyya BJ, Belmadani A, et al. Onset of rosette formation during spontaneous neural differentiation of hESC and hiPSC colonies. *Gene*. 2014;534:400–7.
9. Okita K, Matsumura Y, Sato Y, Okada A, Morizane A, Okamoto S, et al. A more efficient method to generate integration-free human iPSC cells. *Nat Methods*. 2011;5:409–12.
10. Takahashi K, Tanabe K, Ohnuki M, Narita M, Ichisaka T, Tomoda K, et al. Induction of pluripotent stem cells from adult human fibroblasts by defined factors. *Cell*. 2007;131:861–72.
11. Guo S, Wang Y, Zhou D, Li Z. Significantly increased monounsaturated lipids relative to polyunsaturated lipids in six types of cancer microenvironment are observed by mass spectrometry imaging. *Sci Rep*. 2014;4:5959.
12. Berry KA, Hankinn JA, Barkley RM, Spragginsn JM, Caprioli RM, Murphy RC. MALDI imaging of lipid biochemistry in tissues by mass spectrometry. *Chem Rev*. 2011;111:6491–512.
13. Bligh EG, Dyer WJ. A rapid method of total lipid extraction and purification. *Can J Biochem Physiol*. 1959;37:911–7.
14. Koizumi S, Yamamoto S, Hayasaka T, Konishi Y, Yamaguchi-Okada M, Goto-Inoue N, et al. Imaging mass spectrometry revealed the production of lyso-phosphatidylcholine in the injured ischemic rat brain. *Neuroscience*. 2010;168:219–25.
15. Ishikawa S, Tateya I, Hayasaka T, Masaki N, Takizawa Y, Ohno S, et al. Increased expression of phosphatidylcholine (16:0/18:1) and (16:0/18:2) in thyroid papillary cancer. *PLoS One*. 2012;7:e48873.
16. Morita Y, Sakaguchi T, Ikegami K, Goto-Inoue N, Hayasaka T, Hang VT, et al. Lysophosphatidylcholine acyltransferase 1 altered phospholipid composition and regulated hepatoma progression. *J Hepatol*. 2013;59:292–9.
17. Miyamura N, Nakamura T, Goto-Inoue N, Zaima N, Hayasaka T, Yamasaki T, et al. Imaging mass spectrometry reveals characteristic changes in triglyceride and phospholipid species in regenerating mouse liver. *Biochem Biophys Res Commun*. 2011;408:120–5.
18. Rocha B, Cillero-Pastor B, Eijkel G, Bruinen AL, Ruiz-Romero C, Heeren RM, et al. Characterization of lipidic markers of chondrogenic differentiation using mass spectrometry imaging. *Proteomics*. 2015;15:702–13.

Inhibition of L-type amino acid transporter I activity as a new therapeutic target for cholangiocarcinoma treatment

Tumor Biology
March 2017: 1–14
© The Author(s) 2017
Reprints and permissions:
sagepub.co.uk/journalsPermissions.nav
DOI: 10.1177/1010428317694545
journals.sagepub.com/home/tub



Supak Yothaisong^{1,2,3}, Hasaya Dokduang^{2,3}, Naohiko Anzai⁴, Keitaro Hayashi⁵, Nisana Namwat^{1,2,3}, Puangrat Yongvanit^{1,2,3}, Sakkarn Sangkhamanon⁶, Promsuk Jutabha⁵, Hitoshi Endou⁷ and Watcharin Loilome^{1,2,3}

Abstract

Unlike normal cells, cancer cells undergo unlimited growth and multiplication, causing them to require massive amounts of amino acid to support their continuous metabolism. Among the amino acid transporters expressed on the plasma membrane, L-type amino acid transporter-I, a Na⁺-independent neutral amino acid transporter, is highly expressed in many types of human cancer including cholangiocarcinoma. Our previous study reported that L-type amino acid transporter-I and its co-functional protein CD98 were highly expressed and implicated in cholangiocarcinoma progression and carcinogenesis. Therefore, this study determined the effect of JPH203, a selective inhibitor of L-type amino acid transporter-I activity, on cholangiocarcinoma cell inhibition both in vitro and in vivo. JPH203 dramatically suppressed [¹⁴C]-leucine uptake as well as cell growth in cholangiocarcinoma cell lines along with altering the expression of L-type amino acid transporter-I and CD98 in response to amino acid depletion. We also demonstrated that JPH203 induced both G2/M and G0/G1 cell cycle arrest, as well as reduced the S phase accompanied by altered expression of the proteins in cell cycle progression: cyclin D1, CDK4, and CDK6. There was also cell cycle arrest of the related proteins, P21 and P27, in K KU-055 and K KU-213 cholangiocarcinoma cells. Apoptosis induction, detected by an increase in trypan blue-stained cells along with a cleaved caspase-3/caspase-3 ratio, occurred in JPH203-treated cholangiocarcinoma cells at the highest concentration tested (100 μM). As expected, daily intravenous administration of JPH203 (12.5 and 25 mg/kg) significantly inhibited tumor growth in K KU-213 cholangiocarcinoma cell xenografts in the nude mice model in a dose-dependent manner with no statistically significant change in the animal's body weight and with no differences in the histology and appearance of the internal organs compared with the control group. Our study demonstrates that suppression of L-type amino acid transporter-I activity using JPH203 might be used as a new therapeutic strategy for cholangiocarcinoma treatment.

Keywords

L-type amino acid transporter I, cholangiocarcinoma, JPH203, cell cycle arrest, apoptosis, in vivo model

Date received: 26 May 2016; accepted: 23 December 2016

¹Department of Biochemistry, Faculty of Medicine, Khon Kaen University, Khon Kaen, Thailand

²Liver Fluke and Cholangiocarcinoma Research Center, Khon Kaen University, Khon Kaen, Thailand

³Cholangiocarcinoma Screening and Care Program (CASCAP), Khon Kaen University, Khon Kaen, Thailand

⁴Department of Pharmacology, Graduate School of Medicine, Chiba University, Chiba, Japan

⁵Department of Pharmacology and Toxicology, School of Medicine, Dokkyo Medical University, Mibu, Japan

⁶Department of Pathology, Faculty of Medicine, Khon Kaen University, Khon Kaen, Thailand

⁷J-Pharma Co., Ltd., Tokyo, Japan

Corresponding author:

Watcharin Loilome, Department of Biochemistry, Faculty of Medicine, Khon Kaen University, 123 Mittraphap Road, Khon Kaen 40002, Thailand.

Email: watloi@yahoo.com



Introduction

Increased essential nutrient uptake, such as glucose and amino acids, is required for proliferating cells, especially in cancer cells which have lost their normal control of proliferation.¹ Many studies have revealed that numerous nutrient transporters are upregulated in cancer cells to support their massive growth. Among the known amino acid transport systems, system L is a major Na⁺-independent transport agency responsible for the transport of neutral amino acids, including several essential amino acids.² System L has four isoforms: L-type amino acid transporter 1 (LAT1), LAT2, LAT3, and LAT4. While LAT1 and LAT2 require CD98, a heavy chained cell surface antigen forming a heterodimer for the obligatory amino acid exchange on the plasma membrane, LAT3 and LAT4 are facilitated diffusers of amino acid substrates.^{3–7}

LAT1 is one of the most actively studied amino acid transporters in basic research and drug development in human cancers. Many studies have demonstrated that LAT1 is overexpressed and plays a critical role in various human cancers, including cholangiocarcinoma (CCA).^{8–12} CCA is a usually fatal cancer arising from the epithelial cells of the biliary tract. The highest incidence of CCA has been reported from northeast Thailand,¹³ where it is associated with the highest prevalence of liver fluke (*Opisthorchis viverrini*) infection.^{14,15} There is strong evidence indicating that chronic inflammation during liver fluke infection is a key event of CCA carcinogenesis.¹⁶ The lack of effective medical treatment makes radical surgical resection the only chance of cure;¹⁷ however, patients with CCA typically present at an advanced stage of the disease with non-resectable tumors, resulting in a very poor prognosis and only limited therapeutic possibilities.¹⁸ Thus, new approaches to therapy are required to improve patient survival.

JPH203 (also known as KYT0353) is a novel tyrosine analog that selectively inhibits LAT1 transport activity.^{19,20} To date, only three studies have shown that JPH203 has anti-tumor activities in human cancers. JPH203 was highly effective against [¹⁴C]L-leucine uptake and cell growth in human colon cancer cells,¹⁹ human oral cancer cells,²¹ and leukemic cells.²² Moreover, this specific LAT1 inhibitor showed statistically significant growth inhibition against xenografted human colon cancer cells¹⁹ and murine T-lymphoma cells with tPTEN^{-/-} xenografts in the nude mouse model.²² Furthermore, JPH203 was nontoxic to normal murine thymocytes and human peripheral blood lymphocytes,²² suggesting that inhibition of LAT1 activity using JPH203 might be used as a novel therapeutic strategy for cancer treatment.

Our previous study has shown that the expression of LAT1 and CD98 was increased in CCA development during oxidative stress due to *O. viverrini* infection, which might be regulated by the oncogenic signaling pathway,

phosphatidylinositol-3-kinase (PI3K)/AKT. We also showed that CCA tissues exhibited strong LAT1 immunostaining compared to normal bile duct tissues. Furthermore, LAT1 plays an important role as a tumor prognostic factor for CCA patients.¹¹

Based on our previous report, we hypothesized that LAT1 is the main system L-amino acid transporter in CCA, potentially making it a target for CCA cell inhibition. In this study, we investigated the expression of system L-amino acid transporters and CD98 in CCA cell lines. Moreover, we determined, for the first time, the effects of a novel selective LAT1 inhibitor, JPH203, on cell growth and its mechanism for cell growth inhibition in the CCA model. Our results from the in vitro model clearly demonstrated that LAT1 is the main system L-amino acid transporter in CCA cells and that it is expressed together with CD98. Inhibition of LAT1 transport activity using JPH203 could dramatically suppress amino acid uptake and CCA cell growth through altering the cell cycle distribution patterns as well as in inducing apoptosis. Furthermore, JPH203 has anti-tumor activity against CCA cell growth in the in vivo model without general toxicity. This result indicates the possibility of using JPH203 for CCA treatment.

Materials and methods

Cell lines and cell culture

The human CCA cell lines, KKKU-055, KKKU-213, and KKKU-100, were obtained from CCA patients and established at the Liver Fluke and Cholangiocarcinoma Research Center, Khon Kaen University. All of the cell lines were cultured in Ham's F-12 medium (Sigma-Aldrich, St Louis, MO, USA) supplemented with inactivated 10% fetal bovine serum (FBS), 1% penicillin–streptomycin, and NaHCO₃ in a humidified atmosphere containing 5% CO₂.

Antibodies and inhibitor

Antibodies used in this study were as follows: anti-cyclin D1 (#2926D), CDK4 (#2906P), CDK6 (#3136P), P21 (#2946), and P27 (#2552P), purchased from Cell Signaling Technology (Danvers, MA, USA). Antibody against CD98 was purchased from Santa Cruz Biotechnology (Santa Cruz, CA, USA). Anti-caspase-3 (ab32351) and anti-Ki67 were purchased from Abcam (Cambridge, UK). Anti-LAT1 antibody and JPH203 was kindly supplied by J-Pharma (Tokyo, Japan).

Reverse transcription polymerase chain reaction analysis

Reverse transcription polymerase chain reaction (RT-PCR) analysis was performed to determine the expression of the LATs and CD98 at the messenger RNA (mRNA) level.

Total RNAs were prepared from the CCA cells maintained in the growth medium at 37°C in 10 cm Petri dishes using an RNeasy Plus Mini Kit (Qiagen, Hilden, Germany) in accordance with the manufacturer's instruction. RT-PCR analysis was performed with the PrimeScript® RT reagent Kit (Takara Bio Inc., Shiga, Japan) under the conditions recommended by the manufacturer and used as a template for PCR amplification. PCR amplification was performed using the Promega PCR Master Mix (Promega, Madison, WI, USA) following the protocol: 95°C for 2 min; followed by 20 cycles of 95°C for 30 s, 55°C for 30 s, and 72°C for 30 s; with a final extension step of 72°C for 5 min. For LAT1, the forward and reverse primers used were 5'-TGCCGTGTCTTCATCCTG-3' and 5'-CCTCCTGGCTATGTCTCCTG-3', respectively. For LAT2, the forward and reverse primers were 5'-GCCCTCACCTTCTCCAATA-3' and 5'-AATGCATTCTTTGGCTCAG-3', respectively. For LAT3, the forward and reverse primers were 5'-CACGCTACTGCAAGATCCAA-3' and 5'-AGAAGGGCTCTCCTTTCAGG-3', respectively; and for LAT4, the forward and reverse primers were 5'-AAATTGGCCTTCACTGTGG-3' and 5'-ACGACGATGAA GGAGACACC-3', respectively. For CD98, the forward and reverse primers were 5'-CAGAAGGATGATGTC GCTCA-3' and 5'-CCAGTGGCGGATATAGGAGA-3', respectively. A pair of primers, 5'-GCTG CTTT TAAC TCTG GTAA-3' and 5'-CGCGCCATCAC GCCACAGT-3', was used for the PCR amplification of glyceraldehyde 3-phosphate dehydrogenase (GAPDH).

Quantitative western blotting

To confirm the expression of LAT1 and CD98 in CCA cell lines, the cells were grown in 10 cm Petri dishes before harvesting and total protein extraction. To investigate the effects of JPH203, CCA cell lines were plated at 4×10^5 cells in 10 cm Petri dishes, cultured overnight, and then treated with JPH203 at 1–100 μ M and 0.1% dimethyl sulfoxide (DMSO) for 48 h. After incubation, the cells were harvested and subjected to protein extraction and western blotting. Briefly, total proteins were isolated by ice-cold radioimmunoprecipitation assay (RIPA) buffer (50 mM Tris-HCl, pH 7.4, 1% Triton X-100, 0.25% sodium deoxycholate, 150 mM NaCl, 1 mM ethylene glycol-bis (β -aminoethyl ether)-*N,N,N',N'*-tetraacetic acid (EGTA), 1 mM phenylmethylsulfonyl fluoride (PMSF), 2 mM sodium orthovanadate, and 5 mM sodium fluoride) supplied as Completed Protease Inhibitor Cocktails (1 tablet/10 mL of buffer; Roche, Basel, Switzerland). Protein concentrations were calculated using a Pierce® BCA Protein Assay Kit (Thermo Scientific, Rockford, IL, USA). A volume of 40 μ g of proteins were then loaded onto the gels, separated by sodium dodecyl sulfate–polyacrylamide gel electrophoresis (SDS-PAGE), and transferred onto polyvinylidene fluoride (PVDF) membranes (EMD Millipore

Corp., Bedford, MA, USA) using the Bio-Rad western blot system (Bio-Rad Laboratories, Berkeley, CA, USA). After blocking with 5% skim milk in Tris-buffered saline (TBS), the membranes were incubated overnight at 4°C with appropriate primary antibody diluted in blocking buffer. The specific horseradish peroxidase–conjugated secondary antibody incubation was performed for 1 h at room temperature with gentle shaking. The signal was visualized using Pierce ECL Plus Western Blotting Substrate (Thermo Scientific), and the protein densitometric values were analyzed by Multi Gauge software (Fujifilm, Tokyo, Japan). The experiment was replicated three times, and densitometry values for each protein were normalized with the densitometry value of β -actin, which was used as internal control.

Amino acid uptake

To determine the inhibitory effect of JPH203 on amino acid transport in CCA cells, [14 C]L-leucine (Moravex Biochemicals Inc., Brea, CA, USA) was used as the prototypical LAT1 substrate in uptake experiments evaluated via radioactivity. Briefly, the indicated cells were seeded at 2.5×10^4 cells/well in 24-well plates and incubated at 37°C in 5% CO₂ for 2 days. After incubation, the adherent cells were washed three times and pre-incubated for 10 min at 37°C with 0.5 mL of sodium free Hanks' balanced salt solution (Na⁺-free HBSS). Then, the uptake of 1 μ M [14 C]L-leucine was measured in the presence of JPH203 (0.01, 0.1, 1, 3, and 10 μ M) or 0.1% DMSO in Na⁺-free HBSS at 37°C for 1 min and was terminated by washing with cold Na⁺-free HBSS. Next, the cells were solubilized with 0.5 mL of 0.1 N NaOH for 20 min, and the cell lysate mixed with 3 mL of scintillation liquid and radioactivity was measured using an LSC-7200 β -scintillation counter (Hitachi Aloka Medical, Tokyo, Japan). An aliquot of the cell lysate was used to determine the protein concentration using a Pierce BCA Protein Assay kit (Thermo Scientific). All experiments were replicated three times. The IC₅₀ values of [14 C]L-leucine uptake were calculated using GraphPad Prism5 (GraphPad Software Inc., San Diego, CA, USA).

Cell growth inhibition assay

A sulforhodamine B (SRB; Sigma-Aldrich) assay was performed to determine the effect of JPH203 on cell growth inhibition. The CCA cells were seeded at a density of 2×10^3 cells in 100 μ L of medium/well in 96-well plates and maintained at 37°C in 5% CO₂ overnight. Then, the cells were treated with different concentrations of JPH203 (0.1–100 μ M) in 100 μ L of medium, and 0.1% DMSO was used as a control at 24, 48, and 72 h. Later, the cell numbers were estimated using an SRB assay, as previously described.²³ In brief, the adherent cells were

fixed with 100 μ L of 10% trichloroacetic acid (TCA, Wako Pure Chemical Industries Ltd., Tokyo, Japan) for 1 h at 4°C. Then, they were washed with deionized water and stained with 0.4% SRB dye in 1% acetic acid for 30 min. After removal of the SRB dye, the cells were washed with 1% acetic acid and were allowed to air dry. Thereafter, SRB-stained cellular proteins were dissolved in 200 μ L of 10 mM Tris base (pH 10.5). The optical densities were measured at 540 nm in an enzyme-linked immunosorbent assay (ELISA) plate reader, Varioskan Flash (Thermo Fisher Scientific, Vantaa, Finland). The percent viability of the cells in each well was calculated. The experiments were replicated three times, and the IC₅₀ values were calculated using GraphPad Prism 5 (GraphPad Software Inc.).

Cell cycle analysis

CCA cells were seeded and treated with JPH203 as described in section "Quantitative western blotting." After incubation, 1×10^6 cells per experimental condition were harvested and washed with cold phosphate-buffered saline (PBS). Thereafter, the cells were fixed with 70% cold ethanol and kept at -20°C until analysis. After fixation, the cells were washed with cold PBS and incubated with 100 μ g/mL RNaseA (Applichem Inc., Cheshire, CT, USA), and the cell cycle distribution was determined by staining the DNA with 40 μ g/mL of propidium iodide (PI; Invitrogen, Paisley, UK) for 30 min. The results were analyzed by flow cytometry (FACS Calibur, BD Biosciences, San Jose, CA, USA). All experiments were done in triplicate.

Trypan blue dye exclusion assay

Six-well culture plates were used for cell culture. After plating the CCA cells at 1×10^5 cells/well and culturing for overnight, designed concentrations of JPH203 were added for 48 h. After the treatment period, the cells were trypsinized and washed with PBS. The cells were then mixed thoroughly and 10 μ L of cell suspension was added to 10 μ L of 0.4% trypan blue dye (Bio-Rad Laboratories, Inc., Watford, UK) solution. Dead cells were characterized by the uptake of the dye and expressed as the percentage of cells staining blue. The results were detected using a TC20™ Automated Cell Counter (Bio-Rad Laboratories, Inc., Berkeley, CA, USA). All experiments were done in triplicate.

Experimental animals

Six-week-old male athymic BALB/c nude mice (Clea Japan, Inc., Tokyo, Japan) were housed and monitored under pathogen-free conditions in accordance with institutional principals. Food and tap water were provided ad libitum. Mice were subcutaneously injected with 2×10^6 KKKU-213 cells in 0.5 mL of medium into the dorsal area.

After 3 days, the mice were randomly divided into four groups: a control group ($n=5$), JPH203 6.3 mg/kg treatment group ($n=5$), JPH203 12.5 mg/kg treatment group ($n=5$), and JPH203 25 mg/kg treatment group ($n=5$). On the day of grouping (day 0), body weights and diameters of the tumor (length and width) were measured. The tumor volumes were calculated using the standard formula: tumor volume (mm^3) = longer diameter \times (shorter diameter)²/2. After grouping, the mice were intravenously injected with 0.2 mL of normal saline solution (NSS) daily for the control group and JPH203 for the treatment groups for 20 days. Tumor volumes and body weights were assessed twice a week. The tumor volumes were expressed relative to the initial tumor volume (day 0). After treatment, all mice were sacrificed for the collection of tumor samples as well as the liver, lungs, spleen, and kidneys. Formalin-fixed paraffin-embedded sections from the internal organs were analyzed by hematoxylin and eosin (H&E) staining according to standard methods. All slides were reviewed by a pathologist and were photographed using an Olympus CKX41 Microscope (Olympus, Tokyo, Japan) with CellSens standard software. The *in vivo* study was approved by the local animal welfare committee and was carried out in accordance with the local regulations.

Immunohistochemistry

The formalin-fixed and paraffin-embedded tumors were sliced into 4 μ m sections and were deparaffinized in xylene and then rehydrated in graded alcohol. Antigen retrieval was accomplished by incubating the slides in Tris-EDTA Buffer (10 mM Tris base, 1 mM EDTA solution, and 0.05% Tween 20; pH 9.0) for 3 min in a pressure cooker. Then, the slides were incubated in 0.3% H₂O₂ for 30 min to suppress endogenous peroxidase activity and then washed with PBS. Next, the slides were blocked with 10% skim milk in PBS for 30 min. The rabbit polyclonal Ki67 antibody was used as primary antibody at a 1:300 dilution in PBS overnight at 4°C. The following day, after several washes with PBS, the slides were incubated with peroxidase-conjugated EnVision™ secondary antibody (Dako, Glostrup, Denmark) for 90 min, and a peroxidase-labeled polymer, Diaminobenzidine tetrahydrochloride (DAB) solution, was used for signal development for 5 min. The sections were counterstained with hematoxylin followed by dehydrating and mounting. Ki67 positive cells of each tumor sections were counted in least five of $\times 400$ power fields.

Statistical analysis

Statistical analysis was performed using GraphPad Prism version 5 (GraphPad Software Inc.). The data are expressed as mean \pm standard deviation (SD) or mean \pm standard error of the mean (SEM). The results of the western blotting were analyzed with one-way analysis of variance (ANOVA)

followed by a Tukey's multiple-comparison test. The results of cell cycle analysis, dye exclusion assay, and percent Ki67 positive cells were analyzed by Student's *t* test. The results of the relative tumor volume were analyzed using a two-way ANOVA. A value of $p < 0.05$ was considered to indicate a statistically significant difference.

Results

Expression of the system L-amino acid transporters and CD98 in CCA cells

The PCR products for LAT1 and CD98 were clearly detected in all cells studied, whereas LAT2, LAT3, and LAT4 were hardly detected (Figure 1(a)). The presence of LAT1 and CD98 in all cells studied was further confirmed by quantitative western blotting. Consistent with the RT-PCR analysis, the CCA cells clearly expressed LAT1 and CD98 (Figure 1(b)). For the functional expression at the plasma membrane, LAT1, a non-glycosylated light chain with an apparent molecular mass of 40 kDa, forms a heterodimeric complex via disulfide bond with a glycosylated heavy chain or CD98 with an apparent molecular mass around 85 kDa. The heterodimeric complex of LAT1–CD98 is approximately 125 kDa. The results from the RT-PCR analysis and western blotting indicate that LAT1 is the main system L-transporter in our CCA cell lines and occurs together with CD98.

JPH203 inhibits [¹⁴C]L-leucine uptake and cell growth in CCA cell lines

The inhibitory effects of JPH203 on [¹⁴C]L-leucine uptake and cell growth in CCA cells are summarized in Figure 1 and Table 1. At the lowest concentration of JPH203 (0.01 μM), [¹⁴C]L-leucine uptake in all CCA cells was slightly increased when compared to the untreated control. However, 0.1–10 μM JPH203 dramatically inhibited [¹⁴C]L-leucine uptake in a dose-dependent manner in all CCA cells studied with low IC₅₀ values. The K KU-213 cell line was more sensitive to JPH203 than K KU-055 and K KU-100 cell lines (Figure 1(c)–(e) and Table 1). The IC₅₀ values (mean ± SD) were 0.20 ± 0.03 μM for K KU-055, 0.12 ± 0.02 μM for K KU-213 cells, and 0.25 ± 0.04 μM for K KU-100 (Table 1).

To determine whether blocking [¹⁴C]L-leucine uptake using JPH203 suppresses CCA cell growth, an SRB assay was performed after treatment of the CCA cells with JPH203 at various concentrations for 24, 48, and 72 h in 96-well plates. As shown in Figure 1 and Table 1, JPH203 could inhibit the proliferation of CCA cells and IC₅₀ values were decreased in a time-dependent manner. However, the drug response for each CCA cell line to JPH203 showed different patterns, as indicated in Figure 1(f). At 0.1 and 1 μM JPH203, there were hardly any inhibition of

K KU-055 CCA cell proliferation compared with K KU-213 and K KU-100 (Figure 1(g) and (h)). Consistent with the result for amino acid uptake, K KU-213 was more sensitive to JPH203 than K KU-055 and K KU-100 (IC₅₀ at 24–72 h for K KU-213 was lower than that of K KU-055 and K KU-100; Table 1).

JPH203 altered LAT1 and CD98 expression

A previous study demonstrated that inhibition system L activity in K KU-213 CCA cells using a broad system L inhibitor, 2-aminobicyclo-(2,2,1)-heptane-2-carboxylic acid (BCH), can upregulate the expression of LAT1 and CD98.⁹ Likewise, upregulated amino acid transporters, including LAT1, CD98, xCT, ASCT1, and ASCT2, were reported in human prostate cancer cell lines treated with BCH and leucine-free media.²⁴ We, therefore, investigated the impact of JPH203 on LAT1 and CD98 expression. In accordance with previous reports, after the treatment of K KU-055 and K KU-213 cell lines with JPH203 (0–100 μM) for 48 h, both LAT1 and CD98 levels increased in a dose-dependent manner as detected by quantitative western blotting (Figure 2(a)–(f)). These results indicate that upregulated LAT1 and CD98 expression is a feedback effect related to amino acid deprivation caused by the suppression of LAT1 activity using JPH203.

JPH203 induced cell cycle arrest through regulating the cell cycle regulators

To determine the mechanism of the anti-proliferative effect of JPH203, cell cycle analysis was performed using flow cytometric analysis after staining the cells with PI. As shown in Figure 3(a), exposure of the K KU-055 cells to 10–100 μM JPH203 for 48 h resulted in a statistically significant increase in G2/M-phase ($p < 0.01$) cells compared with the control. This was accompanied by a significant decrease in G0/G1 phase cells at 10 μM ($p < 0.05$) and a significant decrease in S-phase cells at 100 μM ($p < 0.05$). Unlike K KU-055, the results for K KU-213 showed that the number of cells in the G0/G1 phase was significantly increased in response to 10–100 μM JPH203 ($p < 0.01$ at 10 μM and $p < 0.001$ at 100 μM). Concomitantly, 10–100 μM of JPH203 significantly decreased the number of S-phase cells compared to the control ($p < 0.001$). However, a slight decrease of G2/M-phase cells was detected in a dose-dependent manner, but this was not statistically significant compared with the control (Figure 4(a)).

To gain insight into the mechanism of cell cycle arrest on treatment with JPH203, we further investigated the expression levels of cell cycle-regulator proteins which function in the G0/G1 phase, including cyclin D1, CDK4, and CDK6.²⁵ The expression of the inhibitors of CDKs, P21, and P27, which affect both G1/S and the G2/M,^{26–28} was also investigated in this experiment. The CCA cells

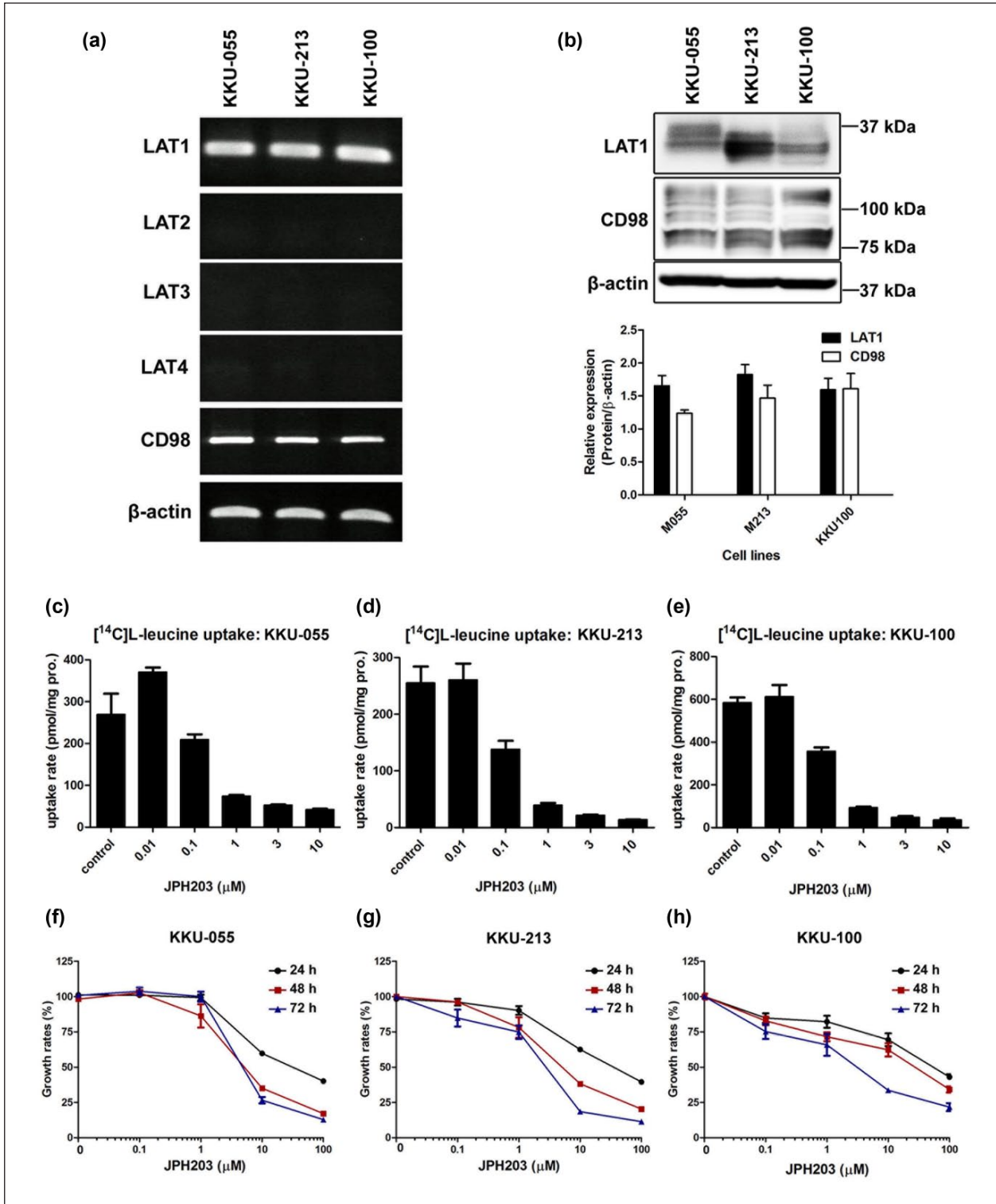


Figure 1. Expression of LAT1 and CD98 and the functional effects of LAT1 inhibition on [14 C]L-leucine uptake and cell growth in CCA cells. (a) Detection of system L-amino acid transporters (LAT1-LAT4) and CD98 by RT-PCR in CCA cells (KKU-055, KKKU-213, and KKKU-100). (b) Expression of LAT1 and CD98 levels in the indicated cells detected by quantitative western blotting. The densitometry value of LAT1 and CD98 was normalized to β -actin. The bar graphs show the average densitometry value \pm SEM from three independent experiments. (c–e) Inhibition of [14 C]L-leucine uptake by JPH203 in CCA cells. [14 C]L-leucine uptake was measured for 1 min in the presence of various concentrations of JPH203. (f–h) JPH203 suppressed cell growth in CCA cells. The indicated cells were treated with various concentrations of JPH203 for 24, 48, and 72 h. The cell viabilities were determined by SRB assays and the growth curves are presented as percentage of untreated control. Each data point represents the mean \pm SEM from three independent experiments.

Table 1. Inhibitory effects of JPH203 on [¹⁴C]-leucine uptake and cell growth inhibition in CCA cells.

Cell line	IC ₅₀ (μM) value for [¹⁴ C]-leucine uptake inhibition	IC ₅₀ (μM) value for growth inhibition		
		24h	48h	72h
KKU-055	0.20 ± 0.03	31.95 ± 1.15	6.16 ± 1.17	5.78 ± 1.15
KKU-213	0.12 ± 0.02	32.95 ± 1.16	5.98 ± 1.16	2.47 ± 1.19
KKU-100	0.25 ± 0.04	48.74 ± 1.22	21.51 ± 1.25	3.00 ± 1.28

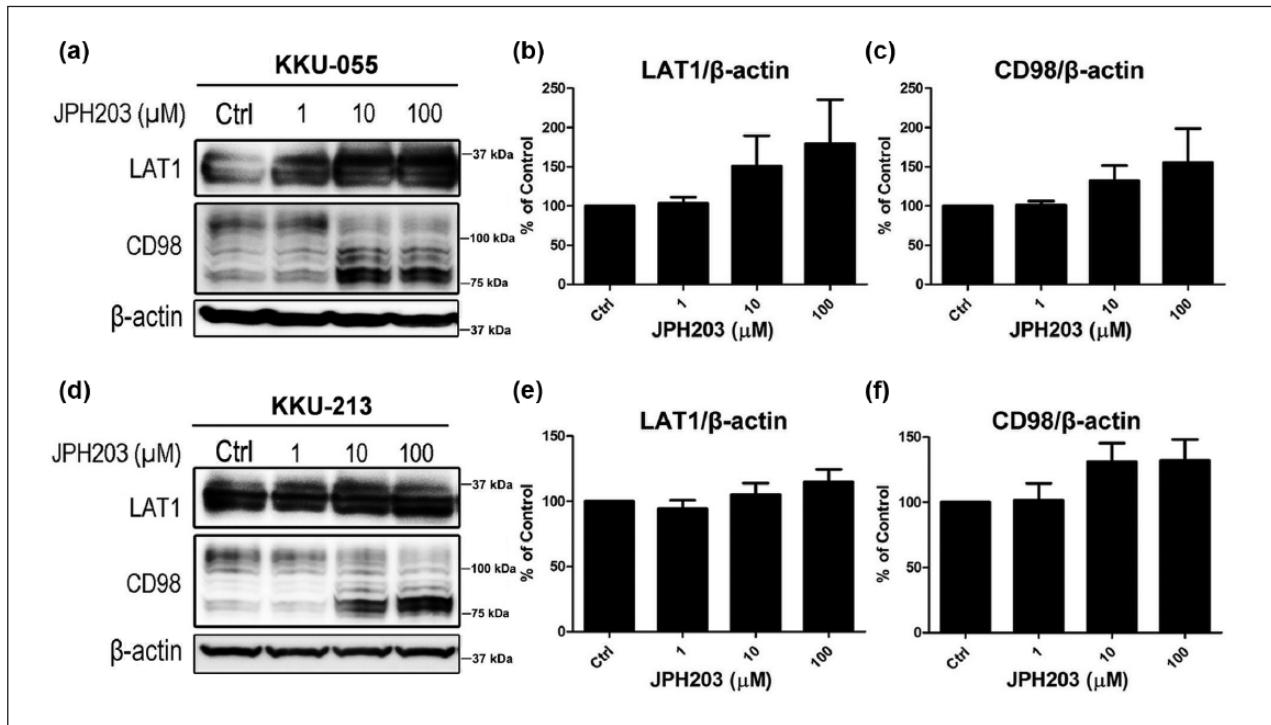


Figure 2. The effect of JPH203 on LAT1 and CD98 expression in CCA cells detected by quantitative immunoblot. (a–c) LAT1 and CD98 expressions were increased in a dose-dependent manner following treatment with JPH203 for 48 h in KKKU-055 cells. (d–f) LAT1 and CD98 expressions were increased in a dose-dependent manner following treatment with JPH203 for 48 h in KKKU-213 cells. The results show a representative western blot for LAT1 and CD98 expression. Bar graphs show the densitometry values normalized to β-actin and were presented as the percentage compared to the untreated control: They show the mean ± SEM from three independent experiments.

were exposed to JPH203 for 48 h and prepared for western blotting. The results in KKKU-055 showed that JPH203 increased the levels of cyclin D1 and CDK4, except that the level of CDK4 at 100 μM was decreased by JPH203 (Figure 3(b)–(d)). In addition, 10–100 μM JPH203 could strongly suppress CDK6 levels ($p < 0.001$) as well as induce higher P21 levels when compared with control (Figure 3(b), (e), and (f)). Moreover, 100 μM of JPH203 markedly increased P27 expression as shown in Figure 3(g). This result indicates that the induction of growth inhibition by JPH203 in KKKU-055 cells was caused by G2/M arrest mainly through elevated P21 levels. However, inhibition of KKKU-055 cell growth at the highest JPH203 concentration (100 μM) is caused by both G2/M arrest and reduced S-phase cells due to

increasing P21 and P27 levels and decreasing CDK4 and CDK6 levels.

As expected, the results for KKKU-213 showed that the levels of cyclin D1, CDK4, and CDK6 which are required for G1/S phase transition were remarkably decreased in a dose-dependent manner when compared to the control, with significant differences being observed at 10–100 μM JPH203 for CDK4 levels ($p < 0.05$ and $p < 0.01$, respectively; Figure 4(b)–(e)). In addition, the levels of P21 increased in a dose-dependent manner, but this was not the case for the CDK inhibitor P27 (Figure 4(b), (f), and (g)). These results indicate that, in KKKU-213 cells, the growth inhibition of JPH203 caused by cell cycle arrest at the G0/G1-phase and reduced S phase occurs via an increase in the CDK inhibitor P21. This may further inhibit the

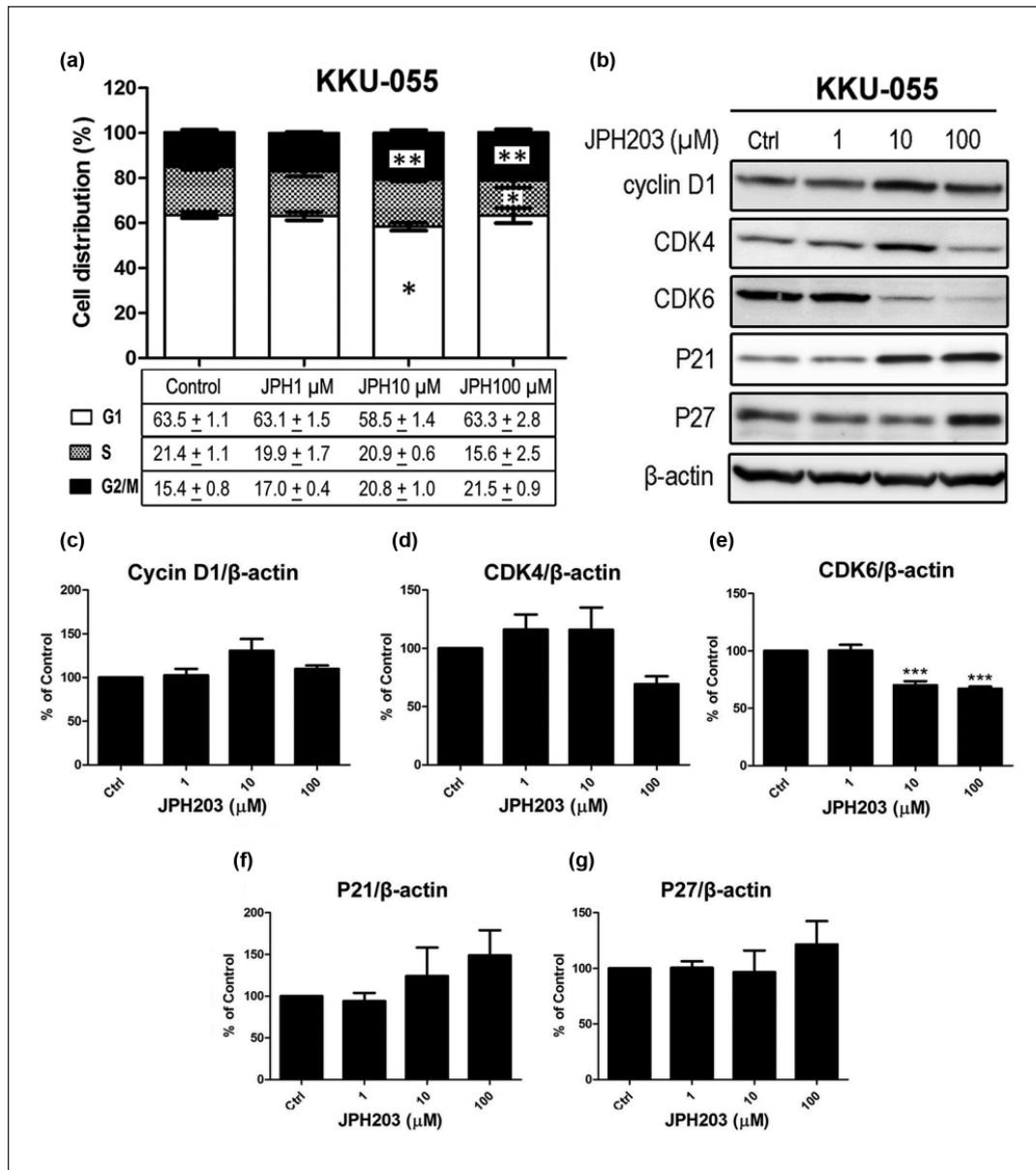


Figure 3. JPH203 induced cell cycle arrest in KKU-055 cells by regulating cell cycle-related proteins. (a) A volume of 10–100 μM JPH203 significantly increased G2/M-phase cells ($p < 0.01$) which was accompanied by significantly decreased G0/G1 phase at 10 μM ($p < 0.05$) and decreased S phase at 100 μM ($p < 0.01$) after treatment for 48h, detected by flow cytometry. Data are expressed as the mean \pm SD of the percentage of cells in each cycle phase from three independent experiments. Results were analyzed by Student's *t* test. (b) A representative western blot for the expression of cell cycle-related proteins, including cyclin D1, CDK4, CDK6, P21, and P27 in KKU-055 cells after treatment with JPH203 for 48h. (c–g) The densitometry values of each protein were normalized to β -actin and were presented as the percentage compared to the untreated control. The mean \pm SEM from three independent experiments are presented (** $p < 0.01$ versus control, one-way ANOVA followed by a Tukey's multiple-comparison test).

activity of cyclin D1–CDK4/CDK6, which is downregulated by this selective LAT1 inhibitor.

Apoptosis induction in response to JPH203 in CCA cells

Since JPH203-induced apoptosis has been demonstrated in human oral cancer²¹ and leukemic cells,²² we investigated the effect of this specific LAT1 inhibitor on apoptosis

induction in our CCA model. To validate the induction of apoptosis in KKU-055 and KKU-213 CCA cells, a trypan blue dye exclusion assay was conducted to measure the percentage of cell death after 48h of JPH203 (0–100 μM) treatment. In addition, the apoptotic-related protein, caspase-3, and its cleaved form were assessed by immunoblot. Our results showed that JPH203 could induce cell death in both CCA cell lines, as shown in Figure 5(a) and (b). Cell death was less than 15% in KKU-055 and 30% in

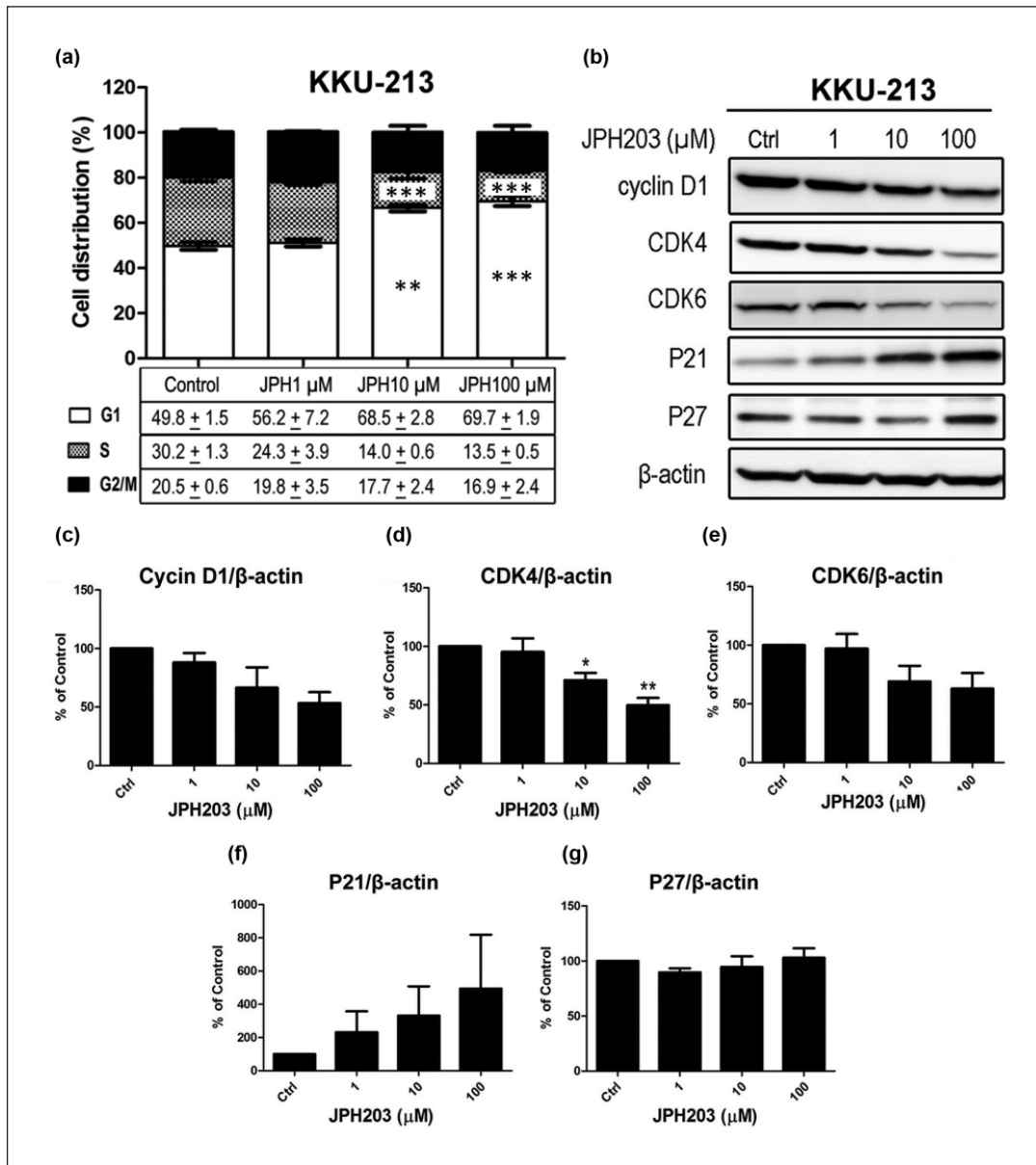


Figure 4. JPH203 induced cell cycle arrest in KKU-213 cells by regulating cell cycle-related proteins. (a) A volume of 10–100 μM JPH203 increased G0/G1-phase cells ($p < 0.01$ and $p < 0.001$ at the dose of 10 and 100 μM , respectively) and decreased S-phase cells ($p < 0.001$) after treatment for 48 h, detected by flow cytometry. Data are expressed as the mean \pm SD of the percentage of cells in each cycle phase from three independent experiments. Results were analyzed by Student's *t* test. (b) A representative western blot for the expression of cell cycle-related proteins, including cyclin D1, CDK4, CDK6, P21, and P27 in KKU-213 cells after treatment with JPH203 for 48 h. (c–g) The densitometry values of each protein were normalized to β -actin and were present as percentage compared to the untreated control. The mean \pm SEM from three independent experiments are presented (* $p < 0.05$, ** $p < 0.01$ vs control, one-way ANOVA followed by a Tukey's multiple-comparison test).

KKU-213 after treatment with 100 μM JPH203. This was a significant change, $p < 0.001$, compared with the control. The percentage of cell death decreased slightly at 1 μM and increased slightly at 10 μM of JPH203 in both CCA cell lines compared to the control. The results from quantitative western blotting showed that the treatment of the CCA cells with JPH203 at 100 μM for KKU-055 and

10–100 μM for KKU-213 increased the cleaved caspase-3/caspase-3 ratio when compared to the control (Figure 5(c)–(e)). A statistically significant difference in the cleaved caspase-3/caspase-3 ratio was observed between KKU-213 treated with 100 μM JPH203 and the control ($p < 0.05$). These results suggest that JPH203-induced apoptosis is regulated by the activation of the caspase cascade under

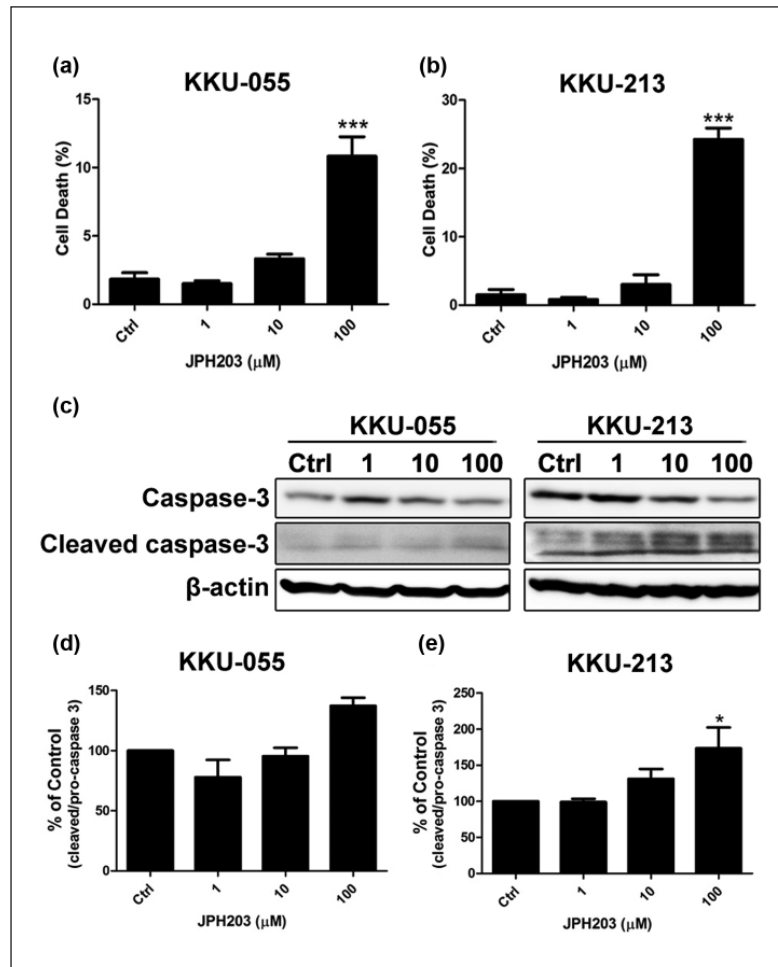


Figure 5. The effects of JPH203 on apoptosis induction in CCA cells. (a and b) CCA cells were treated with various concentrations of JPH203 (0–100 μM) for 48 h. The percentage of cell death was measured by trypan blue staining. The data represent the mean ± SEM from three independent experiments (***) $p < 0.001$ by using a Student's *t* test in comparison with the control). (c) Expression and activation of the apoptotic protein caspase-3 by JPH203 in CCA cells. The indicated cells were stimulated with JPH203 (0–100 μM) for 48 h. The cell lysate was prepared and analyzed by quantitative immunoblot. (d and e) Densitometry values of caspase-3 and its cleaved form were normalized to β-actin and expressed as ratio of the cleaved caspase-3/caspase-3. The mean ± SEM are shown from three independent experiments and analyzed by one-way ANOVA followed by a Tukey's multiple-comparison test (* $p < 0.05$ compared to the untreated control).

the highest concentration tested (100 μM), and that the KKU-213 cell line was more sensitive to JPH203 than the KKU-055 cell line.

JPH203 suppressed CCA cell growth in the *in vivo* model

Our *in vitro* models demonstrated that the KKU-213 cell line was the most sensitive to JPH203 when compared to the other cell lines. Thus, we evaluated the anti-tumor activity of JPH203 in a nude mouse xenograft model derived from KKU-213 CCA cells. JPH203 was administered intravenously daily for 20 days at three different doses (6.3, 12.5, and 25.0 mg/kg) starting at day 3 after the injection of cancer cells. On the days 18 and 21, JPH203 showed dose-dependent inhibition on tumor growth with

significantly inhibited tumor growth in the groups of JPH203 at 12.5 mg/kg (on day 18, $p < 0.05$, and on day 21, $p < 0.01$) and 25 mg/kg (on day 18 and day 21, $p < 0.001$) when compared to the control group (Figure 6(a) and (b)). To confirm our findings on this growth suppression mechanism, immunohistochemical analysis was conducted to identify the expression of a proliferation marker Ki67 in the tumor tissues. Reduction of the cells positive for Ki67 was found in JPH203 treatment groups at 12.5 and 25 mg/kg ($p < 0.01$) compared with control group (Figure 6(c) and (d)). In contrast to the effects on tumor growth, the animals did not show any clinical signs of toxicity, changes in general behavior, or changes in physical activity in the JPH203-treated animals compared to the controls. Mice treated with JPH203 were healthy and had similar body weights to the control mice (Supplementary Figure 1). In

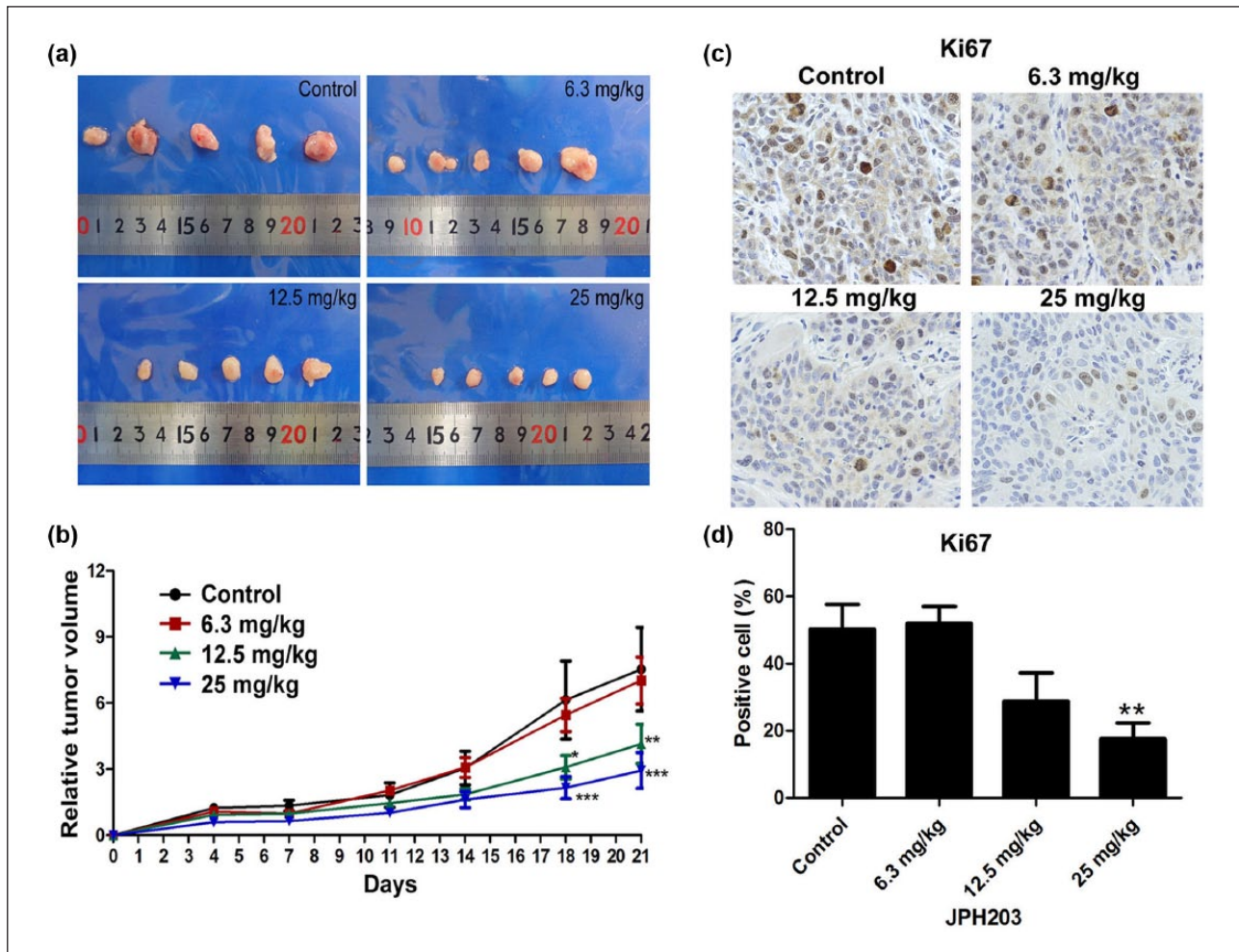


Figure 6. Anti-tumor activity of JPH203 in CCA-inoculated athymic BALB/c nude mice. (a) CCA tumor tissues were obtained from vehicle and JPH203-treated mice ($n = 5/\text{group}$). (b) The tumor volume was expressed relative to the initial tumor volume. The data were analyzed by two-way ANOVA (* $p < 0.05$, ** $p < 0.01$, *** $p < 0.001$ compared to the control group). (c) IHC to identify expression of Ki67 in tumor tissues, magnification $\times 400$. (d) Bar graphs illustrate the proportion of Ki67 positive cells. The data of Ki67 positive cells were expressed as mean \pm SEM (** $p < 0.01$ analyzed by Student's t test).

addition, a histopathological review of the internal organs, including in the liver, lungs, spleen, and kidneys, analyzed by H&E staining showed no discernible toxicity of JPH203 (Supplementary Figure 1). There were no differences in the weight or appearance of the internal organs of mice between the control and treated groups. These results indicate that JPH203 was safe for the animals studied and that it should be considered for use in CCA patients.

Discussion

Although suppressed LAT1 activity using BCH has been reported in CCA,^{8,9} BCH is a broad system L inhibitor that targets all members of LAT family. Therefore, BCH lacks selectivity for both LAT1 and cancer cells, which results in low cytotoxicity for several cancer cell lines, which is undesirable in clinical trials.^{29,30} Our previous study¹¹ showed that LAT1 expression is significantly associated

with *O. viverrini*-induced cholangiocarcinogenesis and a shorter survival time in CCA patients. Moreover, the expression of LAT1 and CD98 in CCA is possibly regulated through the oncogenic PI3K/AKT signaling pathway. Collectively, these data led us to investigate, for the first time, the effects of a selective LAT1 inhibitor in our CCA model.

Our results show that LAT1 is the main system L-transporter, along with CD98, in CCA cells, including the KKU-055, KKU-213, and KKU-100 cell lines, which conforms to a previous study from Janpipatkul et al.⁹ who reported a lower expression of LAT2, LAT3, and LAT4 than LAT1 in KKU-213 cells. Interestingly, our results indicate that JPH203 possesses a higher efficacy for inhibiting CCA cell proliferation than for BCH as shown in previous reports.^{9,8} This phenomenon is possible due to the specificity of JPH203 to LAT1 in CCA cells being much higher than BCH.

The treatment of the CCA cells with JPH203 showed that the IC_{50} values for [^{14}C]L-leucine uptake inhibition were lower than those for cell growth inhibition. This is consistent with two previous studies reporting the effect of JPH203 on human colon cancer¹⁹ and human oral cancer.²¹ Oda et al.¹⁹ suggested that JPH203 inhibits LAT1 by competing with its substrates; therefore, the differences in the IC_{50} values would be caused by the concentrations of LAT1 substrates (neutral amino acids) in the incubation medium. Moreover, we also demonstrated that amino acid deprivation caused by JPH203 treatment for 48 h results in increasing LAT1 and CD98 expressions. This is likely to require a higher concentration of JPH203 to target LAT1 in the cell culture experiments that were performed for 24–74 h when compared to amino acid uptake experiments that were performed with a short incubation period (1 min). Furthermore, the increase in LAT1 and CD98 expressions may function as a compensatory survival mechanism under conditions of amino acid starvation. This result suggests that LAT1 and CD98 expression are regulated by intracellular amino acid levels, which is supported by previous studies in prostate cancer²⁴ and also CCA.⁹

Previous studies have also shown that amino acid depletion mediated by BCH contributes to cell cycle arrest at the G1 phase. This is regulated by cell cycle-related proteins such as cyclin D3, CDK6, and P27 in human oral cancer,³¹ and cyclin D3 along with P27 in human prostate cancer.³² These data are supported by our results; we show that JPH203 clearly induced cell cycle arrest at the G0/G1 phase and reduced S-phase progression in KKU-213 cells via the regulation of cell cycle-related proteins, including cyclin D1, CDK4, CDK6, and P21. Our results also reveal the different growth inhibition mechanism of JPH203 in KKU-055. This specific LAT1 inhibitor induced G2/M cell cycle arrest and reduced S-phase cells via increasing P21 and P27 concentrations in KKU-055. The increase in P21 and P27 during G2/M arrest by anti-cancer agents has been reported in many types of human cancer.^{33–36} For example, gallic acid can induce cell cycle arrest at the G2/M phase through increased P21 and P27 expression in breast cancer.³⁶ However, from our results, the different pattern of cell cycle distribution caused by JPH203 treatment in our CCA cells indicates that JPH203 can selectively target several components of the cell cycle machinery to arrest the cell cycle. This is dependent on both cell type and drug concentration.

Caspase proteins play a critical role in apoptosis and are responsible for many of the biochemical and morphological changes associated with this phenomenon. Therefore, an increased level of activated caspase proteins is one of the most common apoptosis markers that has been used to indicate apoptosis phenotype of cell.^{37,38} Two previous studies reported that JPH203 can induce caspase-dependent apoptosis in cancer cells.^{21,22} The previous study demonstrated that JPH203 can induce

apoptosis of human oral cancer revealed by an increase of apoptosis markers included the cleaved form of caspase-3, caspase-7, and caspase-9, as well as cleaved poly (ADP-ribose) polymerase (PARP) together with 16.5% of Annexin V-FITC-positive cells. These were observed after treatment of the cells with 3 mM of JPH203 for 24 h.²¹ The next study on leukemia reported that JPH203 induced type II cell death, autophagy, followed by caspase-3-dependent apoptosis at 48 h after treatment.²² Consistent with these studies, our data showed that the treatment of CCA cells with JPH203 (100 μ M) for 48 h could increase the ratio of cleaved caspase-3/preform along with an increased number of dead cells, more than 10% and 20% for KKU-055 and KKU-213, respectively. These results indicate that JPH203 induced apoptosis in CCA cells via caspase-3 activation. However, the molecular mechanisms underlying apoptosis caused by JPH203 in the CCA model require more study.

To date, there is only one study on the effect of a LAT1 inhibitor using the CCA xenograft model. Kaira et al.⁸ demonstrated the anti-tumor efficacy of BCH in HuCCT1 CCA xenograft nude mice; however, as indicated above, BCH does not specifically target LAT1 but also other system L-amino acid transporters. Kaira et al.⁸ reported that daily intravenous administration of BCH, up to 200 mg/kg for 14 days, caused a statistically significant delay in tumor growth for 3 weeks after treatment. Compared to Kaira et al.'s study, daily intravenous administration of JPH203 at amounts substantially lower than for BCH (16-fold, 12.5 mg/kg; 8-fold, 25 mg/kg) for 20 days could significantly inhibit KKU-213 CCA cell growth in nude mice starting at day 18. This was confirmed by the decreasing percent of Ki67 positive cells found. Our results indicate that JPH203 is considerably more effective than BCH against CCA cell growth, conforming with the IC_{50} values in inhibiting [^{14}C]L-leucine uptake and cell growth in the in vitro model.^{8,9} Furthermore, our results support the study of Oda et al., the first report of JPH203 in an in vivo model, using intravenously administered JPH203 (12.5 and 25.0 mg/kg). This showed a statistically significant inhibition of growth of HT-29 tumors transplanted to nude mice with only a slight decrease in body weight.¹⁹ However, in our study, there was no statistically significant change that could be attributed to general toxicity, such as changes in the animals' body weight, or the histology or appearance of the internal organs.

Taken together, this study demonstrates that the inhibition of LAT1 activity using JPH203 in CCA cells which show high LAT1 and CD98 expression leads to an intracellular decrease in essential neutral amino acids. This results in an altered expression of LAT1 and CD98, inhibiting cell growth and inducing cell cycle arrest and apoptosis in the in vitro model. Moreover, JPH203 shows anti-tumor efficacy in nude mice bearing human CCA cell xenografts without general toxicity. This study is the first to demonstrate the

effects of a selective LAT1 inhibitor in the CCA model, thus providing useful information for the development of JPH203 as a therapeutic strategy for CCA patients.

Acknowledgements

The authors thank the research technicians (Department of Pathology, School of Medicine, Dokkyo Medical University) who kindly assisted in the processes of paraffin-embedded tissue sections and H&E staining. They also thank Professor Trevor N Petney for editing the article via Publication Clinic KKU, Thailand.

Declaration of conflicting interests

The author(s) declared no potential conflicts of interest with respect to the research, authorship, and/or publication of this article.

Funding

This study was supported by the Invitation Research Grant (grant numbers I57235 and I57305), The Liver fluke and Cholangiocarcinoma Research Center (LFCRC04/2556), as well as a scholarship from the Japanese Government (The Ministry of Education, Culture, Sports, Science and Technology (MEXT)) to S.Y.

References

- Ganapathy V, Thangaraju M and Prasad PD. Nutrient transporters in cancer: relevance to Warburg hypothesis and beyond. *Pharmacol Ther* 2009; 121(1): 29–40.
- Christensen HN. Role of amino acid transport and counter-transport in nutrition and metabolism. *Physiol Rev* 1990; 70(1): 43–77.
- Kanai Y, Segawa H, Miyamoto K, et al. Expression cloning and characterization of a transporter for large neutral amino acids activated by the heavy chain of 4F2 antigen (CD98). *J Biol Chem* 1998; 273(37): 23629–23632.
- Yanagida O, Kanai Y, Chairoungdua A, et al. Human L-type amino acid transporter 1 (LAT1): characterization of function and expression in tumor cell lines. *Biochim Biophys Acta* 2001; 1514(2): 291–302.
- Rossier G, Meier C, Bauch C, et al. LAT2, a new basolateral 4F2hc/CD98-associated amino acid transporter of kidney and intestine. *J Biol Chem* 1999; 274(49): 34948–34954.
- Babu E, Kanai Y, Chairoungdua A, et al. Identification of a novel system L amino acid transporter structurally distinct from heterodimeric amino acid transporters. *J Biol Chem* 2003; 278(44): 43838–43845.
- Bodoy S, Martin L, Zorzano A, et al. Identification of LAT4, a novel amino acid transporter with system L activity. *J Biol Chem* 2005; 280(12): 12002–12011.
- Kaira K, Sunose Y, Ohshima Y, et al. Clinical significance of L-type amino acid transporter 1 expression as a prognostic marker and potential of new targeting therapy in biliary tract cancer. *BMC Cancer* 2013; 13: 482.
- Janpipatkul K, Suksen K, Borwornpinyo S, et al. Downregulation of LAT1 expression suppresses cholangiocarcinoma cell invasion and migration. *Cell Signal* 2014; 26(8): 1668–1679.
- Yanagisawa N, Hana K, Nakada N, et al. High expression of L-type amino acid transporter 1 as a prognostic marker in bile duct adenocarcinomas. *Cancer Med* 2014; 3(5): 1246–1255.
- Yothaisong S, Namwat N, Yongvanit P, et al. Increase in L-type amino acid transporter 1 expression during cholangiocarcinogenesis caused by liver fluke infection and its prognostic significance. *Parasitol Int*. Epub ahead of print 30 November 2015. DOI: 10.1016/j.parint.2015.11.011.
- Li J, Qiang J, Chen SF, et al. The impact of L-type amino acid transporter 1 (LAT1) in human hepatocellular carcinoma. *Tumour Biol* 2013; 34(5): 2977–2981.
- Vatanasapt V, Sriamporn S and Vatanasapt P. Cancer control in Thailand. *Jpn J Clin Oncol* 2002; 32(Suppl.): S82–S91.
- Ohshima H and Bartsch H. Chronic infections and inflammatory processes as cancer risk factors: possible role of nitric oxide in carcinogenesis. *Mutat Res* 1994; 305(2): 253–264.
- Thamavit W, Bhamarapavati N, Sahaphong S, et al. Effects of dimethylnitrosamine on induction of cholangiocarcinoma in *Opisthorchis viverrini*-infected Syrian golden hamsters. *Cancer Res* 1978; 38(12): 4634–4639.
- Yongvanit P, Pinlaor S and Bartsch H. Oxidative and nitrate DNA damage: key events in opisthorchiasis-induced carcinogenesis. *Parasitol Int* 2012; 61(1): 130–135.
- Khuntikeo N, Loilome W, Thinkhamrop B, et al. A comprehensive public health conceptual framework and strategy to effectively combat cholangiocarcinoma in Thailand. *PLoS Negl Trop Dis* 2016; 10(1): e0004293.
- Blechacz B and Gores GJ. Cholangiocarcinoma: advances in pathogenesis, diagnosis, and treatment. *Hepatology* 2008; 48(1): 308–321.
- Oda K, Hosoda N, Endo H, et al. L-type amino acid transporter 1 inhibitors inhibit tumor cell growth. *Cancer Sci* 2010; 101(1): 173–179.
- Wempe MF, Rice PJ, Lightner JW, et al. Metabolism and pharmacokinetic studies of JPH203, an L-amino acid transporter 1 (LAT1) selective compound. *Drug Metab Pharmacokinet* 2012; 27(1): 155–161.
- Yun DW, Lee SA, Park MG, et al. JPH203, an L-type amino acid transporter 1-selective compound, induces apoptosis of YD-38 human oral cancer cells. *J Pharmacol Sci* 2014; 124(2): 208–217.
- Rosilio C, Nebout M, Imbert V, et al. L-type amino-acid transporter 1 (LAT1): a therapeutic target supporting growth and survival of T-cell lymphoblastic lymphoma/T-cell acute lymphoblastic leukemia. *Leukemia* 2015; 29(6): 1253–1266.
- Yothaisong S, Dokduang H, Techasen A, et al. Increased activation of PI3K/AKT signaling pathway is associated with cholangiocarcinoma metastasis and PI3K/mTOR inhibition presents a possible therapeutic strategy. *Tumour Biol* 2013; 34(6): 3637–3648.
- Wang Q, Tiffen J, Bailey CG, et al. Targeting amino acid transport in metastatic castration-resistant prostate cancer: effects on cell cycle, cell growth, and tumor development. *J Natl Cancer Inst* 2013; 105(19): 1463–1473.
- Sherr CJ. Mammalian G1 cyclins. *Cell* 1993; 73(6): 1059–1065.

26. Li Y, Jenkins CW, Nichols MA, et al. Cell cycle expression and p53 regulation of the cyclin-dependent kinase inhibitor p21. *Oncogene* 1994; 9(8): 2261–2268.
27. Xiong Y, Hannon GJ, Zhang H, et al. p21 is a universal inhibitor of cyclin kinases. *Nature* 1993; 366(6456): 701–704.
28. Coats S, Flanagan WM, Nourse J, et al. Requirement of p27Kip1 for restriction point control of the fibroblast cell cycle. *Science* 1996; 272(5263): 877–880.
29. Kim CS, Cho SH, Chun HS, et al. BCH, an inhibitor of system L amino acid transporters, induces apoptosis in cancer cells. *Biol Pharm Bull* 2008; 31(6): 1096–1100.
30. Wang Q and Holst J. L-type amino acid transport and cancer: targeting the mTORC1 pathway to inhibit neoplasia. *Am J Cancer Res* 2015; 5(4): 1281–1294.
31. Kim CS, Moon IS, Park JH, et al. Inhibition of L-type amino acid transporter modulates the expression of cell cycle regulatory factors in KB oral cancer cells. *Biol Pharm Bull* 2010; 33(7): 1117–1121.
32. Wang Q, Bailey CG, Ng C, et al. Androgen receptor and nutrient signaling pathways coordinate the demand for increased amino acid transport during prostate cancer progression. *Cancer Res* 2011; 71(24): 7525–7536.
33. Kumar AP, Garcia GE and Slaga TJ. 2-methoxyestradiol blocks cell-cycle progression at G(2)/M phase and inhibits growth of human prostate cancer cells. *Mol Carcinog* 2001; 31(3): 111–124.
34. Ou TT, Wang CJ, Lee YS, et al. Gallic acid induces G2/M phase cell cycle arrest via regulating 14-3-3beta release from Cdc25C and Chk2 activation in human bladder transitional carcinoma cells. *Mol Nutr Food Res* 2010; 54(12): 1781–1790.
35. Han JH, Lee J, Jeon SJ, et al. In vitro and in vivo growth inhibition of prostate cancer by the small molecule imiquimod. *Int J Oncol* 2013; 42(6): 2087–2093.
36. Hsu JD, Kao SH, Ou TT, et al. Gallic acid induces G2/M phase arrest of breast cancer cell MCF-7 through stabilization of p27(Kip1) attributed to disruption of p27(Kip1)/Skp2 complex. *J Agric Food Chem* 2011; 59(5): 1996–2003.
37. Elmore S. Apoptosis: a review of programmed cell death. *Toxicol Pathol* 2007; 35(4): 495–516.
38. Cohen GM. Caspases: the executioners of apoptosis. *Biochem J* 1997; 326(Pt 1): 1–16.

Roles of organic anion transporters (OATs) in renal proximal tubules and their localization

Naoyuki Otani¹ · Motoshi Ouchi¹ · Keitaro Hayashi¹ · Promsuk Jutabha¹ · Naohiko Anzai^{1,2} 

Received: 28 March 2016 / Accepted: 27 August 2016 / Published online: 10 September 2016
© Japanese Association of Anatomists 2016

Abstract Organic anions (OAs) are secreted in renal proximal tubules in two steps. In the first step, OAs are transported from the blood through basolateral membranes into proximal tubular cells. The prototypical substrate for renal organic anion transport systems, *para*-aminohippurate (PAH), is transported across basolateral membranes of proximal tubular cells via OAT1 (*SLC22A6*) and OAT3 (*SLC22A8*) against an electrochemical gradient in exchange for intracellular dicarboxylates. In the second step, OAs exit into urine through apical membranes of proximal tubules. This step is thought to be performed by multidrug efflux transporters and a voltage-driven organic anion transporter. However, the molecular nature and precise functional properties of these efflux systems are largely unknown. Recently, we characterized an orphan transporter known as human type I sodium-phosphate transporter 4, hNPT4 (*SLC17A3*), using the *Xenopus* oocyte expression system. hNPT4 acts as a voltage-driven efflux transporter (“human OATv1”) for several OAs such as PAH, estrone sulfate, diuretic drugs, and urate. Here, we describe a model for an OA secretory pathway in renal tubular cells in which OAs exit cells and enter the tubular lumen via hOATv1 (hNPT4). Additionally, hOATv1 functions as a common renal secretory pathway for both

urate and drugs, indicating that hOATv1 may be a leak pathway for excess urate that is reabsorbed via apical URAT1 to control the intracellular urate levels. Therefore, we propose a molecular mechanism for the induction of hyperuricemia by diuretics: the diuretics enter proximal tubular cells via basolateral OAT1 and/or OAT3 and may then interfere with the NPT4-mediated apical urate efflux in the renal proximal tubule.

Keywords Organic anion · Transporter · Uric acid · Drugs

Introduction

The kidney plays an important role in homeostasis, as it cleanses the body of harmful metabolites, medications, and xenobiotics. The primary site in the kidney at which organic anions (OAs) are removed from the blood and discharged into the urine is the proximal tubule. Renal secretion of OAs, including exogenous substrates (e.g., drugs) and endogenous substrates (e.g., urate), is carried out in at least two steps in proximal tubular cells (Møller and Sheikh 1982). In the first step, OAs in the blood cross basolateral membranes and are transported into proximal tubular cells. When they are transported in this direction, which is opposite to that of the electrochemical gradient, OAs are exchanged for α -ketoglutarate and other intracellular dicarboxylates (Shimada et al. 1987). In the second step, OAs cross the apical membranes of tubular epithelial cells and are excreted into the urine. This energetically favorable process for OAs is thought to be mediated by membrane transporters. Because most OAs are bound to proteins, such as albumin in blood, they are not filtered through the glomerulus. Instead, they are transported from the blood across basolateral membranes into proximal

Naoyuki Otani and Motoshi Ouchi contributed equally to this work.

✉ Naohiko Anzai
anzai@chiba-u.jp

¹ Department of Pharmacology and Toxicology, Dokkyo Medical University, 880 Kitakobayashi, Mibu, Shimotsuga, Tochigi 321-0293, Japan

² Department of Pharmacology, Chiba University Graduate School of Medicine, 1-8-1 Inohana, Chuo-ku, Chiba 260-8670, Japan

tubules, and are then exported across apical membranes of tubular epithelial cells into urine.

In tubular cells, there are specific transporters for essential nutrients (e.g., glucose and amino acids) that are filtered by glomerulus to keep them in the blood (Wright 1985). In contrast, the transport of various endogenous and exogenous substances that are harmful to the body is carried out by transport systems that are characterized as “multiselective;” i.e., one transporter recognizes many types of substances as transport substrates. Because such compounds can be harmful, the body is protected by organs (such as the kidneys, liver, and intestines) that biotransform the compounds into less active metabolites and excrete them. Eventually, drugs and environmental toxicants are excreted—particularly from the kidney—into the urine. Transporters of OAs, known as organic anion transporters (OATs), play a major role in determining several properties of drugs, such as their pharmacokinetics and pharmacodynamics.

The reabsorption pathways for urate—one of the clinically important OAs—are mediated by the apical human urate/anion transporter, which was identified in 2002 (Enomoto et al. 2002) and designated urate transporter 1 (URAT1)/*SLC22A12*, and also by the basolateral voltage-driven urate transporter 1 (URATv1)/glucose transporter 9 (GLUT9)/*SLC2A9*, which was reported by our group and others (Vitart et al. 2008; Anzai et al. 2008; Caulfield et al. 2008). The urate secretory transporters in renal proximal tubular cells are not as specific as the reabsorptive ones. They have been identified as multispecific organic anionic drug transporters OAT1 and OAT3, located at the basolateral membrane (Hosoyamada et al. 1999; Cha et al. 2001). The voltage-driven OAT 1 (OATv1), identified by us in pig kidneys in 2003, functions as an excretion pathway for OAs, and is found on the luminal membranes of proximal tubules. One of the substrates transported by porcine OATv1 (pOATv1) is urate (Jutabha et al. 2003). Thus, the pOATv1 protein is considered to be involved in the voltage-sensitive pathway for apical urate secretion. Human Na⁺-phosphate cotransporter 4 (hNPT4), which belongs to the type 1 sodium-phosphate cotransporter family classified as *SLC17A3*, is a multispecific OA efflux transporter that has also been characterized as a novel urate transporter (Jutabha et al. 2010).

Organic anion transporter systems in the kidney

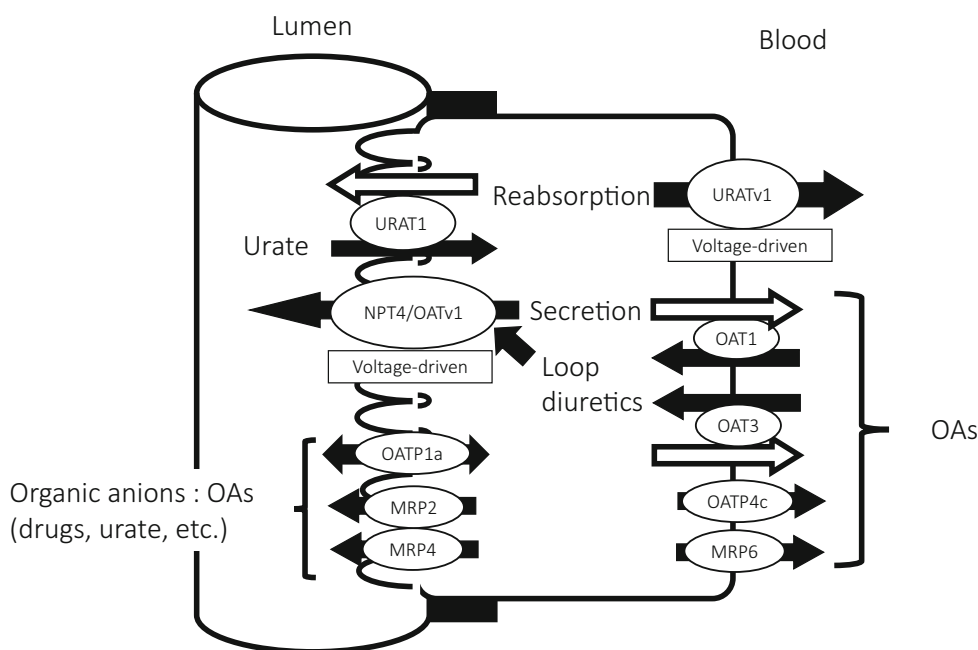
Many classes of OAs have been shown to be eliminated by the kidney (Anzai et al. 2006), including endogenous substances, such as urate and prostaglandins, and essential drugs, such as antibiotics, furosemide, nonsteroidal anti-inflammatory drugs, angiotensin-converting enzyme

inhibitors, and sulfate and glucuronide conjugates of drugs. Molecular cloning has identified several families of elimination-involved OA transporters, including the OAT family (Sekine et al. 1997; Sweet et al. 1997), the organic anion transporting polypeptide (OATP) family (Jacquemin et al. 1994), and the type 1 sodium-phosphate cotransporter (NPT) family (Reimer and Edwards 2004). ATP-dependent OATs, such as multidrug resistance-associated proteins (MRPs), act as active efflux pumps (Giacomini et al. 2010) (Fig. 1).

OAT family SLC22

Substrates of the *para*-aminohippurate (PAH) transporter have been suspected to include endogenous OAs, uremic substances, drugs, and environmental compounds. Because the PAH transporter is multispecific, it is suitable for eliminating various endogenous metabolites and xenobiotics. In the kidney, the PAH transport system is believed to participate in “tubular secretion.” After being isolated by expression cloning methods, the PAH transporter was designated OAT1 (Sekine et al. 1997; Sweet et al. 1997), and OAT 2, 3, and 4 were subsequently identified (Anzai and Endou 2007). In the kidney, the transport of OAs into cells at the basolateral membrane is a tertiary active transport process. The first step in this process is the countertransport of an OA (e.g., PAH) against its electrochemical gradient in exchange for the movement of an intracellular dicarboxylate (e.g., α -ketoglutarate) in the same direction as its electrochemical gradient (Anzai et al. 2006). After the gradient of decarboxylate has been directed outward, it is then maintained by being metabolized and transported across the basolateral membrane into cells via the Na⁺/dicarboxylate cotransport system. The Na⁺ gradient, which is directed inward and drives this process, is maintained by a transport step that requires energy, i.e., the extracellular transport of Na⁺ is performed at the basolateral membrane by Na⁺/K⁺-ATPase. Human proteins OAT1–3 are localized on the basolateral membranes of proximal tubular cells. The OAT4 mRNA is expressed in the kidneys, and the OAT4 protein is found on the apical membranes of proximal tubular cells. The OAT4 protein comprises 550 amino acids and shares its secondary structure with other OAT proteins (Cha et al. 2000). The OAT1 protein has extremely broad selectivity for substrates, which include endogenous substrates such as urate, dicarboxylates (Shimada et al. 1987), cyclic nucleotides, and prostaglandins, as well as exogenous substrates such as glucuronides, sulfate conjugates, environmental compounds, and anionic drugs (e.g., β -lactam antibiotics, diuretics, nonsteroidal anti-inflammatory drugs, angiotensin-converting enzyme inhibitors, and methotrexate).

Fig. 1 Proposed model of transcellular urate transport in the renal proximal tubule (Anzai et al. 2010). URAT1 at the apical membrane participates in proximal tubular urate reabsorption, and the reabsorbed urate exits cells via basolateral URATv1. The secretory pathway for urate is known to be mediated by OAT1 and OAT3, located on the basolateral side, and the exit pathway on the apical side involves a long-hypothesized voltage-driven transporter that is compatible with NPT4/OATv1. The latter is also proposed to be the exit path for diuretics



OATP family SLC21/SLCO

The OATP family was first identified in the rat liver by the expression cloning method as a family of sodium-independent bile acid transporters (Jacquemin et al. 1994). Several OATPs are selectively involved in the hepatic uptake of bulky and hydrophobic organic anions; however, most OATPs are expressed in various types of tissue and various locations, such as the blood–brain barrier, choroid plexus, heart, lungs, intestines, kidneys, placenta, and testes. The members of the OATP family are divided into six subfamilies (OATP1–6). Of the OATPs found in humans, the only one that is expressed mainly in the kidneys is OATP4C1 (Mikkaichi et al. 2004). Several substances that chiefly undergo renal excretion are substrates of OATP family transporters. For example, digoxin, methotrexate, and thyroid hormones such as triiodothyronine are transported with high affinity by OATP4C1, which is expressed only in the basolateral membranes of the proximal tubular cells.

NPT family SLC17

The SLC17 proteins, which were first considered to be phosphate carriers, have since been shown by molecular studies to be expressed at the apical membranes of renal proximal tubular cells and to mediate the transport of OAs (Reimer and Edwards 2004). Various OAs are transported via mouse NPT1 and hNPT1 in a chloride-dependent manner. Furthermore, because hNPT1 tends to combine with PAH, as earlier studies with brush-border membrane vesicles have shown, it is also believed to be a classical voltage-dependent transporter of PAH.

However, whether the transport of PAH is affected by membrane potential is unclear (Uchino et al. 2000).

MRP family ABCC

The ATP-dependent excretion of both drugs and xenobiotics is mediated by P-glycoprotein (P-gp). This protein is expressed in the luminal membranes of the small intestine and the blood–brain barrier and in the apical membranes of excretory cells, such as hepatocytes and the epithelial cells of kidney proximal tubules (Giacomini et al. 2010).

The multidrug resistance-associated protein (MRP) family primarily comprises active transporters with an ATP-binding cassette motif. The protein P-gp is this family's prototype (Ford and Hait 1990) and extrudes various hydrophobic molecules, in particular antineoplastics such as adriamycin, daunorubicin, vinblastine, and vincristine. In addition, multidrug resistance is conferred by P-gp (Gottesman et al. 2002). In proximal tubular cells, the members of the MRP family are believed to function as extrusion pumps on the apical membrane for OAs, especially those that are large and hydrophobic. Two isoforms of the MRP family, MRP2 and MRP4, deserve particular attention with respect to renal physiology and pharmacology. One of the physiological roles of MRP2 is to transport conjugated bilirubin from the liver into bile. In the kidney, MRP2 plays a role in the transport of highly lipophilic organic compounds across the apical membranes of tubular cells into urine. In contrast, the MRP4 isoform is involved in the efflux of several small hydrophilic OAs, including urate, prostaglandins, and cephem antibiotics into the tubular lumen.

Analysis of the function of NPT4 (SLC17A3) as OATv1

pOATv1 was first isolated as a voltage-driven OAT from the pig kidney cortex (Jutabha et al. 2003). It mediates facilitated diffusion driven by membrane voltage. In humans, NPT1 belongs to the SLC17 family and displays the highest homology to pOATv1. Dehghan et al. have found that NPT4, as well as URATv1, are causative genes of hyperuricemia (Dehghan et al. 2008). We have discovered that hNPT4, which belongs to the same family as hNPT1, is a voltage-dependent OAT, as is porcine OATv1.

In 2010, Jutabha and Anzai et al. described an hNPT4 protein localized to the apical membranes of renal proximal tubular cells (Jutabha et al. 2010). The localization of this protein in the liver is still unknown and warrants further investigation.

hNPT4 mediates the transport of PAH, estrone sulfate, estradiol glucuronide, bumetanide, and ochratoxin A (Anzai et al. 2010), and it interacts with various anionic compounds, such as probenecid, diuretics, nonsteroidal anti-inflammatory drugs, and steroid sulfates. Therefore, it is a multispecific OAT that overlaps in substrate selectivity with OAT family (*SLC22*) members (Anzai et al. 2006). Many substrates for OATs, except for dicarboxylates and penicillin G, interact with hNPT4. Thus, it would be interesting to determine the common mechanisms responsible for the similar substrate selectivities of structurally different OATs. hNPT4 interacts strongly with various diuretics, such as thiazides and loop diuretics. Bumetanide and furosemide inhibit PAH transport via hNPT4 in a dose-dependent manner. It was reported that hNPT4 functions as a luminal voltage-dependent excretion pathway for loop diuretics in proximal tubules (Ellison and Wilcox 2008). Considering that hNPT4 is a voltage-driven facilitated transporter which is localized on the apical membranes of proximal tubules, it may represent a highly suitable exit pathway for OAs via the apical membranes of renal proximal tubules. Thus, the role of hNPT4 in PAH transport is similar to that of pOATv1, initially characterized by classical expression cloning (Jutabha et al. 2003).

The transporter pOATv1 has an amino acid sequence that is quite similar to that of hNPT1 (63 %) and less similar to that of hNPT4 (45 %). Furthermore, pOATv1 is expressed in the liver and in the kidney, the latter being involved in the renal elimination of anionic drugs such as PAH and diuretics and the secretion of endogenous substrates such as urate (Jutabha et al. 2010). PAH transport by pOATv1, but not by hNPT4, has been shown to be chloride sensitive. Since we could not determine the reason for this difference between the transporters, we were not able to conclude that hNPT4 is a human ortholog of pOATv1.

Two splice variants of NPT4

hNPT4 has two splice variants of NPT4 mRNA reported in the GenBank database. One variant, hNPT4_L (variant 1: NM_001098486), contains an open reading frame encoding a putative 498-amino-acid protein (NP_001091956), and the other, hNPT4_S (variant 2: NM_006632), encodes a 420-amino-acid protein (NP_006623). The difference between these two isoforms is the presence of a fourth exon in hNPT4_L. mRNAs for both hNPT4 isoforms have been detected only in the kidneys and liver by reverse transcription polymerase chain reaction (Jutabha et al. 2010; Ruddy et al. 1997). Following injection of complementary RNAs (cRNAs) into *Xenopus* oocytes, hNPT4_L, but not hNPT4_S, has been found to be expressed on the plasma membrane (Jutabha et al. 2011a), corresponding to the results of a previous study showing that NPT4 (U90545, short isoform) is localized on the endoplasmic reticulum following transfection of cDNA into COS (an abbreviation for “CV-1 in origin with SV40 genes”) cells (Melis et al. 2004).

hNPT4 as a renal secretory pathway for urate

Urate is generated from purine metabolism, and sustained hyperuricemia is a pathogenetic cause of gout, chronic renal diseases, hypertension, and cardiovascular diseases. The serum level of uric acid is largely determined by the intrarenal reabsorption and secretion of urate. The renal reabsorption of urate is controlled by two proximal tubular urate transporters: apical URAT1 (Enomoto et al. 2002) and basolateral URATv1 (Vitart et al. 2008; Anzai et al. 2008; Caulfield et al. 2008). In contrast, hNPT4, an orphan transporter, is a multispecific OA efflux transporter that is expressed by the kidneys and the liver. hNPT4 is localized on the apical side of the renal tubule, and it functions as a voltage-driven urate transporter (Jutabha et al. 2011b). In addition, hNPT4 interacts significantly with loop diuretics such as furosemide and bumetanide. Therefore, hNPT4 likely acts as a common secretion route for drugs, and may play an important role in diuretic-induced hyperuricemia (Jutabha et al. 2010). After URATv1, which is a basolateral urate efflux transporter, and hNPT4, which is an apical OA efflux transporter, were identified, a three-factor model was proposed for the transepithelial transport of urate in renal proximal tubules (Anzai and Endou 2012). However, because the molecules involved in renal urate handling play physiological and pathophysiological roles that are still somewhat unclear, it is important to continue to investigate those roles.

In 2008, a genome-wide association study found that the NPT4-encoding gene *SLC17A3* is, like two other genes, associated with the concentration of uric acid and the risk of gout (Dehghan et al. 2008). Recently, NPT4 has been functionally characterized as a novel urate efflux transporter, and two loss-of-function mutations (not polymorphisms) of *SLC17A3* have been found in patients with gout and reduced excretion of renal urate (Jutabha et al. 2011b). Because it is a protein that is apically expressed in renal tubules, NPT4 is believed to be an exit path for urate when it is transtubularly secreted.

Single nucleotide polymorphisms in *SLC17A3*/NPT4

There are currently 10 nonsynonymous *SLC17A3* single nucleotide polymorphisms (SNPs) reported in the public SNP database (NCBI dbSNP). The functional properties of five of the NPT4 variants (A100T, G239 V, V257F, G279R, and P378L, as reported at the time of determination) were characterized using the *Xenopus* oocyte expression system (Jutabha et al. 2011a). The transport activities of urate, PAH, estrone sulfate, and bumetanide were studied. Compared with a wild-type clone, P378L did not show any transport function for any of the above four substrates tested. V257F and G279R displayed moderately reduced transport activities, whereas A100T did not exhibit altered transport of any of the four substrates. In terms of the structure–function relationship, the reduction of transport function in V257F but the lack of a reduction in transport function in G239 V is interesting because both residues are in the same (fifth) transmembrane domain. The NPT4 protein has been detected at the plasma membranes of oocytes injected with cRNAs derived from all NPT4 mutants. It has been suggested that the reduced transport activity caused by some SNPs is not due to an absence of surface membrane expression. These functionally relevant NPT4 variants may explain some of the interindividual differences in susceptibility to certain diseases, such as gout (Pascual and Perdiguerro 2006), that are observed in individuals with altered NPT4 function. Diuretics are NPT4 substrates, so it would be interesting to further investigate whether individuals who possess SNPs in NPT4 are resistant to diuretic treatment. Functional analysis of other hNPT isoforms that have same amino acid replacement in the corresponding position to hNPT4 may provide further insight about the importance of these residues on OA transport in SLC17 members.

Renal urate transporters as causes of diuretic-induced hyperuricemia

Hyperuricemia is a well-known adverse effect of diuretic treatment (Ravnan et al. 2002). Diuretics are thought to have direct actions on urate transporters in renal proximal

tubules by enhancing urate influx and causing an increase in the serum urate. We focused on whether hNPT4 is a transporter of urate.

Both membrane transporters and metabolic enzymes are involved in the clearance of drugs from the kidney and liver; therefore, if these organs show altered drug transport activity, the pharmacokinetics of the substrate drugs might be affected (Anzai and Endou 2007). One substrate transported by hNPT4 is bumetanide, so polymorphic changes in hNPT4 might affect the pharmacokinetics of this and other loop diuretics (Jutabha et al. 2010). For example, the phenomenon known as “diuretic resistance” is exhibited by about one-third of patients with chronic heart failure (Ravnan et al. 2002). This phenomenon has been defined as a failure to decrease extracellular fluid volume despite the liberal administration of diuretics. A possible cause of this phenomenon is decreased tubular delivery of loop diuretics, which is often attributed to decreased renal perfusion in patients with heart failure. Furthermore, the differences in function of the hNPT4 variants mentioned earlier probably explain some of the interindividual differences in diuretic response. Thus, it would be interesting to determine if diuretic resistance is sometimes explained by altered hNPT4 function (Jutabha et al. 2011b).

Common diuretics, such as loop diuretics (furosemide and bumetanide) and thiazide, also reduce urinary uric acid excretion and increase the serum uric acid level (Russel et al. 2002). The protein hNPT4 likely serves as a common secretion route for drugs and urate. The dose-dependent inhibitory effects of furosemide and bumetanide on hNPT4-mediated urate transport suggest that the inhibition of urate efflux through this transporter by loop diuretics may be responsible for diuretic-induced hyperuricemia (Jutabha et al. 2011b).

Conclusions

We have demonstrated that hNPT4 is a multispecific OA efflux transporter expressed in the kidneys and liver. In the kidneys, it is localized on the apical sides of renal tubules and functions as a voltage-driven urate transporter. The kidneys play a dominant role in maintaining the serum urate level. Renal urate excretion is a function of the balance between reabsorption and secretion. It has recently been demonstrated that the uptake of luminal urate into renal proximal tubular cells is mediated by the urate-anion exchanger URAT1, and that the voltage-driven urate efflux transporter URATv1/GLUT9 facilitates the exit of intracellular urate from the cells into the interstitium/blood space. OAT1 and/or OAT3, located on the basolateral sides of renal proximal tubular cells, have been proposed to act as uptake transporters for urate from the interstitium/blood

space into cells; however, the molecular identity of the apical urate transporter that excretes intracellular urate into the luminal (urine) space is elusive. We suggest that NPT4/OATv1 is the missing component of the three-factor model because it functions in renal tubular efflux and the elimination of various anionic drugs, such as PAH and diuretics, as well as in the secretion of endogenous substrates such as urate. In addition to a known effect on renal urate uptake transporters, another mechanism for diuretic-induced hyperuricemia may be an inhibition of NPT4-mediated urate secretion. Therefore, the NPT4/OATv1-mediated efflux of urate may represent a new drug target for hyperuricemia.

Acknowledgments This study was supported in part by grants from from the Japan Society for the Promotion of Science [JSPS KAKENHI 24590328 (K.H.), 23590647 (P.J.), 26461258 (N.A.)], the Strategic Research Foundation Grant-aided Project for Private Universities (S1412001), the Science Research Promotion Fund of the Japan Private School Promotion Foundation, the Gout Research Foundation of Japan, the Shimabara Science Promotion Foundation (K.H.), a Dokkyo Medical University Investigator-Initiated Research Grant (N.O., M.O.), and Research grant of Seki Minato Memorial Awards of the Seki Minato Foundation (P.J., N.A.).

Compliance with ethical standards

Disclosure of potential conflicts of interest There are no conflicts of interest associated with the authors who contributed to this manuscript.

References

- Anzai N, Endou H (2007) Drug transport in the kidney. In: You G, Morris ME (eds) Drug transporters: molecular characterization and role in drug disposition. Wiley, Hoboken, pp 463–493
- Anzai N, Endou H (2012) Renal basis of hyperuricemia. In: Terkeltaub R (ed) Gout and other crystal arthropathies. Elsevier Saunders, Philadelphia, pp 51–58
- Anzai N, Kanai Y, Endou H (2006) Organic anion transporter family: current knowledge. *J Pharmacol Sci* 100:411–426
- Anzai N, Ichida K, Jutabha P, Kimura T, Babu E, Jin CJ, Srivastava S, Kitamura K, Hisatome I, Endou H, Sakurai H (2008) Plasma urate level is directly regulated by a voltage-driven urate efflux transporter URATv1 (SLC2A9) in humans. *J Biol Chem* 283:26834–26838
- Anzai N, Jutabha P, Endou H (2010) Molecular mechanism of ochratoxin A transport in the kidney. *Toxins (Basel)* 2:1381–1398
- Caulfield MJ, Munroe PB, O'Neill D, Witkowska K, Charchar FJ, Doblado M, Evans S, Eyheramendy S, Onipinla A, Howard P, Shaw-Hawkins S, Dobson RJ, Wallace C, Newhouse SJ, Brown M, Connell JM, Dominiczak A, Farrall M, Lathrop GM, Samani NJ, Kumari M, Marmot M, Brunner E, Chambers J, Elliott P, Kooner J, Laan M, Org E, Veldre G, Viigimaa M, Cappuccio FP, Ji C, Iacone R, Strazzullo P, Moley KH, Cheeseman C (2008) SLC2A9 is a high-capacity urate transporter in humans. *PLoS Med* 5:e197
- Cha SH, Sekine T, Kusuhara H, Yu E, Kim JY, Kim DK, Sugiyama Y, Kanai Y, Endou H (2000) Molecular cloning and characterization of multispecific organic anion transporter 4 expressed in the placenta. *J Biol Chem* 275:4507–4512
- Cha SH, Sekine T, Fukushima JI, Kanai Y, Kobayashi Y, Goya T, Endou H (2001) Identification and characterization of human organic anion transporter 3 expressing predominantly in the kidney. *Mol Pharm* 59:1277–1286
- Dehghan A, Köttgen A, Yang Q, Hwang SJ, Kao WL, Rivadeneira F, Boerwinkle E, Levy D, Hofman A, Astor BC, Benjamin EJ, van Duijn CM, Witteman JC, Coresh J, Fox CS (2008) Association of three genetic loci with uric acid concentration and risk of gout: a genome-wide association study. *Lancet* 372:1953–1961
- Ellison DH, Wilcox CS (2008) Brenner and Rector's the kidney, 8th edn. Saunders Elsevier, Philadelphia, pp 1646–1678
- Enomoto A, Kimura H, Chairoungdua A, Shigeta Y, Jutabha P, Cha SH, Hosoyamada M, Takeda M, Sekine T, Igarashi T, Matsuo H, Kikuchi Y, Oda T, Ichida K, Hosoya T, Shimokata K, Niwa T, Kanai Y, Endou H (2002) Molecular identification of a renal urate anion exchanger that regulates blood urate levels. *Nature* 23:447–452
- Ford JM, Hait WN (1990) Pharmacology of drugs that alter multidrug resistance in cancer. *Pharmacol Rev* 42:155–199
- Giacomini KM, Huang SM, Tweedie DJ, Benet LZ, Brouwer KL, Chu X, Dahlin A, Evers R, Fischer V, Hillgren KM, Hoffmaster KA, Ishikawa T, Keppler D, Kim RB, Lee CA, Niemi M, Polli JW, Sugiyama Y, Swaan PW, Ware JA, Wright SH, Yee SW, Zamek-Gliszczynski MJ, Zhang L, International Transporter Consortium (2010) Membrane transporters in drug development. *Nat Rev Drug Discov* 9:215–236
- Gottesman MM, Fojo T, Bates SE (2002) Multidrug resistance in cancer: role of ATP-dependent transporters. *Nat Rev Cancer* 2:48–58
- Hosoyamada M, Sekine T, Kanai Y, Endou H (1999) Molecular cloning and functional expression of a multispecific organic anion transporter from human kidney. *Am J Physiol Renal Physiol* 276:F122–F128
- Jacquemin E, Hagenbuch B, Stieger B, Wolkoff AW, Meier PJ (1994) Expression cloning of a rat liver Na⁺-independent organic anion transporter. *Proc Natl Acad Sci USA* 91:133–137
- Jutabha P, Kanai Y, Hosoyamada M, Chairoungdua A, Kim DK, Iribe Y, Babu E, Kim JY, Anzai N, Chatsudthipong V, Endou H (2003) Identification of a novel voltage-driven organic anion transporter present at apical membrane of renal proximal tubule. *J Biol Chem* 278:27930–27938
- Jutabha P, Anzai N, Kitamura K, Taniguchi A, Kaneko S, Yan K, Yamada H, Shimada H, Kimura T, Katada T, Fukutomi T, Tomita K, Urano W, Yamanaka H, Seki G, Fujita T, Moriyama Y, Yamada A, Uchida S, Wempe MF, Endou H, Sakurai H (2010) Human sodium phosphate transporter 4 (hNPT4/SLC17A3) as a common renal secretory pathway for drugs and urate. *J Biol Chem* 285:35123–35132
- Jutabha P, Anzai N, Kimura T, Taniguchi A, Urano W, Yamanaka H, Endou H, Sakurai H (2011a) Functional analysis of human sodium-phosphate transporter 4 (NPT4/SLC17A3) polymorphisms. *J Pharmacol Sci* 115:249–253
- Jutabha P, Anzai N, Wempe MF, Wakui S, Endou H, Sakurai H (2011b) Apical voltage-driven urate efflux transporter NPT4 in renal proximal tubule. *Nucleosides Nucleotides Nucleic Acids* 30:1302–1311
- Melis D, Havelaar AC, Verbeek E, Smit GP, Benedetti A, Mancini GM, Verheijen F (2004) NPT4, a new microsomal phosphate transporter: mutation analysis in glycogen storage disease type Ic. *J Inherit Metab Dis* 27:725–733
- Mikaichi T, Suzuki T, Onogawa T, Tanemoto M, Mizutamari H, Okada M, Chaki T, Masuda S, Tokui T, Eto N, Abe M, Satoh F, Unno M, Hishinuma T, Inui K, Ito S, Goto J, Abe T (2004) Isolation and characterization of a digoxin transporter and its rat

- homologue expressed in the kidney. *Proc Natl Acad Sci USA* 101:3569–3574
- Møller JV, Sheikh MI (1982) Renal organic anion transport system: pharmacological, physiological, and biochemical aspects. *Pharmacol Rev* 34:315–358
- Pascual E, Perdiguero M (2006) Gout, diuretics and the kidney. *Ann Rheum Dis* 65:981–982
- Ravnan SL, Ravnan MC, Deedwania PC (2002) Pharmacotherapy in congestive heart failure: diuretic resistance and strategies to overcome resistance in patients with congestive heart failure. *Congest Heart Fail* 8:80–85
- Reimer RJ, Edwards RH (2004) Organic anion transport is the primary function of the SLC17/type I phosphate transporter family. *Pflugers Arch* 447:629–635
- Ruddy DA, Kronmal GS, Lee VK, Mintier GA, Quintana L, Domingo R Jr, Meyer NC, Irrinki A, McClelland EE, Fullan A, Mapa FA, Moore T, Thomas W, Loeb DB, Harmon C, Tsuchihashi Z, Wolff RK, Schatzman RC, Feder JN (1997) A 1.1-Mb transcript map of the hereditary hemochromatosis locus. *Genome Res* 7:441–456
- Russel FG, Masereeuw R, van Aubel RA (2002) Molecular aspects of renal anionic drug transport. *Annu Rev Physiol* 64:563–594
- Sekine T, Watanabe N, Hosoyamada M, Kanai Y, Endou H (1997) Expression cloning and characterization of a novel multispecific organic anion transporter. *J Biol Chem* 272:18526–18529
- Shimada H, Moewes B, Burckhardt G (1987) Indirect coupling to Na^+ of *p*-aminohippuric acid uptake into rat renal basolateral membrane vesicles. *Am J Physiol* 253:F795–F801
- Sweet DH, Wolff NA, Pritchard JB (1997) Expression cloning and characterization of ROAT1. The basolateral organic anion transporter in rat kidney. *J Biol Chem* 272:30088–30095
- Uchino H, Tamai I, Yamashita K, Minemoto Y, Sai Y, Yabuuchi H, Miyamoto K, Takeda E, Tsuji A (2000) *p*-Aminohippuric acid transport at renal apical membrane mediated by human inorganic phosphate transporter NPT1. *Biochem Biophys Res Commun* 270:254–259
- Vitart V, Rudan I, Hayward C, Gray NK, Floyd J, Palmer CN, Knott SA, Kolcic I, Polasek O, Graessler J, Wilson JF, Marinaki A, Riches PL, Shu X, Janicijevic B, Smolej-Narancic N, Gorgoni B, Morgan J, Campbell S, Biloglav Z, Barac-Lauc L, Pericic M, Klaric IM, Zgaga L, Skaric-Juric T, Wild SH, Richardson WA, Hohenstein P, Kimber CH, Tenesa A, Donnelly LA, Fairbanks LD, Aringer M, McKeigue PM, Ralston SH, Morris AD, Rudan P, Hastie ND, Campbell H, Wright AF (2008) SLC2A9 is a newly identified urate transporter influencing serum urate concentration, urate excretion and gout. *Nat Genet* 40:437–442
- Wright EM (1985) Transport of carboxylic acids by renal membrane vesicles. *Annu Rev Physiol* 47:127–141

ミニレビュー

プロスタグランジンと有機アニオンのトランスポーター

獨協医科大学医学部薬理学講座*

安西 尚彦, 岡本 和久, 花田 健治, 阿部 篤朗, 大谷 直由, 大内 基司

Vitamins (Japan), **89** (9), 441-445 (2015)**Transporters for prostaglandins and organic anions**

Naohiko Anzai, Kazuhisa Okamoto, Kenji Hanada, Tokuro Abe, Naoyuki Otani, Motoshi Ouchi

Department of Pharmacology and Toxicology, Dokkyo Medical University School of Medicine, Tochigi 321-0293, Japan

Organic anion transporters (OATs) play a fundamental role in the elimination of numerous endogenous and exogenous organic anions from the body. The secretion of numerous organic anions including endogenous metabolites, drugs, and xenobiotics, is an important physiological function of excretory organs such as kidney and the process of secretion of organic anions through the proximal tubule cells is achieved via unidirectional transcellular transport. To date, several families of multispecific organic anion transporters, including organic anion transporter (OAT) family, organic anion-transporting polypeptide (OATP) family, sodium-phosphate transporter (NPT) family and ATP-dependent organic anion transporters such as multidrug resistance-associated protein (MRP) are identified by molecular cloning. Among them, some members of OATP (SLC21/SLCO) family and OAT (SLC22) family are thought to contribute to the membrane permeation of prostaglandins (PGs), for example, PGE₂ and PGF_{2α}, that play various physiological and pathophysiological roles. The first PG-specific transporter PGT (prostaglandin transporter), a member of SLC21/SLCO family, was identified in 1995. This transporter may play a primary role in the removal of bioactive PGs from the circulation. Recently, we identified a novel member of the SLC22 family expressed in mouse kidney and designated this member as OAT-PG (organic anion transporter for prostaglandins). This OAT-PG specifically transports PGs which are localized in proximal tubules.

Key words: organic anion, prostaglandin, transporter, OAT, OATP

(Received May 11, 2015)

有機アニオンとは

ビタミン・バイオフィクターには水溶性の高い物質も含まれ、それらの一部は「有機イオン」に分類される。有機イオンは正電荷を持つ有機カチオン(有機塩基)と負電荷を持つ有機アニオンに分けられる。すなわち、

有機アニオンとは炭素骨格を有し、生理学的条件下において陰性の荷電を帯びている物質の総称である(表1)¹⁾。臨床医療の現場において重要な有機アニオンといえば、抗生物質、利尿薬、非ステロイド性抗炎症薬(NSAIDs)、ACE阻害薬などの薬物およびその代謝産物がこれに該当する。有機アニオンの細胞膜輸送とい

*〒 321-0293 栃木県下都賀郡壬生町北小林 880 獨協医科大学医学部薬理学講座 E-mail : anzai@dokkyomed.ac.jp

うと生体異物の排出というイメージがあるが、実際には有機アニオンの中には、生体にとって(有用な)内因性物質、すなわち、プロスタグランジン(PG)やステロイド抱合体、その他に尿酸などが含まれており、有機アニオン輸送は必ずしも排泄のみを示すものではない。有機アニオンはイオンという性質上、水溶性であり、脂質で構成された細胞膜を自由に通過することはできない。細胞膜透過のためには特定の膜タンパク質であるトランスポーターが必要となり、いわゆる一群の有機アニオントランスポーターがこれを担っている。

有機アニオントランスポーター

有機アニオントランスポーターとして、これまでに OAT (organic anion transporter) ファミリー、OATP (organic anion transporting polypeptide) ファミリー、NPT (sodium-phosphate transporter) ファミリー、そして ATP 駆動型トランスポーターの MRP (multidrug resistance-associated protein) ファミリーが分子同定されている(表 2)²⁾。SLC22 に分類される OAT ファミリーは、1997 年に PAH (パラアミノ馬尿酸) の取り込み活性を指標にし

た発現クローニング法により OAT1 (SLC22A6) が同定され、その後ヒトでは OAT2, 3, 4, 7, さらに URAT1 および OAT10 が続けて同定された。OAT1 ~ 4 および URAT1, OAT10 は腎臓に発現し、OAT7 は肝臓に存在している³⁾。OATs の有機アニオン取り込みは、細胞内に蓄積された有機酸との交換輸送により行われることが示唆されている。SLCO/SLC21 に分類される OATP ファミリーは、肝機能検査試薬として知られる有機アニオンの BSP (bromosulphophthalein) / 胆汁酸トランスポーターとしてクローニングされ、主に肝臓に発現し、大型の有機アニオンの輸送に関与する。近年、SLC17 に分類される NPT ファミリーも有機アニオン排泄機構の一つであると考えられている。MRPs は癌細胞に多剤耐性を付与する抗癌剤排出ポンプとして知られる MDR1 とともに、ABC (ATP Binding Cassette) トランスポータースーパーファミリーに属し、ATP の水解エネルギーを用いて細胞内から細胞外へ各種抗癌剤を排出する。肝臓での抱合型ビリルビン輸送に関与する MRP2 (ABCC2) は、腎臓では近位尿細管管腔側膜に存在して、アニオン性の高脂溶性化合物の尿中への分泌を担うと考えられている。また、同ファミリーの MRP4 (ABCC4) も近位尿

表 1 有機イオンの分類

	性状	輸送基質	
		生体異物・薬物	内因性物質
有機カチオン (有機塩基)	正電荷を持つ 水溶性有機物質	利尿薬アミロライド, 抗潰瘍薬シメチジン, 抗腫瘍薬シスプラチン	ヒスタミン, ドパミン, ノルアドレナリン, セロトニン, クレアチニン
有機アニオン (有機酸)	負電荷を持つ 水溶性有機物質	抗生物質 (PcG, セフェム), 利尿薬 (フロセミド, チアジド), 抗炎症薬 NSAIDs (サリチル酸, インドメタシン), 抗腫瘍薬 MTX, バルプロ酸	胆汁酸, クレアチニン, ヌクレオチド (cAMP, cGMP), プロスタグランジン (PGE ₂ , PGF _{2α}), 尿酸, ケトン体, 短鎖脂肪酸, TCA サイクル中間代謝体

水溶性有機物質は荷電の状況により、正電荷を持つ有機カチオン(有機塩基)と陰電荷を持つ有機アニオン(有機酸)に分類される。

表 2 有機アニオントランスポーターの分類

1. Organic Anion Transporter (OAT) family : SLC22 (有機アニオントランスポーターファミリー)
OAT1, OAT2, OAT3, OAT4, OAT7, URAT1
2. Sodium-phosphate transporter family : SLC17 (Na⁺依存性リン酸トランスポーターファミリー)
NPT1, NPT4, OATv1
3. Organic Anion Transporting Polypeptide (OATP) family : SLCO (肝特異的有機酸トランスポーターファミリー)
OATP1A2 (OATP-A), OATP1B1 (OATP-C), OATP1B3 (OATP8), OATP2A1 (PGT), OATP2B1 (OATP-B), OATP4C1 (OATP-R)
4. MRP (multidrug resistance-associated protein) family : ABCC (多剤耐性関連タンパク質ファミリー)
MRP1, MRP2, MRP3, MRP4, MRP5, MRP6
5. Organic Solute Transporter (OST) (有機溶質トランスポーター)
OSTα -OSTβ

ヒトの体内での有機アニオン輸送を担う分子群として5つのトランスポーターファミリーが知られている。

細管腔側膜に存在し、プロスタグランジンや尿酸に加え、セフェム系抗生物質などのアニオン性薬物の分泌を担うと考えられている⁴⁾。

プロスタグランジンの細胞膜透過

有機アニオンの一つであるプロスタグランジン(PG)は、アラキドン酸を基質としてPGH合成酵素であるシクロオキシゲナーゼ(COX)により生成される生理活性物質である。細胞内で合成されたPGは、オートクラインないしパラクラインにより細胞外に放出され、細胞膜表面にある受容体に結合し、多彩な生理作用を発現する。細胞外に放出されて作用発現に寄与したPGは、細胞内に取込まれて15-ヒドロキシPG脱水素酵素(15-PGDH)による代謝を受けて15-ケト-PGとなり不活性化される。PGは高い疎水性を持つため、脂質二重層を容易に透過するものと考えられてきたが、実際にはその膜透過性は非常に低いため、合成されたPGの細胞外放出および作用したPGの細胞内への取込みには、トランスポーターと呼ばれる膜輸送タンパク質が必要となる⁴⁾。PGがオートコイドとして

作用するためには、①細胞内での産生、②細胞外での膜受容体への作用、③細胞内での不活性化、という3つの段階を経る必要がある(図1)。極めて膜透過性の低いPGが①から②、そして②から③という細胞膜の内外での移動を迅速に行うためにはトランスポーターが必要となる。

PG トランスポーター

PGトランスポーターの分子実体としては、1995年Schusterらの研究グループが世界に先駆けてPGに特異性の高い分子としてPGT(SLCO/SLC21ファミリー)のクローニングに成功している⁵⁾。PGTに続き著者らの研究グループが、薬物等の体外排泄を担う有機酸トランスポーターOAT(SLC22ファミリー)がPGを輸送することを明らかにした。また、ABCトランスポーターのMRP4や、新規有機溶質トランスポーターのOST α -OST β によるPG輸送も報告されている(表3)。

A) PGT (Prostaglandin transporter)

ステロイドホルモン抱合体を輸送することが知られ

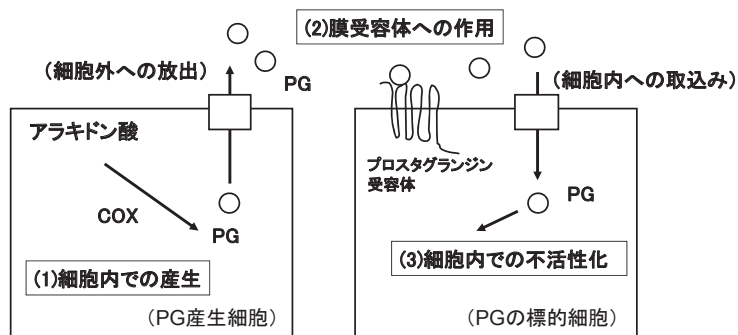


図1 プロスタグランジン(PG)の経細胞膜輸送(文献⁴⁾改変)

PGがオートコイドとして作用するためには、①細胞内での産生、②細胞外での膜受容体への作用、③細胞内での不活性化、という3つの段階を経る必要がある。①と②、および②と③の段階をそれぞれつなぐものがトランスポーターによる(1)細胞外への放出と(2)細胞内への取込みである。

表3 プロスタグランジントランスポーターの分類

1. Organic Anion Transporting Polypeptide(OATP) family: SLCO(肝特異的有機酸トランスポーターファミリー)
OATP2A1(PGT)
2. Organic Anion Transporter(OAT) family: SLC22(有機アニオントランスポーターファミリー)
OAT1, OAT2, OAT3, OAT4
3. MRP(multidrug resistance-associated protein) family: ABCC(多剤耐性関連タンパク質ファミリー)
MRP4
4. Organic Solute Transporter(OST) (有機溶質トランスポーター)
OST α -OST β

ヒトの体内でのプロスタグランジン輸送を担う分子群として有機アニオントランスポーターの中でも4つのファミリーが担うことが報告されている。

ている OATP (SLCO/SLC21) ファミリーの中から同定されたものが PGT である⁵⁾。OATP ファミリーには輸送基質の一つとして PG を輸送するクローンがいくつかあることが知られているが、PGT は OATP ファミリーの中では、構造的にも機能的にも特異な存在であり、輸送基質は PG に限られている。PGT による各種プロスタグランジンの細胞内取り込み速度は、 $PGE_2 \sim PGE_2 > PGF_{2\alpha} > TXB_2 > 6\text{-ケト-PGF}_{1\alpha} \sim \text{iloprost (PGI}_2 \text{ アナログ)}$ の順である。PGT は PGH_2 も輸送することが報告されている ($K_m = 376 \pm 34 \text{ nM}$)⁶⁾。最近、ラット PGT mRNA は肺、肝、腎、胃、十二指腸、空腸、回腸、結腸、睪丸、子宮、脳、眼などに存在するが、心筋、骨格筋などには認められない。ラット PGT mRNA は、PG 代謝が最も盛んな肺に非常に多く存在する。また、ラット PGT mRNA は腎では乳頭部 > 髓質 > 皮質の順に発現しているとされており、糸球体、集合管主細胞、髓質の間質細胞と乳頭部細胞などに発現するとされる⁷⁾。ヒト PGT mRNA は、さらに心筋と骨格筋にも認められる。これまでに述べたように、強力な作用を有する PG は受容体に作用した後、速やかに局所で代謝されなければならない。しかし、PG の代謝酵素は細胞内にあるので、PG を不活性化するためにはまず細胞内へ取り込まれる必要がある (図 2)。生体全体としては肺循環が重要で、各臓器で作用を終え代謝し切れなかった PG は肺で代謝され、体循環に回らないようにしている。腎臓では PG の産生、

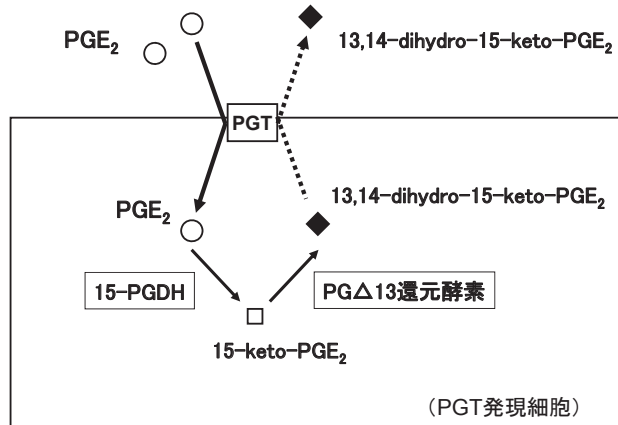


図2 プロスタグランジントランスポーター PGT と PG 不活性化の連関

PG は受容体に作用した後、PGT により取込まれ、細胞内の PG 代謝酵素 (15-PGDH) により代謝される。さらに PG Δ 13 還元酵素などにより分解された代謝産物 (13,14-dihydro-15-keto-PGE₂) は PG 取込みの交換基質となって効率的に細胞外に放出される。

作用、代謝が原則的に腎臓内部で行われ、PG は局所調節に関与していると考えられている。

B) OAT-PG (prostaglandin-specific organic anion transporter)

OATs による PG 輸送の特性は 2002 年に Kimura らにより報告されている⁸⁾。ヒト OAT1 (hOAT1), hOAT2, hOAT3, hOAT4 それぞれの安定発現細胞を用いて、RI 標識 PGE₂ と PGF_{2 α} の細胞内取込みを調べたところ、それぞれの細胞で時間および濃度依存性の取込みが認められ、その K_m は PGE₂ に対しては 154 ~ 970 nM であり、PGF_{2 α} に対しては 575 ~ 1092 nM であった。最近、Shiraya らは SLC22 ファミリーのオーファントランスポーターの中から、PG 特異的な輸送を行うクローンを見出し、prostaglandin-specific organic anion transporter (OAT-PG) と名付けた⁹⁾。OAT-PG は、近位尿細管の基底側膜に限局して発現し、先述の 15-PGDH の局在と一致することから、PG シグナルの不活化に重要な役割を持つことを示唆している (図 3)。OAT-PG は、エイコサノイドでは PGE₂ や PGH₂ を対向基質として PGE₂ 排出が促進される (トランス亢進) だけでなく、他のエイコサノイドである 12-HPETE (12-hydroper-

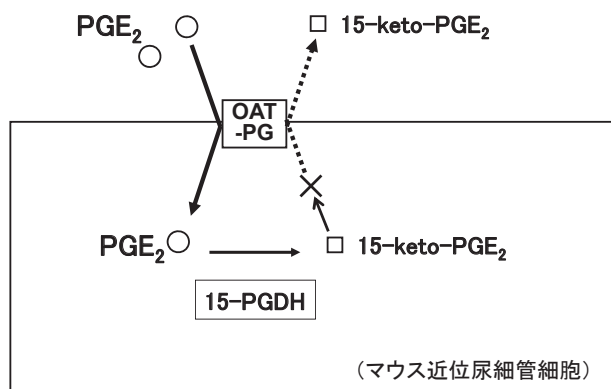


図3 OAT-PG と PG 不活性化酵素 (15-PGDH) との連関
マウスの近位尿細管の基底側膜に限局して発現し PG 特異的な輸送を行う prostaglandin-specific organic anion transporter (OAT-PG) は、先述の PG 代謝酵素 15-PGDH の局在と一致し、受容体に作用した後の PG を細胞内に取込み続けて酵素 15-PGDH による不活化が行われると考えられている。OAT-PG は、エイコサノイドでは PGE₂ や PGH₂ を対向基質として PGE₂ 排出が促進される (トランス亢進) だけでなく、他のエイコサノイドである 12-HPETE (12-hydroperoxyeicosatetraenoic acid), 15-HPETE, 15-HETE (15-hydroxyeicosatetraenoic acid) などトランス亢進を示す。15-ケト-PGE₂ などの PGE₂ 不活性化代謝産物によるトランス亢進が存在するのかどうかについては今後の検討が待たれる。

oxyeicosatetraenoic acid), 15-HPETE, 15-HETE (15-hydroxyeicosatetraenoic acid) などもトランス亢進を示すことが示され, 興味深いがその生理学的意味は不明であり, PGTにみられるような13,14-ジヒドロ-PGE₂や13,14-ジヒドロ-15-ケト-PGE₂などのPGE₂不活性化代謝産物によるトランス亢進が存在するのかどうかについては解析がなされておらず, 不活性化酵素との機能的な連関についての今後の検討が待たれる.

(平成 27.5.11 受付)

文 献

- 1) 安西尚彦, 遠藤仁 (2003) 有機物質の輸送—トランスポーター. 別冊医学のあゆみ 腎疾患—state of arts 2003-2005 (浅野泰, 小山哲夫編). pp.79-82, 医歯薬出版, 東京
- 2) Anzai N, Kanai Y, Endou H (2006) Organic anion transporter family: current knowledge. *J Pharmacol Sci* **100**, 411-442
- 3) 宮崎博喜, 安西尚彦, 関根孝司, 遠藤 仁 (2005) 有機陰イオン輸送—最近の進歩. *Annual Review 腎臓* 2005 (伊藤克己, 遠藤仁, 御手洗哲也, 東原英二, 秋澤忠男編). pp.26-33, 中外医学社, 東京
- 4) 安西尚彦 (2011) 生理活性脂質のトランスポーター. 栄養・食品機能とトランスポーター (日本栄養・食糧学会監修). pp.105-119, 建帛社, 東京
- 5) Kanai N, Lu R, Satriano JA, Bao Y, Wolkoff AW, Schuster VL (1995) Identification and characterization of a prostaglandin transporter. *Science* **268**, 866-869
- 6) Chi Y, Schuster VL (2010) The prostaglandin transporter PGT transports PGH₂. *Biochem Biophys Res Commun* **395**, 168-172
- 7) Bao Y, Pucci ML, Chan BS, Lu R, Ito S, Schuster VL (2002) Prostaglandin transporter PGT is expressed in cell types that synthesize and release prostanoids. *Am J Physiol Renal Physiol* **282**, F1103-F1110
- 8) Kimura H, Takeda M, Narikawa S, Enomoto A, Ichida K, Endou H (2002) Human organic anion transporters and human organic cation transporters mediate renal transport of prostaglandins. *J Pharmacol Exp Ther* **301**, 293-298
- 9) Shiraya K, Hirata T, Hatano R, Nagamori S, Wiriyasermkul P, Jutabha P, Matsubara M, Muto S, Tanaka H, Asano S, Anzai N, Endou H, Yamada A, Sakurai H, Kanai Y (2010) A novel transporter of SLC22 family specifically transports prostaglandins and co-localizes with 15-hydroxyprostaglandin dehydrogenase in renal proximal tubules. *J Biol Chem* **285**, 22141-22151